The research reported in this document was supported jointly by the Dept. of the Army, the Dept. of the Navy, and the Dept. of the Air Force under Air Force Contract No. AF 19 (122)-458.

division 6 · lincoln laboratory · MIT · lexington 73, massachusett

17 January 1955

Approved

Robert R. Everett

ACKNOWLEDGMENT

The author is grateful to Dr. John B. Goodenough for guidance and encouragement in the supervision of this thesis, and to the staff of Groups 35, 37 and 63, Lincoln Laboratory, for their many invaluable assistances.

Sincere appreciation is extended to Mr. Robert E. Lepore for many tedious hours spent in sample preparation, to Mrs. Muriel I. Durso for a painstaking preparation of the manuscript, and to Miss Mary Matas for her cooperation in the preparation of the illustrations.

MAGNETOSTRICTION IN FERRITES POSSESSING A SQUARE HYSTERESIS LOOP

ABSTRACT

The development of ceramic materials with an intrinsically square hysteresis loop for use as storage elements in high-speed electronic computers has been largely empirical. A fundamental understanding of the basic mechanism responsible for the square hysteresis loop is necessary for further significant improvements in these materials. The investigation reported in this paper was undertaken to obtain magnetostriction data on a compositional series of ferrites in which there exists an important variation in the character of the hysteresis loop. A significant correlation was found between the magnetostriction and the hysteresis data. The isotropic saturation magnetostriction for these polycrystalline materials was found to change sign, going through zero at the optimum composition for hysteresis-loop squareness in this compositional series. In addition, the sign of the magnetostriction at low fields, which in nearly all cases is opposite to that at high fields, also changes at this optimum composition. These data have been analyzed, and it has been concluded that the effective domain anisotropy and the polycrystalline saturation magnetostriction are zero at the optimum composition. A possible mechanism is advanced which explains the observed data as the result of a grain-to-grain alignment of the magnetic moments due to the anisotropy of the single-crystal magnetostriction.

* * * * * *

Because it presents information of general interest this thesis report, which has had only very limited distribution, is being issued as a Division 6 Report.

Philip K. Baltzer (J.B.S.)

Philip K. Baltzer

TABLE OF CONTENTS

LIST OF ILLUSTRATIONS

LIST OF ILLUSTRATIONS
(continued)

LIST OF ILLUSTRATIONS
(continued)

CHAPTER I

INTRODUCTION

A. The General Problem

Materials possessing hysteresis loops rectangular in shape have been known for some time.[1] Since the exploitation of this hysteresis-loop characteristic was conceived as a means for retaining information in an electronic-computer memory,[2] a great impetus has been given to the study of the basic mechanisms responsible for rectangular hysteresis loops.

Both metallic and ceramic materials have been developed which possess a square hysteresis loop. However, little is known concerning the basic mechanism that is responsible for this hysteresis-loop characteristic. This is particularly true for the polycrystalline ceramics which are considered in this paper.

Extremely square B-H loops have been obtained for the polycrystalline ceramics called ferrites. The hysteresis characteristics of these materials are primarily dependent upon the chemical composition. Therefore, this study is concerned both with an understanding of the macroscopic mechanism responsible for the square B-H loop in ferrites and with the influence of the chemical composition upon this physical mechanism; such an understanding should lead to the creation of new materials with improved magnetic properties.

B. Historical Background

Before the specific problem can be considered, the basic concepts of magnetism and their associated terminology will be reviewed.

Most materials are composed of atoms which are located in a periodic geometric configuration called the crystalline structure.

The atoms exist as charged particles, ions, which may possess a magnetic moment. The magnetic moment of these ions is produced by their electronic configuration. Since these ions are in close proximity to one another in the crystal lattice, the way in which their electronic configurations interact determines the magnetic character of the material. FERROMAGNETISM is defined as the case when all the moments of these ions are parallel to one another and pointed in the same direction. The energy involved in maintaining this alignment is called the magnetic EXCHANGE ENERGY and is expressed as $A\bar{r}$, where A is the EXCHANGE PARAMETER and $\bar{r}$ is an average distance to near-neighbor magnetic atoms. The exchange parameter is a measure of the strength of coupling between the magnetic moments.

In some crystal structures interpenetrating sublattices exist in which the magnetic moments within each sublattice are parallel and in the same direction but in opposition to the moments of the other sublattices. A material is called FERRIMAGNETIC when a nonzero net moment exists and is called ANTIFERROMAGNETIC when the net moment is zero. The energies involved in producing these magnetic configurations are also called magnetic exchange energies. The CURIE TEMPERATURE, T_c, is the temperature at which the exchange energies responsible for ferromagnetism, ferrimagnetism, or antiferromagnetism are just overwhelmed by the thermal energy of the system. At temperatures above T_c the magnetic moments are oriented in a random fashion with respect to one another, and the material is called PARAMAGNETIC. Since the Curie temperature, like the exchange parameter, is a measure of the strength of coupling between magnetic moments, T_c is proportional to A.

The geometry of the crystal structure and the exchange coupling produce energetically preferred or easy directions for the total magnetic moment in a crystal. The energy per unit volume required to rotate the

magnetic moment from an easy direction of magnetization to an energetically unfavorable or hard direction is defined as the CRYSTALLINE ANISOTROPY ENERGY, K. The sign of K is indicative of the direction of easy magnetization in the crystal. In a cubic crystal, the directions along the cube edges are all equivalent by symmetry and are called $\langle 100 \rangle$ directions. The directions along the cube diagonals are also all equivalent and are called $\langle 111 \rangle$ directions. The directions of easy magnetization for $K > 0$ are the $\langle 100 \rangle$ directions and for $K < 0$ the $\langle 111 \rangle$ directions.

The crystalline structure of most magnetic materials is physically distorted as the direction of magnetization is varied. This phenomenon is called MAGNETOSTRICTION. Magnetostriction has a strong influence on the use and characteristics of magnetic materials and will be treated in detail in Chapter III.

Most magnetic materials are actually composed of many small regions or DOMAINS which are each saturated magnetically but differ in their direction of magnetization. In zero applied field, the direction of the magnetic moments in each domain is usually determined by the crystalline anisotropy K. The boundary layers between the magnetic domains are called DOMAIN WALLS. The flux reversal of a magnetic material possessing a domain configuration is largely a process of domain walls moving through the material (see Figure 1-1). Thus the total magnetic moment of a material is dependent upon the existing domain configuration, which can be changed by the application of an external field.

Through a domain wall the magnetic moments are directed parallel to the moment of one domain on one side and are progressively turned parallel to the magnetic moment of the other. Since the magnetic moments within the wall are not directed along an easy direction and are

A-61494

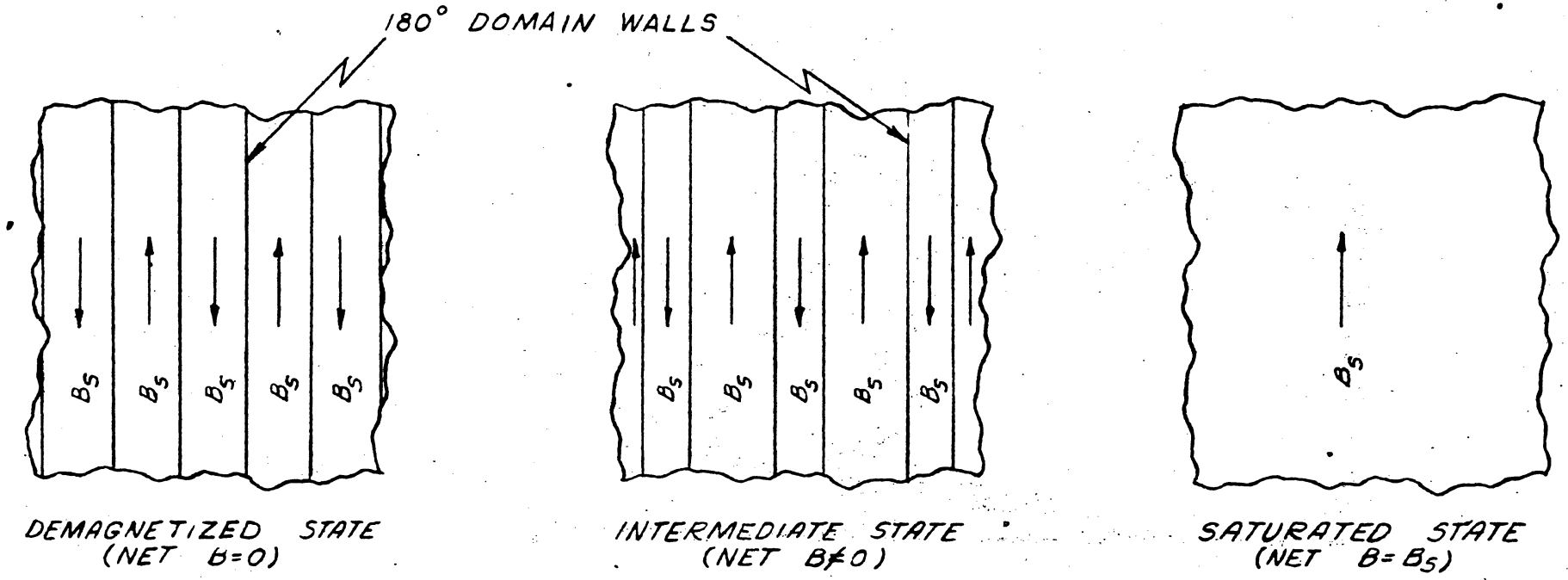

FIG.1-1

DOMAINS IN A MAGNETIC MATERIAL

not parallel to one another, work is done against the EFFECTIVE WALL ANISOTROPY, K_w, and the exchange energy. Therefore a domain wall possesses a DOMAIN-WALL ENERGY SURFACE DENSITY, $\sigma_w \propto \sqrt{K_w A}$. It is K_w which restricts the thickness of a domain wall to a small value. Therefore when $K_w = 0$, discrete domain walls will not exist. The K_w is the combined effect of the crystalline anisotropy energy K and the magnetoelastic energy.[3] The magnetoelastic energy is caused by the strains produced by magnetostriction. Both the crystalline anisotropy energy and the magnetostriction must be zero for $K_w = 0$. Hence if the magnetostriction is nonzero, domain walls can exist even when the crystalline anisotropy energy $K = 0$.

It does not seem to have been brought out in the literature that a difference exists, in general, between K_w and K_d, the EFFECTIVE DOMAIN ANISOTROPY ENERGY influencing the direction of domain magnetization. Therefore this point must be made clear. The volume of a domain wall is so small with respect to the volume of the domains on either side that the lattice dimensions within the domain wall will essentially be determined by the magnetostriction in the adjacent domains. Since the magnetoelastic energy associated with the magnetic moments within the wall would be lower if the lattice dimension within the wall were not so constrained, work must be done to rotate a moment from its direction in a domain to its direction in a wall. The effective anisotropy energy within the wall is therefore different from that in the domains. K_d may therefore be considered as a macroscopic effect influencing the direction of magnetization, whereas K_w is a microscopic effect influencing the rotation of moments through a domain wall. It is possible that the influence of magnetostriction could decrease K_d while at the same time increasing K_w. Further comments on these effects will be made in Chapter VI.

The terminology associated with the magnetic hysteresis loop is indicated in Figure 1-2, where

B_s = saturation-flux density;

B_r = remanent-flux density;

H_c = coercive force, the field for B = 0; and

B_m = the maximum flux density for a nonsaturated loop at the maximum applied field H_m.

The squareness R_s of the B-H (or hysteresis) loop will be defined as the ratio of the flux density at $-\frac{H_m}{2}$ to B_m. It is because of this definition that R_s will vary with the applied field. A maximum R_s often occurs for $H_m \simeq H_c$, where H_c is the coercive force for the saturation loop.

Rectangular or square hysteresis loops have been obtained in single crystals of magnetic materials.[4] A square B-H loop was obtained in these cases by cutting a sample from a single crystal, such that the path of the magnetic flux is always in a direction parallel to a preferred orientation of the magnetization within the material. When this was done, the reversal of magnetization was accomplished through a very small change in the applied field, producing the square B-H loop.

A polycrystalline material can be considered a closely packed assemblage of individual single crystals. The single crystallites in a polycrystal are not in general oriented with respect to one another in any way. Therefore the problem of obtaining a square B-H loop is far more difficult for a polycrystalline material than for a single crystal. However, if the crystalline axes of each of these crystallites were aligned with one another, a pseudosingle crystal would be obtained. A square B-H loop would then be obtainable in the same manner as in the case of an actual single crystal. Precisely this has been done with metallic tapes where the rolling and annealing process can produce an

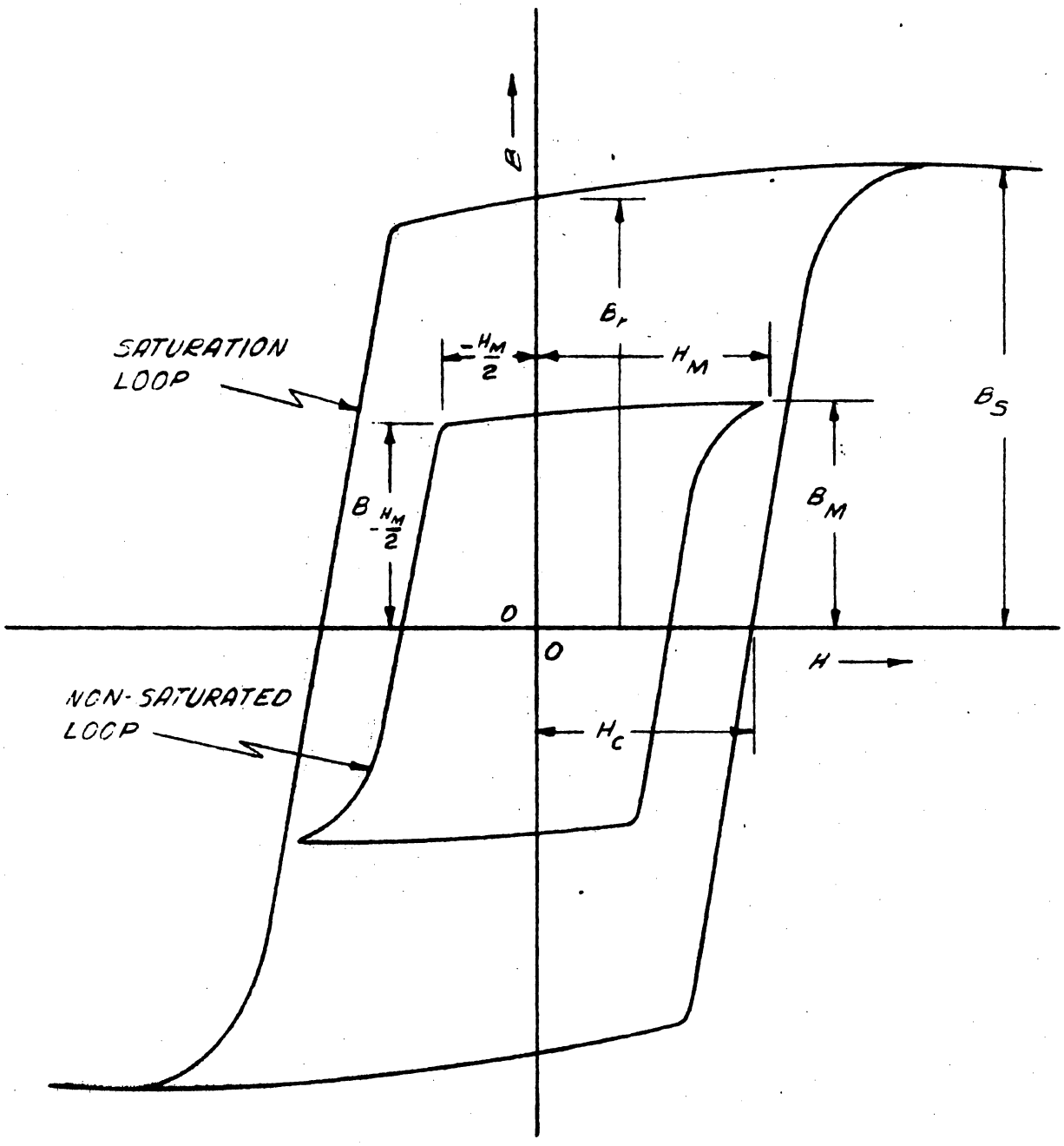

FIG. 1-2

HYSTERESIS LOOP TERMINOLOGY

A-61496

actual alignment of the crystallites within the material.

In some materials it has been found possible to produce a square B-H loop without an alignment of the crystallites. It is sometimes possible to align the magnetic moments of the individual crystallites by the application of an external compressive or tensile stress. This has been done with both metals[1] and ferrites.[5,6] The necessary requirement is that the direction of magnetization within each crystallite be determined by the directional stress applied. In a few materials the alignment of a crystallite magnetic moment with its neighbors is also possible by cooling the material slowly through the Curie temperature with a magnetic field applied.[7]

Since it had always been necessary to have an alignment of the magnetic moments in a square-looped polycrystal, it was thought essential to have alignment of the moments if square hysteresis loops were to be obtained. However, certain ceramic oxides of iron called ferrites have been developed[8] which possess very square hysteresis loops, without the use of any conscious alignment mechanism whatsoever(see Figure 1-3). It is these materials, called square B-H looped ferrites, which are investigated in this paper.

Although ferrites have been developed with very high maximum squareness ($R_s > 0.9$), there are basic improvements which, if made, would increase the applicability of these materials. Losses and high excitation still severely limit the use of these materials in high-speed circuitry having low power levels. Efforts to meet this problem have produced theories concerning both the square B-H loop[9] and the dynamics of the mechanism of flux reversal.[10]

When a material is saturated in a given direction, domain walls have been eliminated, and the material is effectively one single domain.

A-61505

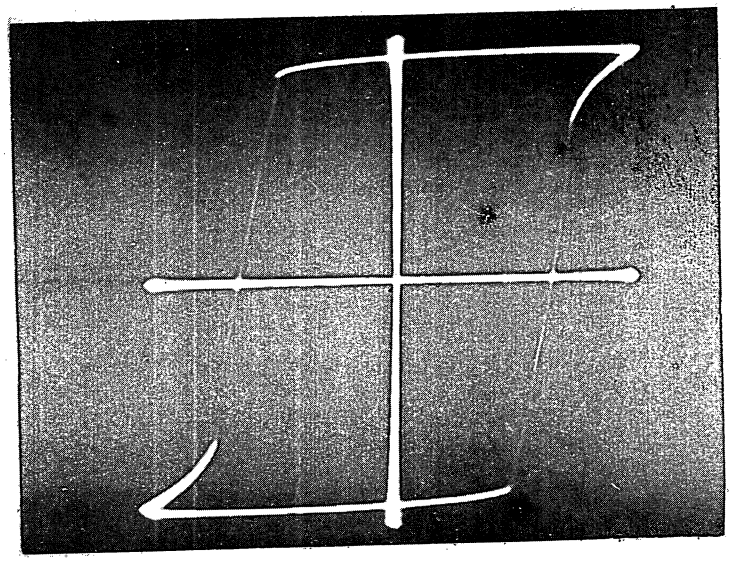

SATURATION LOOP

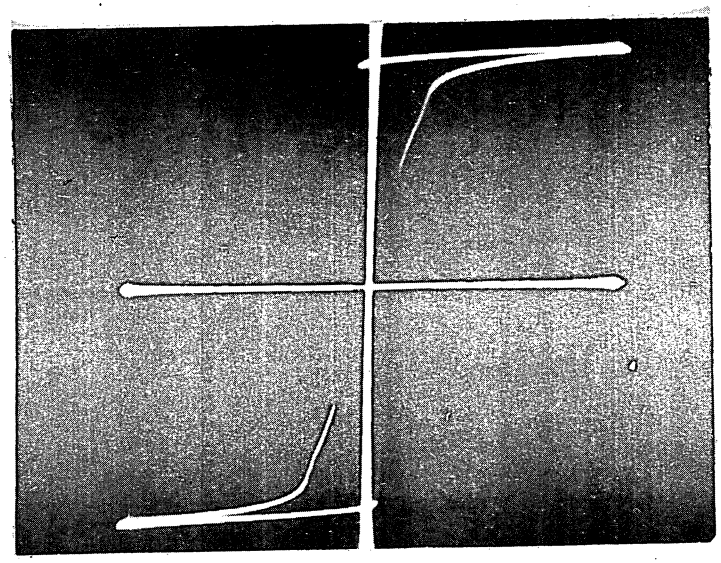

MAXIMUM SQUARENESS LOOP

NOTE:
THE DIMENSIONS OF BOTH LOOPS
HAVE BEEN NORMALIZED

FIG. 1-3

TYPICAL HYSTERESIS LOOPS FOR SQUARE-LOOPED FERRITES

Therefore, at the remanent state of very square-looped materials, domain walls may not be in existence. Domains of reverse magnetization must be first nucleated in this case before a flux reversal is possible. The square B-H loop observed for single crystals or pseudosingle crystals is thus obtained when both nucleation of domains of reverse magnetization and all domain-wall motion are restricted to a single threshold field, above which the created domain walls move throughout the material producing a sudden flux reversal. The square B-H loop may therefore be explained in terms of a nucleation model, whereby nuclei of domains of reverse magnetization form at grain boundaries. There are essentially three important energy relations which determine the critical external field at which nucleation would occur.

1. Free magnetic-pole energy density at a grain boundary is produced by the grain-to-grain misalignment of the directions of the magnetization of any two adjacent grains. This free-pole energy is the result of the demagnetizing fields which are in opposition to the magnetic moments producing them.

2. Domain-wall energy must be considered, since in the formation of a nucleus of reverse magnetization a domain wall must be created. Since there is a rotation of magnetic moments within a domain wall against the anisotropy and exchange energies, the energy of the system considered is directly increased by an increase in the total domain-wall area.

3. Magnetic-energy density is $(-\vec{B}\cdot\vec{H}/4\pi)$, where a positive direction of field is defined as that favoring a complete flux reversal. Therefore, the formation of a nucleus of reverse magnetization would reduce the total energy. The total effective field is a sum of the applied field and the demagnetizing field due to free poles.

At the value of the applied field for which a nucleation of reverse magnetization becomes energetically more favorable in terms of the sum of the three energies involved, a nucleus would form to reduce the total configuration energy. If nucleation occurs at a field which is greater than the threshold field for domain-wall motion, domain-wall motion will produce a complete flux reversal without a further increase in the applied field. This then is the condition that must be fulfilled to have a square B-H loop according to the model employed; it has been expressed in terms of fundamental parameters: $L(\omega^*)^2 < 60\,\sigma_\omega$, where L is a mean grain diameter, ω^* is the grain-surface pole density, and σ_ω is the energy per unit area of a 180° domain wall. The grain-surface pole density $\omega^* = I_s(\cos\theta_1 - \cos\theta_2)$, where I_s is the saturation moment and the $(\cos\theta_1 - \cos\theta_2)$ term is a measure of the grain-to-grain alignment of the magnetization which approaches zero for complete grain-to-grain alignment.

In the case of high grain-to-grain alignment of the magnetization, ω^* is reduced to an extremely low value, and a square loop is produced. If the saturation moment of a material is sufficiently low, the condition for squareness might be fulfilled if each crystallite was magnetized along the easy direction of magnetization nearest to the direction of the applied field. This is the tentative explanation given to the phenomenon of the square B-H loop ferrites.

It should be noted with respect to this theory for B-H loop squareness that the maximum squareness for a material is not a saturation loop. In a nonsaturation loop there are domains of reverse magnetization as an initial condition. Therefore, to apply the nucleation theory to this case, it was tacitly assumed that the domain walls present

at the initial state are frozen in their position by grain boundaries, voids, etc., and therefore do not participate in the flux reversal over the nonsaturation B-H loop being considered. This assumption may or may not be a valid one. If the assumption is not valid, the theory as presented is not applicable.

The force on a unit surface of a 180° domain wall is $HB_s \cos \theta/2\pi$, where θ is the angle between the magnetization and the field. In the case of high grain-to-grain alignment of the magnetic moments $\cos \theta \simeq 1$ for all crystallites. Therefore, the force on all domain walls would essentially be the same value, and when the threshold of domain-wall motion is reached, a complete flux reversal would occur over a small increment of applied field, producing a square B-H loop. For this mechanism to prevail, the threshold field for all the walls participating must be the same. Therefore, regardless of the mechanism involved, it may be stated that a grain-to-grain alignment of the magnetic moments within a polycrystal is the most important single condition that produces B-H loop squareness.

The square B-H loop materials used in computer-storage devices must have a response to low-pulse excitation that has a duration in the order of microseconds.[8] Therefore, it is desirous to minimize both the time for flux reversal in these materials and the necessary pulse excitation to produce this flux reversal. A theory of the flux-reversal mechanism in polycrystalline materials has been advanced[10] using the model of expanding cylindrical domains of reverse magnetization. The shape of the voltage response of a polycrystalline ferrite to pulse excitation can be explained mainly on the basis of the change in effective domain-wall area. A figure of merit for the magnetization reversal is

defined as the switching coefficient $S_w = (H_m - H_o)\tau$, where τ is the time required to reverse the magnetization, H_m is the applied magnetic field, and H_o is the threshold-field value at which the average domain-wall velocity is zero.

The equation of motion of a cylindrical 180° domain wall has been derived in Appendix I. Since the effective mass of a domain wall is very low, the complete equation of motion can be expressed in a simplified form:

$$\beta\dot{\rho} + \frac{3}{2}\alpha\rho + \frac{\sigma_w}{\rho} = 2H_m I_c \cos\theta,$$

where ρ is the radius of the cylindrical domain wall, σ_w is the domain-wall energy surface density, β is the viscous damping coefficient which is proportional to σ_w, α is the stiffness coefficient, H_m is the applied field, I_s is the saturation moment, and θ is the angle between H_m and I_s. Rewriting the equation of motion one obtains the following relationship:

$$\beta\dot{\rho} = 2(H_m - H_o)\, I_s \cos\theta, \text{ where } H_o = \left(\frac{\sigma_w}{\rho} + \frac{3}{2}\alpha\rho\right)/2I_s \cos\theta.$$

The switching time $\tau = d/v$, where d is an average distance a domain wall travels in the time τ and v is the average wall velocity. Therefore, the coefficient $S_w = (H_m - H_o)\,\tau$ can be shown to be $S_w = \frac{\beta d}{2I_s \cos\theta}$.

The switching coefficient S_w has been measured on both metals and ferrites. The switching coefficient is low ($S_w \simeq 0.4$ oe-μsec for metallic tapes) because of the high saturation moment and high grain-to-grain alignment of the magnetic moments in these materials. $S_w \simeq 1$ oe-μsec for most ferrites. Therefore, in this respect, present square B-H ferrites are inferior to metals.

C. The Specific Problem

The importance of grain-to-grain orientation of the magnetization has been shown for both metals and ferrites. Therefore, it is possible that the moments in square B-H loop ferrites could be given a grain-to-grain alignment by some internal mechanism. The crystalline anisotropy can produce a partial alignment when the magnetic moments lie along directions of easy magnetization nearest to the direction of the field. However, any internal mechanism producing a greater alignment must be the result of either an orientation of the crystallites or the influence of magnetostriction.

Since there is no apparent alignment of the crystallites, a study of the polycrystalline magnetostriction of a compositional series in the system containing square-looped ferrites has been made. The customary methods of measuring magnetostriction in ferrites would not be valid, if an alignment does exist. Therefore, a different experimental technique has been used which permits meaningful data to be obtained. The polycrystalline magnetostriction data has been analyzed in terms of a model for the polycrystal which permits a qualitative interpretation of both the single-crystal magnetostriction and the degree of grain-to-grain alignment within the material.

Large magnetostriction effects have been observed in some ferrites possessing nonsquare B-H loops. However, when this investigation was initiated, there had not been any systematic investigation of magnetostriction in ferrites possessing square B-H loops. Since the initiation of this work, others have published a paper which reports magnetostriction data obtained on a compositional series of ferrites which possess varying hysteresis-loop squareness.[11] The experimental data

that is reported is compatible with the results of this work; however, the conclusions are completely different from those of this investigation. A critique of the work has therefore been necessary.

CHAPTER II

COMPOSITIONAL SURVEY

An extensive investigation by M.I.T.'s Lincoln Laboratory concerns the compositional effect on the square B-H loop properties of ferrites. Many compositional systems have been investigated; however, the most significant and complete data were collected on the two systems that will be discussed.

It seems advisable to mention briefly at this point some of the difficulties involved both in controlling and in determining the chemistry of these materials. In most compositions that have been considered, both manganese and iron ions exist in the same structure. Both of these elements are multivalent. In the process of making polycrystalline ferrites, it is necessary to sinter the material at a temperature of 1350 C to 1450 C. At these temperatures there is an oxidation of some of the Mn^{+2} ions to Mn^{+3} to give Mn_3O_4 and a reduction of some of the Fe^{+3} ions to Fe^{+2} ions to give Fe_3O_4 in solid solution with the original ferrite.

Since Mn_3O_4 is, by itself, tetragonal, an excessive amount of this component may cause a precipitation of a second phase. If Fe^{+3} ions are not reduced simultaneously with the oxidation of the Mn^{+2} ions, there may be an excess of Fe^{+3} which is precipitated out as $\alpha - Fe_2O_3$. Both a second phase and the presence of Fe_3O_4 are undesirable in these materials. The second phase would produce demagnetizing fields within the material, tending to inhibit a square B-H loop. The high conductivity of Fe_3O_4 makes the presence of this component undesirable. Further, even if a second phase is not formed, the oxidation process takes place more readily

near an exposed surface. Therefore, as one goes into the material from the surface, there is a compositional change due to a change in the amount of oxidation that has taken place; thus air sintering produces inhomogeneous products. Homogeneity may be improved, however, by annealing the products in an inert atmosphere after sintering. This anneal appears to reduce most of the Mn^{+3} ions back to Mn^{+2} ions without appreciably affecting the iron valencies.

Not only is it difficult to control the valence of the Mn and Fe ions, but it is also difficult (impossible at present) to ascertain the actual valence of these ions in the final product. This is again due to the fact that both of these elements are multivalent, and present methods of analysis do not permit determination of the valencies when two multivalent ions are present. The total amount of each element can be determined and agrees with the as-mixed components. Therefore, it is only possible to express the compositions in a simplified form; it is recognized that this simple case does not actually exist.

The first compositional system to be considered may be expressed in terms of the following general formula:

$$(MgOFe_2O_3)_{(1-\alpha)(1-\gamma)} + (MnOFe_2O_3)_{\alpha(1-\gamma)} + (Mn_3O_4)_{\gamma},$$

where the compositional parameters α and γ can vary from 0 to 1. $MgOFe_2O_3$ is magnesium ferrite, $MnOFe_2O_3$ is manganese ferrite and Mn_3O_4 is called hausmannite. Therefore, in this system Mn_3O_4 is being added to a mixed stoichiometric mixture of Mg and Mn ferrite. Both Mg ferrite and Mn ferrite are magnetic and have a cubic spinel structure. On the other hand, Mn_3O_4 is paramagnetic and has a tetragonal spinel structure.

The other compositional system is quite similar in its general formula: $(MgOFe_2O_3)_{(1-\beta)(1-\gamma)} + (ZnOFe_2O_3)_{\beta(1-\gamma)} + (Mn_3O_4)_{\gamma}$, where β and γ are

compositional parameters which can vary between 0 and 1. This system differs in that zinc ferrite, $ZnOFe_2O_3$, has replaced the manganese ferrite and the parameter β has replaced α. Zinc ferrite is paramagnetic and has a cubic spinel structure.

Maximum B-H loop squareness, R_s, has been plotted in Figure 2-1 as a contour map with γ as the ordinate and with α and β as the abscissae for the right and left sides, respectively. It is apparent from this figure that R_s is mainly a function of the parameter γ with an optimum occurring for any fixed α or β at $\gamma \simeq 0.15$. Starting from the line $\alpha = 0$, an increase in α increases the magnitude of R_s and broadens the influence of γ up to about $\alpha = 0.3$. For $0.3 \leqslant \alpha \leqslant 1$, the contour map is essentially a broad plateau with a small singular peak for $\alpha \simeq 0.6$ and $\gamma = 0.15$. The influence of β is very similar to the effect of α; the paramagnetic character of zinc ferrite, however, dilutes the magnetic exchange to reduce the Curie point T_c to room temperature or below for $\beta \geqslant 0.65$.

Although the Mn ions of Mn_3O_4 have large magnetic moments, the moments of some ions apparently do not interact with the other magnetic moments in the crystal structure. Therefore, T_c and room-temperature B_s decrease as γ increases beyond a critical value. As α is increased, T_c and the room-temperature B_s both increase because of the large magnetic moment of Mn ferrite. On the other hand, as β is increased, the paramagnetic Zn ferrite dilutes the magnetic-exchange forces and eventually reduces T_c below room temperature. The saturation moment, however, is increased as β increases to $\beta \simeq 0.45$ because of a displacement of Fe^{+3} ions to different crystallographic positions.

Since B-H loop squareness is the main concern in this investigation, it was decided to give first priority to a study of the effect of the

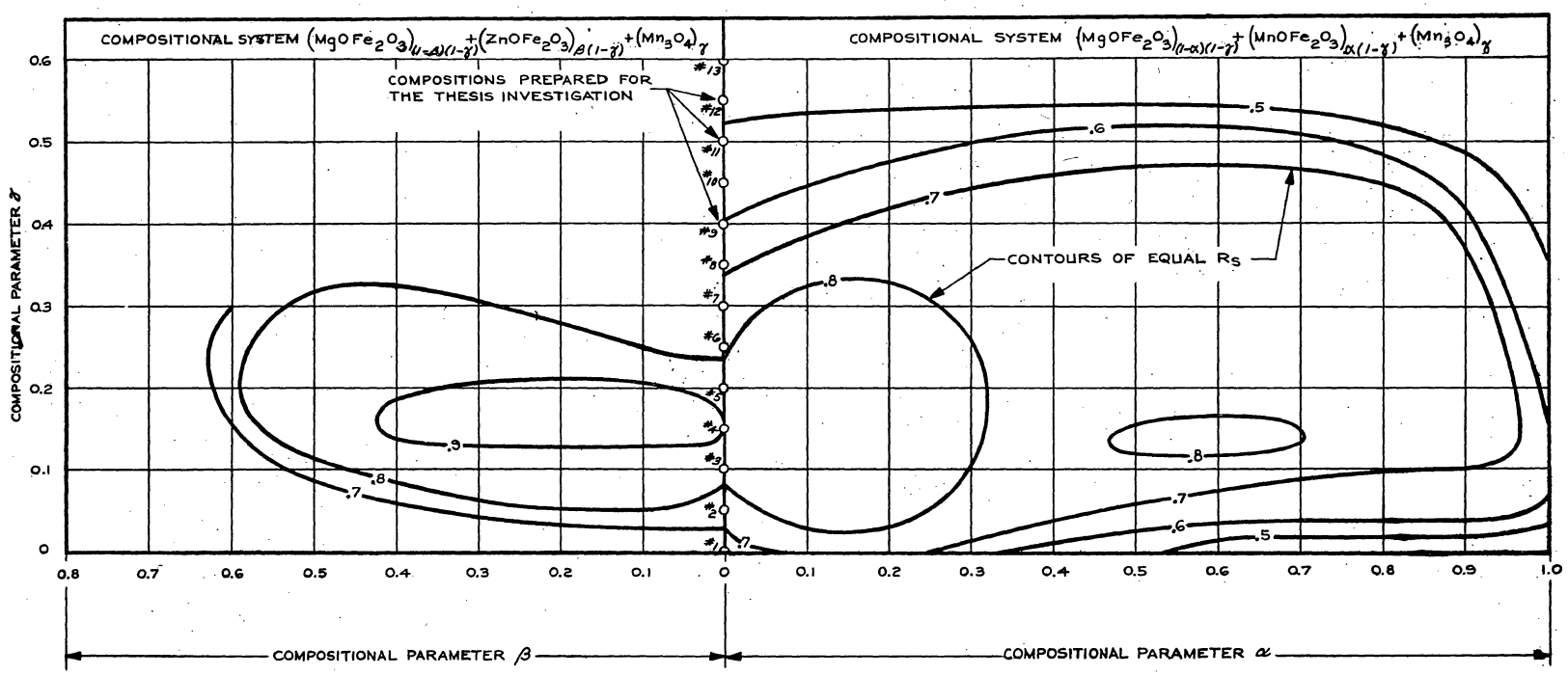

FIG. 2-1

MAXIMUM B-H LOOP SQUARENESS (R_S) AS A FUNCTION OF COMPOSITION

parameter γ; a study of the effect of the parameters α and β was left to later investigation. Therefore, the common boundary between the two ternary systems discussed, the binary system $(MgOFe_2O_3)_{1-\gamma}(Mn_3O_4)_{\gamma}$, was selected for study. Thirteen compositions were selected in which γ varies from 0 to 0.6 in steps of 0.05.

CHAPTER III

MAGNETOSTRICTION

A. Single-Crystal Phenomenon

The phenomenon of magnetostriction was first observed by Joule[12] in 1842. Magnetostriction is the name given to the change in size and shape of a material as influenced by its magnetization. A phenomenological expression for magnetostriction has been derived by Becker and Döring;[13] nevertheless, little is known concerning the actual physical mechanism causing the phenomenon. However, calculations of Van Vleck[14] concerning the crystalline anisotropy and those of Vonsovsky[15] concerning magnetostriction indicate that both of these phenomena depend strongly on the spin-orbit coupling of the magnetic ions. The orbital angular momentum of the electron configuration in each magnetic ion is usually strongly related to the crystalline structure in which the ion is located. The magnetic moment of an ion is determined almost entirely by its spin angular momentum. Hence it is quite understandable that if there is a spin-orbit coupling, the magnetization is influenced by the crystalline structure, and conversely the crystalline structure is influenced by the magnetization.

A brief and simplified outline of the derivation of the single-crystal-magnetostriction equation, as given by Kittel,[3] will be given to acquaint the reader with the principles involved. Since the magnetostriction is so closely associated with the crystalline anisotropy, it can be formally considered as the strain dependence of the crystalline anisotropy. The free energy in any physical system must be a minimum for stable equilibrium. Therefore, for a material in zero effective field, the total of the sum of the following three energy densities must be

a minimum: (1) elastic-energy density U_e, (2) anisotropy-energy density U_A, and (3) magnetoelastic energy U_c.

The elastic-energy density, U_e, is due to physical deformations of the crystal lattice and the associated stresses involved. U_e can be expressed generally as $U_e = 1/2 \sum_{nm} C_{mn} e_m e_n$, where the C_{mn} are the moduli of elasticity and the e_m or e_n are the strain coefficients describing the distortion of the crystal lattice.[16] If the symmetry property of the C_{mn} matrix elements and the symmetry properties of the cubic-crystal lattice are used, the expression for U_e can be greatly simplified to the following form:

$$U_e = \frac{1}{2} C_{11}(e_{xx}^2 + e_{yy}^2 + e_{zz}^2) + C_{12}(e_{xx}e_{yy} + e_{yy}e_{zz} + e_{zz}e_{xx}) + \frac{1}{2} C_{44}(e_{yz}^2 + e_{zx}^2 + e_{xy}^2).$$

Because of the symmetry of the cubic lattice, the anisotropy-energy density U_A can be expressed, to first order, in the following form:

$$U_A = K (\alpha_1^2\alpha_2^2 + \alpha_1^2\alpha_3^2 + \alpha_2^2\alpha_3^2),$$

where K is the anisotropy coefficient and the α_i are the direction cosines of the magnetization direction relative to the crystalline cubic axes.

The magnetoelastic energy expresses the coupling between the magnetic and elastic phenomena and is therefore the energy term from which the magnetostriction is derived. If the change in volume is neglected, this energy can be expressed, to first order approximation, as

$$U_c = B_1(\alpha_1^2 e_{xx} + \alpha_2^2 e_{yy} + \alpha_3^2 e_{zz}) + B_2(\alpha_1\alpha_2 e_{xy} + \alpha_2\alpha_3 e_{yz} + \alpha_3\alpha_1 e_{zx}),$$

where B_1 and B_2 are called magnetoelastic coupling coefficients.

In an unconstrained system, the equilibrium value of the strain components for any direction of magnetization can be determined from the condition

$$\frac{\partial [U_e + U_A + U_c]}{\partial e_{ik}} = 0.$$

It should be noted that, if constraints are present, the α_i's are functions of the strain components e_{ik}, and U_A enters explicitly into the problem. Thus e_{ik} is found as a function of the direction cosines α_i.

The relative change in length $\delta\ell/\ell$ in a direction determined by the direction cosines β_i can be expressed as a function of the strain components: $\left(\frac{\delta\ell}{\ell}\right)_{\alpha_i\beta_i} = \sum_k e_{ik}\beta_i\beta_k$. Therefore, by substitution of $e_{ik}(\alpha_i)$ in the expression for the relative change in length, the equation for first-order single-crystal magnetostriction is found:

$$\frac{\delta\ell}{\ell} = \frac{3}{2}\lambda_{100}(\alpha_1^2\beta_1^2 + \alpha_2^2\beta_2^2 + \alpha_3^2\beta_3^2 - \frac{1}{3}) \qquad (3\text{-}1)$$

$$+ 3\lambda_{111}(\alpha_1\alpha_2\beta_1\beta_2 + \alpha_1\alpha_3\beta_1\beta_3 + \alpha_2\alpha_3\beta_2\beta_3),$$

where $\lambda_{100} = -\frac{2B_1}{3(C_{11}-C_{12})}$, $\lambda_{111} = -\frac{B_2}{3C_{44}}$, the α_i are the direction cosines of the magnetization, and the β_i the direction cosines of the measuring direction. By the insertion of a constant term, the $-1/3$ in the coefficient of λ_{100}, Equation 3-1 has arbitrarily been expressed so that $\frac{\delta\ell}{\ell} = 0$ for a completely random distribution of the α_i and β_i. When the magnetization is along one of the cubic axes, the $\langle 100\rangle$ direction, then $\alpha_1 = 1$, $\alpha_2 = \alpha_3 = 0$ and Equation 3-1 reduces to

$$\frac{\delta\ell}{\ell} = \frac{3}{2}\lambda_{100}(\beta_1^2 - \frac{1}{3}). \qquad (3\text{-}2)$$

Similarly when the magnetization is along a $\langle 111\rangle$ direction $\alpha_1 = \alpha_2 = \alpha_3 = \frac{1}{\sqrt{3}}$ and Equation 3-1 reduces to

$$\frac{\delta\ell}{\ell} = \lambda_{111}(\beta_1\beta_2 + \beta_1\beta_3 + \beta_2\beta_3). \qquad (3\text{-}3)$$

Similar expressions for $\frac{\delta\ell}{\ell}$ in terms of the α_i are also found for the cases where the direction of measurement is known and is along first the $\langle 100\rangle$ direction and then along the $\langle 111\rangle$ direction. Therefore, the reason for the use of λ_{100} and λ_{111} for the magnetostriction coefficients becomes apparent.

The coefficients λ_{100} and λ_{111} vary considerably from one material to another, both in magnitude and sign. A few typical examples are given below:

Material	$\lambda_{100} \times 10^6$	$\lambda_{111} \times 10^6$
Iron	+19.5	-18.8
Nickel	-46	-25
Magnetite [24]	-19.4	+86.4
Nickel ferrite [17]	-36	-4
Cobalt ferrite [17]	-515	+45

A positive sign indicates an expansion and the negative sign a contraction in the direction considered. For example, if iron was magnetized along a $\langle 100 \rangle$ direction the material would elongate in the direction of magnetization and if magnetized along a $\langle 111 \rangle$ direction it would contract in the direction of magnetization. Equation 3-1 indicates that the magnetostriction is a function only of the direction of magnetization. This is true for most materials at low fields, but at high fields the linear magnetostriction is effected through a volume change due to the high fields. This effect due to high fields is usually so small that it can be neglected.

B. Polycrystalline Phenomena

Since the square B-H loop ferrites are polycrystals, it is desirable that a model be constructed which can utilize the single-crystal magnetostriction formalism. This would permit evaluation of polycrystalline magnetostriction data in terms of the single-crystal phenomenon. In the selected model a polycrystal is considered an ensemble of single crystallites, and crystallites are assumed to possess single-crystal magnetostriction characteristics and differ only in their relative crystallographic orientations. In order to construct a relationship between the

polycrystalline behavior and that for the single crystal, the simplifying assumptions stated below are necessary.

1. A macroscopic strain measured on the polycrystal in a given direction can be expressed as a simple summation of the strains in the crystallites along that direction. Experimentally, it is known that this is a reasonable assumption. It should be noted that the volume change neglected in the single-crystal formalism still holds for this polycrystalline model.

2. The distribution of crystallite orientations within the polycrystal is usually not known. In sintered ferrites it is reasonable to assume a random distribution of these crystallites.

3. Since the material as a whole is not mechanically constrained, each crystallite can be considered as without constraints. This assumption can be justified as a first approximation provided that the fraction of the total magnetoelastic energy which influences the magnetic-moment direction in crystallites is small. This condition can be reasonably fulfilled when the total magnetoelastic energy is large with respect to the crystalline anisotropy energy K. This condition can also be fulfilled when the magnetic moments are aligned by a saturating external field. However, when this condition is not fulfilled, the magnitude of the macroscopic strain would be reduced, since constraints would then be placed upon each crystallite of sufficient magnitude to inhibit strains due to magnetostriction.

4. The distribution of the magnetic moments within the polycrystal is, in most cases, not known and must be assumed. It is this assumption that must be given careful consideration for each situation.

One of the few cases for which the distribution of magnetic moments is known is the case of magnetic saturation of the polycrystal. Therefore, if the measurement is in a direction parallel to the saturation direction, $\alpha_i = \beta_i$ in each crystallite, and Equation 3-1 can be reduced to the following form:

$$\frac{\delta \ell}{\ell} = \lambda_{100}\left[1 + 3(\varepsilon - 1)\left(\beta_1^2\beta_2^2 + \beta_1^2\beta_3^2 + \beta_2^2\beta_3^2\right)\right], \qquad (3\text{-}4)$$

where $\varepsilon = \lambda_{111} / \lambda_{100}$. The average macroscopic magnetostriction which is measured in a polycrystal parallel to the direction of the saturating field, when the saturating field is applied, is obtainable from Equation 3-4 by averaging the direction cosines β_i over all crystallographic directions. Actually it is the direction of crystallite orientation which should be averaged. Since a random distribution of crystallite orientation has been assumed, the average over-all single-crystal directions without a weighting function is justified. The averaged cosine term of Equation 3-4 is $\overline{\left(\beta_1^2\beta_2^2 + \beta_1^2\beta_3^2 + \beta_2^2\beta_3^2\right)} = \frac{1}{5}$.

Equation 3-4 may now be written as an averaged magnetostriction:

$$\overline{\left(\frac{\delta \ell}{\ell}\right)} = \overline{\lambda}_{\parallel(S)} = \frac{(3\varepsilon + 2)}{5}\lambda_{100} \qquad (3\text{-}5)$$

The average magnetostriction coefficient $\overline{\lambda}_{\parallel(S)}$ is an isotropic quantity for a polycrystal regardless of the orientation of the sample. For the case of an isotropic magnetostriction, a simple angular dependence exists for the first-order change in length at any angle θ from the saturation direction:

$$\frac{\delta \ell}{\ell} = \frac{3}{2}\overline{\lambda}_{\parallel(S)}\left(\cos^2\theta - \frac{1}{3}\right). \qquad (3\text{-}6)$$

Other simplifying cases of the distribution of magnetic moments within a polycrystal are the cases when all the moments in the individual crystallites are along either the $\langle 100 \rangle$ or $\langle 111 \rangle$ direction nearest to

a specified direction in the polycrystal. In these cases Equation 3-1 reduces to Equations 3-2 and 3-3, respectively, for the individual crystallites:

$$\frac{\delta l}{l} = \frac{3}{2}\lambda_{100}\left(\beta_1^2 - \frac{1}{3}\right) \qquad (3\text{-}2)$$

$$\frac{\delta l}{l} = \varepsilon\,\lambda_{100}(\beta_1\beta_2 + \beta_1\beta_3 + \beta_2\beta_3) \qquad (3\text{-}3)$$

The averaging of the direction cosines β_i in these equations should not be taken over all crystallographic directions since the distribution of the direction of magnetization among the equivalent directions specified is not isotropic. Equation 3-2 has been appropriately averaged by Becker and Döring:[13]

$$\overline{\left(\frac{\delta l}{l}\right)} = \bar{\lambda}_{\parallel(100)} = \frac{\sqrt{3}}{\pi}\lambda_{100} = 0.55\,\lambda_{100}, \qquad (3\text{-}7)$$

where the symbol $\bar{\lambda}_{\parallel(100)}$ is the macroscopic magnetostriction of a polycrystal when the individual moments of the crystallites are along the $\langle 100\rangle$ direction nearest to a reference direction in the polycrystal and the direction of measurement is parallel to this reference direction. Equation 3-3 has been appropriately averaged in Appendix B:

$$\overline{\left(\frac{\delta l}{l}\right)} = \bar{\lambda}_{\parallel(111)} = \frac{2}{\pi}\,\varepsilon\,\lambda_{100} = 0.64\,\varepsilon\,\lambda_{100}, \qquad (3\text{-}8)$$

where $\varepsilon = \dfrac{\lambda_{111}}{\lambda_{100}}$. The symbol $\bar{\lambda}_{\parallel(111)}$ has the same meaning as $\bar{\lambda}_{\parallel(100)}$ except for the difference in the direction of magnetization of the individual crystallites.

The parameter $\varepsilon = \dfrac{\lambda_{111}}{\lambda_{100}}$ is a measure of the anisotropy of the single-crystal magnetostriction. Therefore, the macroscopic magnetostriction of a polycrystal as a function of field is dependent on both the angular distribution of the magnetic moment of the crystallites and the parameter ε. The isotropic case is that for which $\varepsilon = 1$. In the

isotropic case the polycrystalline magnetostriction is a function of only the $\overline{(\cos^2\theta)}$ where θ is the angular relationship between individual magnetic moments and the direction of measurements. However, when $\varepsilon \neq 1$, the magnetostriction of a polycrystal cannot have a simple interpretation in terms of the directions of magnetization within the material.

Since in the general expression for the single-crystal case two constants are involved, λ_{100} and ε, these constants can theoretically be determined from polycrystalline data if two independent distributions of the magnetic moments are actually known. Magnetic saturation is one case where the distribution is known. For this case Equation 3-5 gives the expression $\overline{\lambda}_{\parallel (S)}$ for the magnetostriction parallel to the saturation direction.

If the effective domain anisotropy $K_d > 0$ and large, then $\overline{\lambda}_{\parallel (100)}$ could be measured parallel to the direction of saturation when the saturating field has been removed. Similarly if $K_d < 0$ and large, then $\overline{\lambda}_{\parallel (111)}$ could be measured parallel to the direction of saturation when the saturating field is removed. Therefore, if either of these cases exists and the material can still be saturated so as to measure $\overline{\lambda}_{\parallel (S)}$, the constants λ_{100} and ε can be determined. However, in most polycrystalline materials little is known about the actual domain configuration at H = 0. Although λ_{100} cannot, in general, be determined from polycrystalline measurements, an analysis of the observed data in terms of the idealized situations mentioned can be quite relevant concerning the qualitative influence of λ_{100} and ε. An analysis of this sort will be made in this paper concerning the experimental data.

CHAPTER IV

EXPERIMENTAL METHODS

A. Critique of Present Methods

The concepts expressed in Chapter III have been known for some time. However, much magnetostriction data presently available should be critically examined as to its meaning on the basis of the experimental technique employed. Most existing experimental data on ferrites has been obtained on long-bar samples or long ellipsoids of revolution,[18] and some data have been obtained from toroidal samples.[19] In the case of long-rod samples or ellipsoids, the external magnetic field has been applied in only one direction, along the long axis of the specimen, and the magnetostrictive strain measured on only the long dimension. For the case of toroidal samples a circumferential field is applied and the magnetostrictive strain measured on a diameter of the toroid. These methods are essentially the same, except that for the case of the toroid there is not the demagnetizing field which is present for the rod and ellipsoidal samples.

The magnetostrictive strain as measured by the techniques just mentioned is plotted versus the applied field as the field is increased from zero to a saturating value. The major criticism that can be made of this method is that it makes the arbitrary assumption of zero magnetostriction at zero field. The zero for the derived magnetostriction for a single crystal is arbitrary (see Chapter III); this arbitrary zero reference is held throughout the derivation for polycrystalline magnetostriction and cannot be assumed to occur at zero fields it must be established experimentally before data can be meaningful.

As shown in Chapter III, the polycrystalline magnetostriction is dependent upon the distribution of magnetic moments throughout the material. The zero reference at zero field for polycrystalline magnetostriction corresponds to a completely random, or isotropic, distribution of the magnetic moments. The assumption that a random distribution of the magnetic moments exists at a zero field can be justified for some materials. However, for the general case, and especially for materials possessing a square hysteresis loop and therefore a high remanent-flux density, this assumption is not valid.

If the assumption of an initially random distribution is not valid, the magnetostriction at zero field along a measured direction could be highly positive or negative, depending on the actual distribution of the moments and the values of the single-crystal constants λ_{100} and ε. Therefore, it is conceivable that a saturation magnetostriction as determined by these methods could not only be incorrect in magnitude but also in sign.

Another point should be made concerning the way in which the applied field is controlled. Some workers using long-rod samples have reported the magnetostrictive strain as a function of the applied field which is directed along the axis of the specimen and then reversed.[20] In general, the flux reversal of most materials at low fields is accomplished both by a rotation of the magnetic moments and by the motion of domain walls. In fact, for most materials possessing a square hysteresis loop, 180° domain-wall motion unquestionably plays a major role in the flux reversal. Magnetostriction is dependent on the angular orientation of the magnetic moment and not on the polarity of the moment. The motion of 180° domain walls, however, serves just to change the polarity

of the magnetic moment and does not produce any magnetostriction effects. Although the magnetization goes through zero in a flux reversal due to 180°-wall motion, the magnetostriction does not. The assumption of zero magnetostriction at zero field, or even at demagnetization, is clearly not justified in these measurements.

It must be concluded that any assumptions concerning a zero reference for the magnetostriction at zero field would not be valid for the general case, and especially for materials possessing a square hysteresis loop. The zero reference must be experimentally established.

B. Technique Employed

In view of the criticism that can be made of the usual techniques for obtaining magnetostriction in ferrite in general, and especially ferrites possessing square B-H loops, a somewhat different method was used by the author. The technique that was used employed thin-disc samples approximating an oblate spheroid. The magnetostrictive strain was measured along a fixed diameter as shown, and the saturating field was applied in the plane of the disc (Figure 4-1).

It has been shown in Chapter III that the magnetostriction for a saturated polycrystal can be expressed in the following form:

$$\frac{\delta \ell}{\ell} = \frac{3}{2} \overline{\lambda}_{11_{(S)}} (\cos^2 \theta - 1), \qquad (4\text{-}1)$$

where θ is the angle between the direction of measurement and the direction of the saturation moment. Therefore, rotation of the sample in a saturating field, as shown in Figure 4-1 would produce just the magnetostrictive strain in the measured direction which is given by Equation 4-1. Measurement of the strain for $\theta = 0$ and $\theta = \frac{\pi}{2}$ provides both a measurement of $\overline{\lambda}_{11_{(S)}}$ and a determination of the zero reference for additional magnetostriction data. Essentially the same method has been used

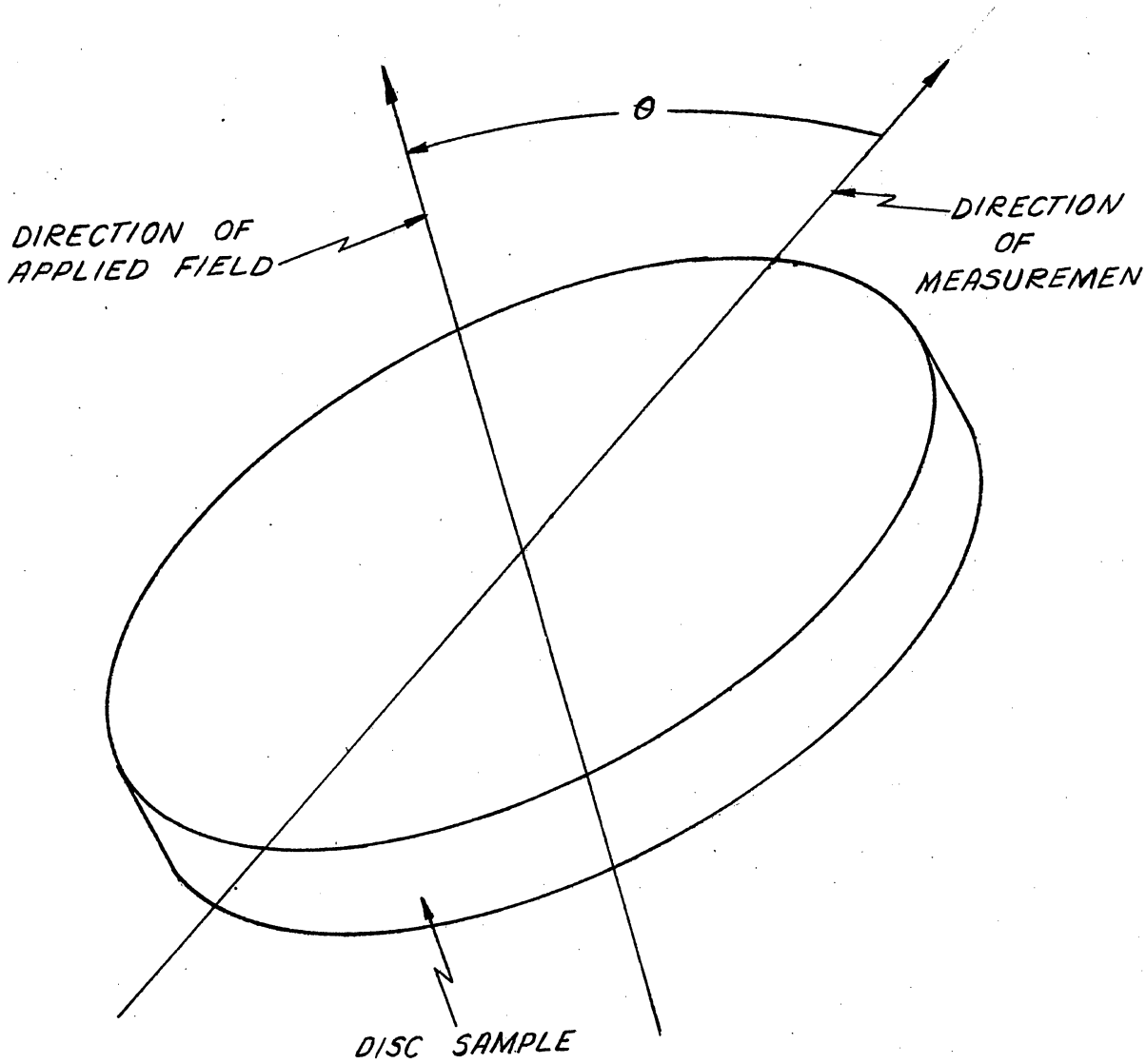

FIG. 4-1

DISC SAMPLE IN MAGNETIC FIELD

A-61495

by others for the determination of $\lambda_{11(S)}$ for metals[18,21] but is not known to have been applied to ferrites.

Magnetostriction data has also been obtained as a function of the applied field. Considerable care has been exercised in order to obtain meaningful data. Most magnetostriction data is obtained by changing the field from zero to the desired value and recording the accompanying strain in the direction of the applied field. However, for low fields there is little possibility that the direction of measurement is actually an axis of symmetry for the angular configuration of the magnetic moments within the material. Therefore, in this paper magnetostriction data has been obtained for the case of changing the field to the desired value from the saturation value as a reference. Thus the direction of the saturating field becomes an axis of symmetry for the angular configuration of the magnetic moment regardless of the field applied. These data in conjunction with the zero reference determined as above provide data which can be given a fundamental interpretation.

C. Equipment

The magnetostrictive strain of most materials is extremely small and is a relative change of the order of 10^{-6}. To measure this strain, some workers have used a mechanical-optical system.[18] Goldman[21] and others have utilized resistance-wire strain gages for this purpose. These strain gages are made by the Baldwin-Lima-Hamilton Corporation; they have been found to be extremely reliable and do not require individual calibration. Therefore, because of the ease of measurement, resistance-wire strain gages were used for this investigation. A typical strain gage is shown in Figure 4-2. The gage consists of a fine grid of constantan wire which when placed in intimate contact with a material is

A-61503

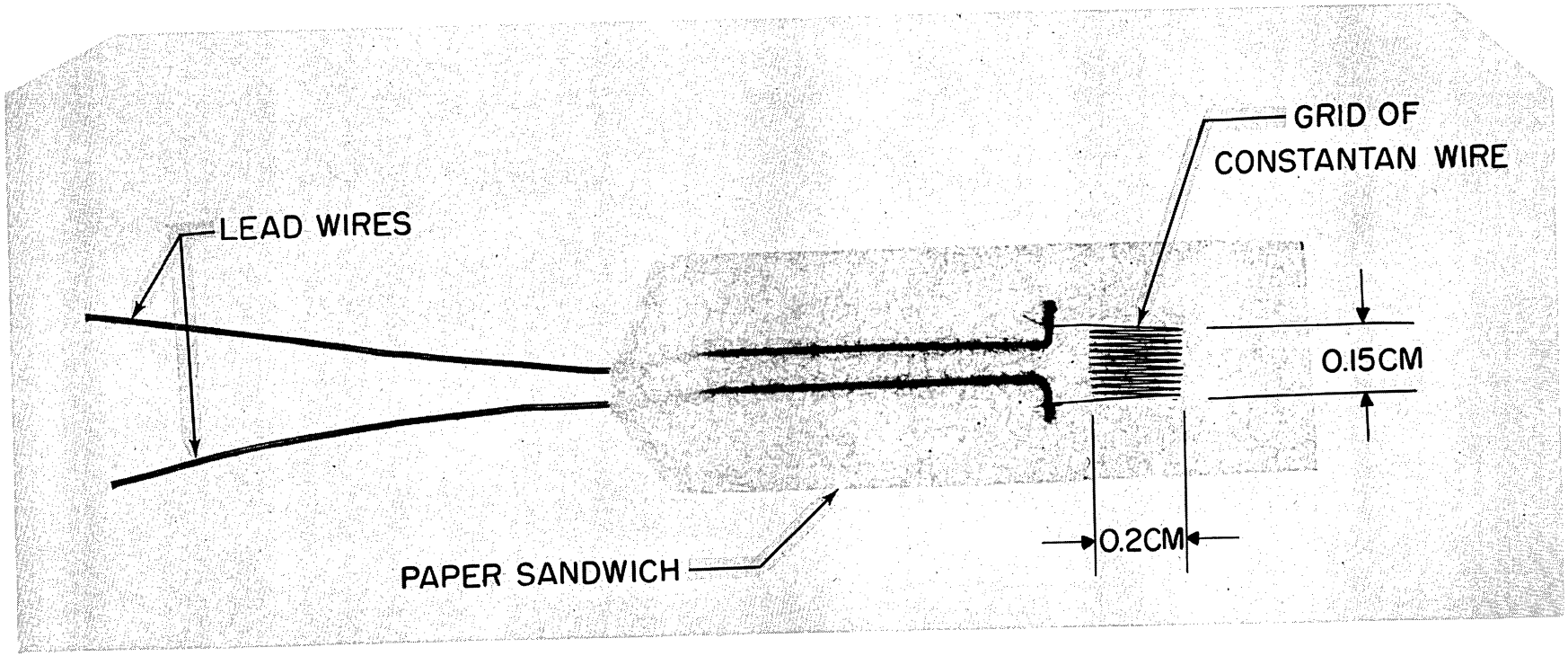

FIG 4-2

RESISTANCE-WIRE STRAIN GAGE

(BALDWIN-LIMA-HAMILTON CORP. SRA TYPE A-19)

expanded or contracted according to a strain of the sample. The expansion or contraction of the wire grid produces a corresponding change in the cross-sectional area of the wire; this in turn increases or reduces the total resistance of the wire composing the grid. The relative change in resistance of the strain gage is a linear function of the strain to be measured. The constant of proportionality between the measured strain and the change in resistance is of the order of unity and is called the gage factor. The gages of a given manufacturing lot are calibrated by the manufacturer. The wire grid of the strain gage is mounted sandwich style between two sheets of paper, thus providing a means of handling the wire grid. This sandwich is then glued to the sample; the glue and method used were those recommended by the manufacturer.

The relative change in length of the strain gage can be measured with comparative ease by means of a simple d-c bridge circuit (Figure 4-3). It has been shown[22] that maximum sensitivity of the bridge will occur for the case when all bridge arms are approximately of the same impedance. Therefore, each bridge arm consists of a strain gage, and balance is obtained by shunting one arm with a high-impedance decade box. Thermal equilibrium for all wire junctions and components is required to keep all thermal noise constant relative to the desired sensitivity. Also the thermal-resistance change of the measuring gage must be compensated by maintaining one of the other arms of the bridge at the same temperature as the measuring gage. Therefore, the measuring gage and the compensating gage are kept at the temperature of the sample. The other two gages of the bridge are kept at room temperature.

The balance voltage of the bridge is detected by an ultrasensitive d-c breaker amplifier and recorded on a recording milliammeter.

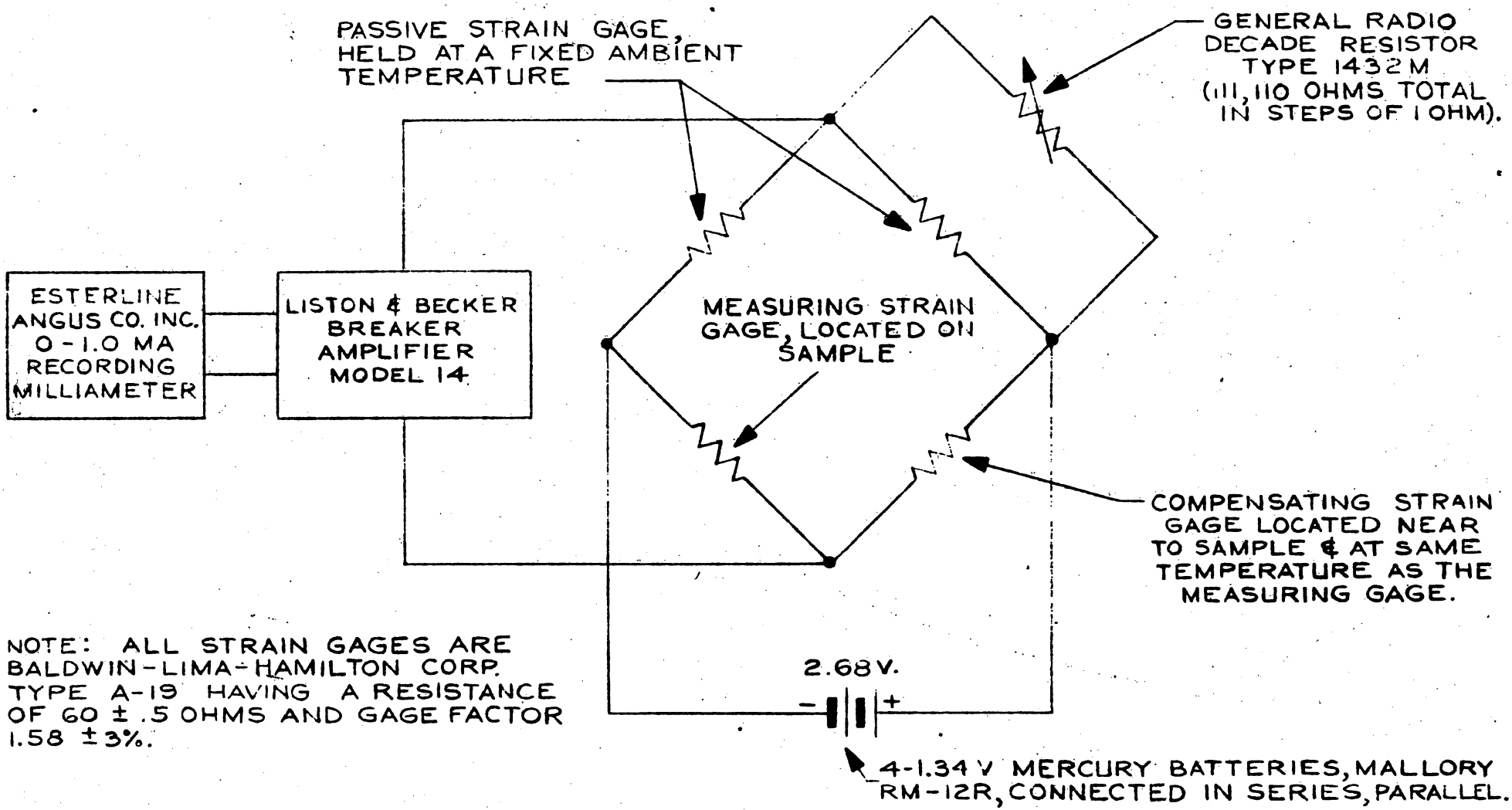

FIG. 4-3

CIRCUIT SCHEMATIC FOR THE MEASUREMENT OF MAGNETOSTRICTION

The amplifier used was a Liston-Becker Model 14 which has a sensitivity of 10^{-8} volts with an input impedance of 100 ohms. A voltage is developed across the amplifier when the bridge is perturbed from an initial state of balance by a change in strain-gage resistance; this voltage can be shown to be approximately $\varepsilon = E\ \delta r/r$, where r is the resistance of the gage and E is the d-c. potential applied to the bridge. For the strain gages used $\delta r/r \simeq 1.6\ \delta\ell/\ell$, and the voltage was $E \simeq 3$ volts. Therefore the amplifier sensitivity of 10^{-8} volts corresponded to a strain of approximately 2×10^{-9}, which was very adequate for the measurements reported here. A sensitivity of 10^{-8} was found experimentally.

The wiring of the experimental apparatus is shown in Figure 4-4. All bridge components and connections, except for the decade box and the compensating and measuring gages, are located within the copper box shown. The box provides both thermal and electrostatic shielding for the components within. The two gages within the box were thermally stabilized by clamping them between two large copper blocks. Each wiring connection was also made on a copper block for thermal stability.

An exploded view of the sample holder is shown in Figure 4-5. The problem was to

1. Suspend the disc sample in a magnetic field at an equilibrium temperature;
2. Permit rotation of the sample in a field;
3. Provide for a measuring and compensating strain gage; and
4. Permit a measurement of sample temperature.

The compensating gage was glued to the gage plate, and the thermocouple was clamped to this plate. The sample plate containing the disc sample with strain gage glued on one side was made easily replaceable. Thermal

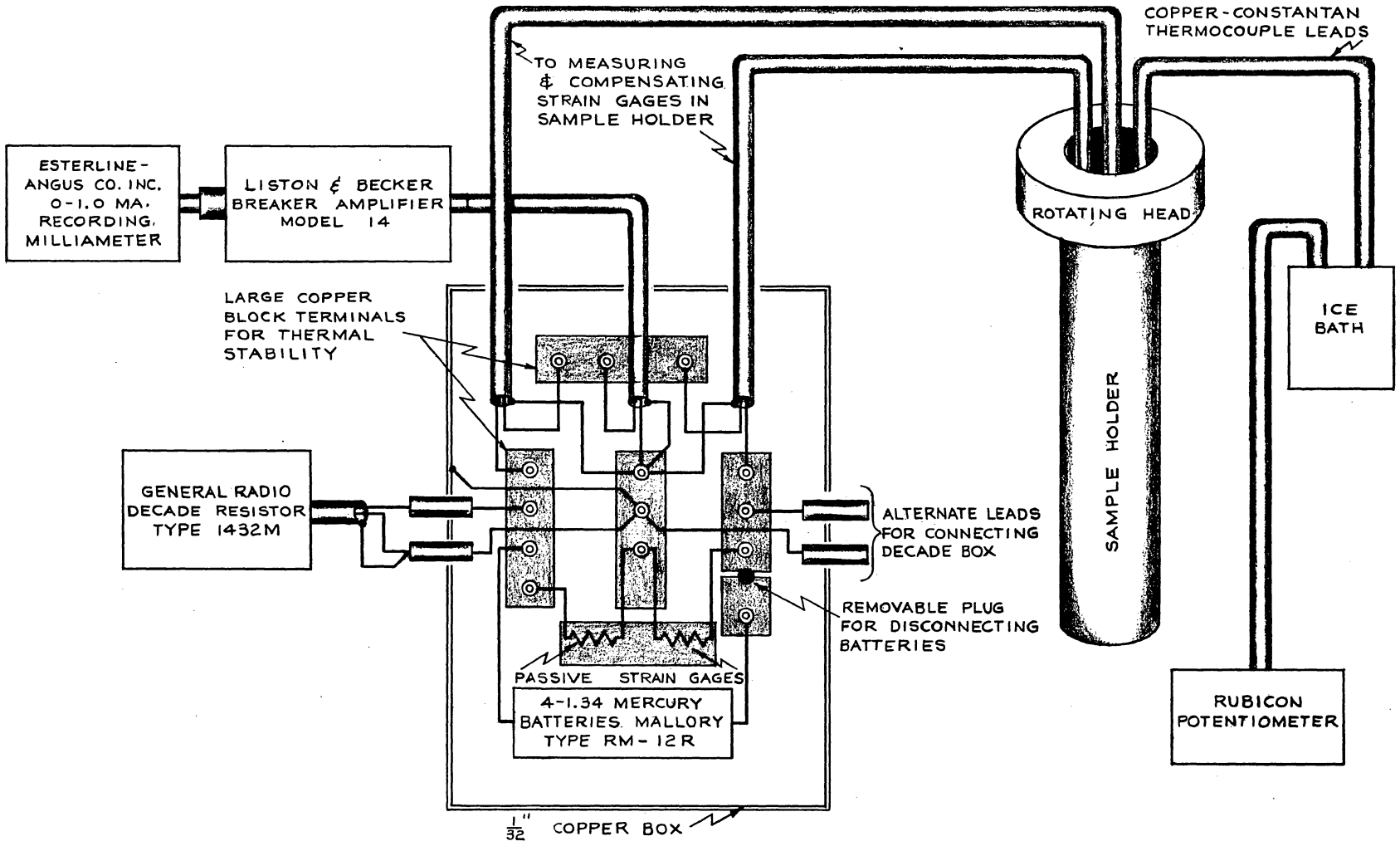

FIG. 4-4

WIRING DIAGRAM OF EQUIPMENT FOR MEASURING MAGNETOSTRICTION

D-61457

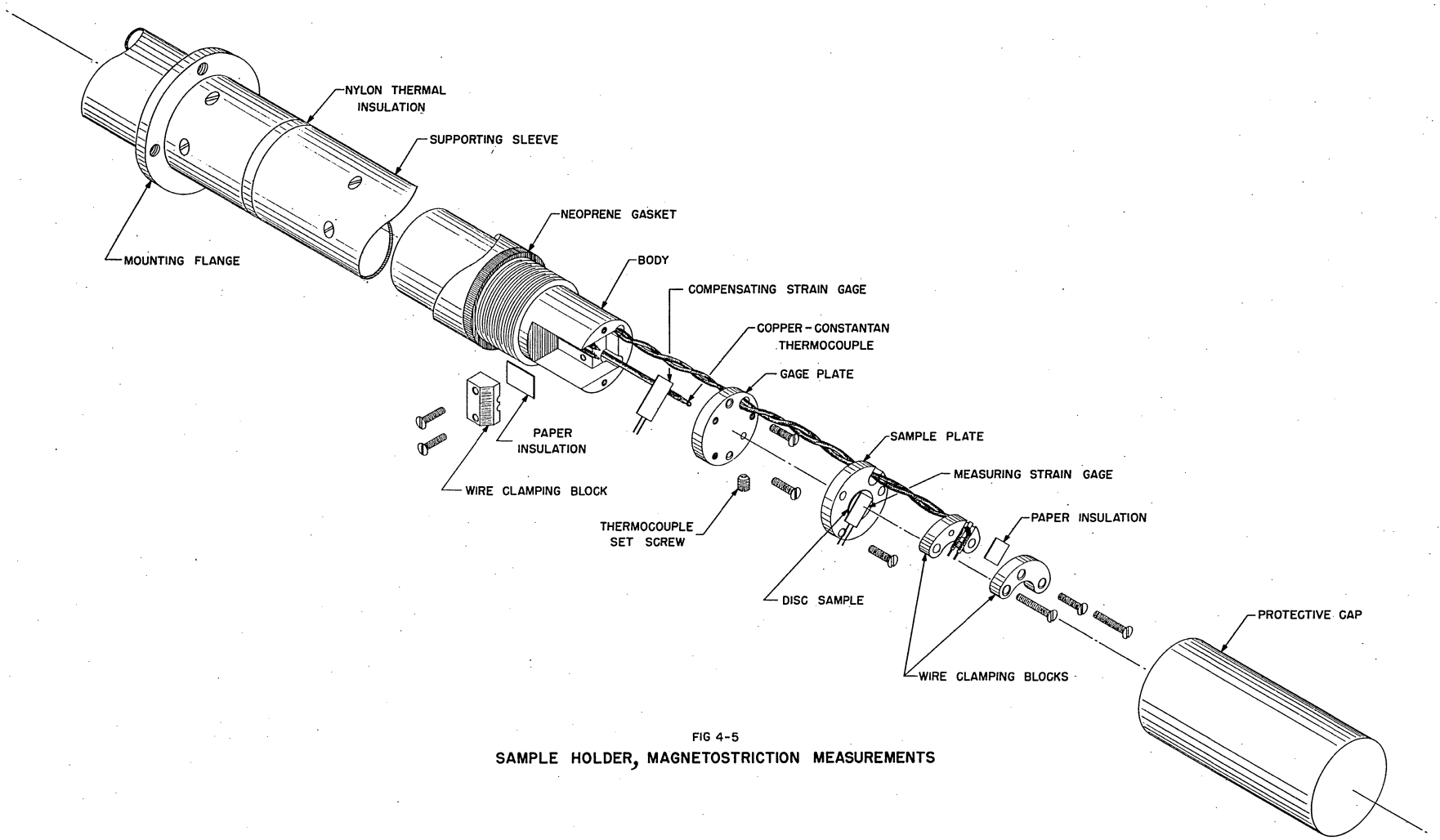

FIG 4-5

SAMPLE HOLDER, MAGNETOSTRICTION MEASUREMENTS

insulation was accomplished by a nylon thermal insulator. All parts are brass except where noted. Hence a satisfactory thermal stability was established for sample and strain gages. The protecting cap and neoprene gasket permit emersion of the sample holder into any desired coolant.

Rotation of the sample holder is provided by the rotating head shown in Figure 4-6. The dial plate was engine divided, and the vernier permits an accuracy of 0.1 degree. The worm drive is mounted in a rocking arm which permits the worm to be disengaged from the worm gear with relative ease. This feature permits a rapid rotation of the sample through any large angle.

Suspension of the sample in a magnetic field was provided by a yoke which rested on the magnet. The sample holder, rotating head, and yoke are shown assembled in Figure 4-7. The entire experimental setup for magnetostriction measurements is shown in Figure 4-8; the sample holder is inside of a Dewar flask in the magnet. A Varian V-4007 magnet was used with a Varian V-2200 regulated power supply. The pole pieces were 6 inches in diameter and 4 inches apart; the maximum field available at the center was 3,500 oersteds.

D. Procedure

At each sample temperature the following steps were taken to determine the saturation magnetostriction constant $\overline{\lambda}_{\parallel(S)}$:

1. After thermal transients due to the setup of equipment had sufficiently subsided, the bridge was balanced.

2. The maximum field was applied and the sample rotated. The amplifier gain was adjusted to produce a maximum deflection of about 0.5 milliampere on the recording milliammeter. This technique results in an accuracy in the strain measurements as a function of the applied field of about

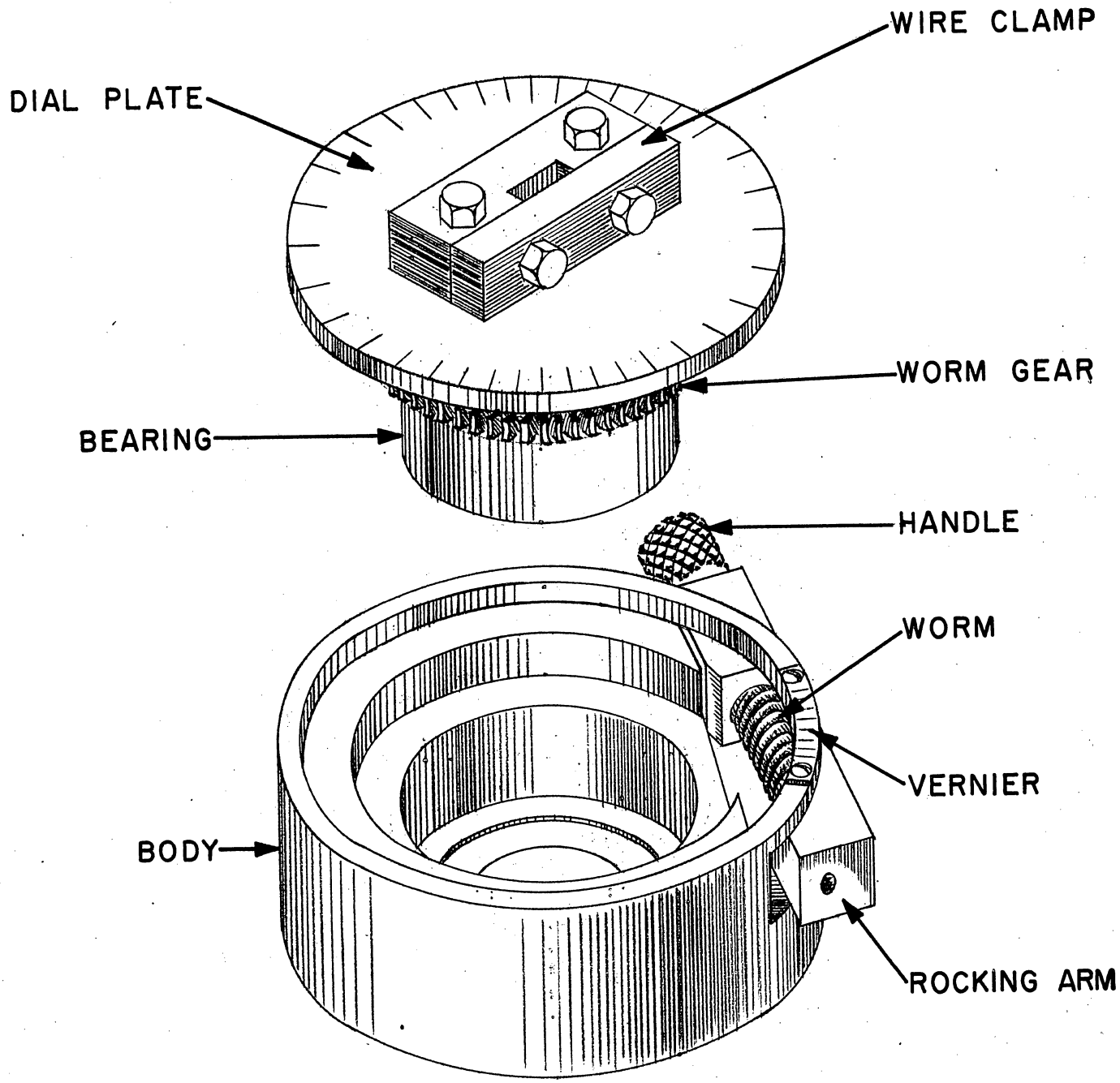

FIG. 4-6

ROTATING HEAD FOR MAGNETOSTRICTION MEASUREMENTS

A-61460

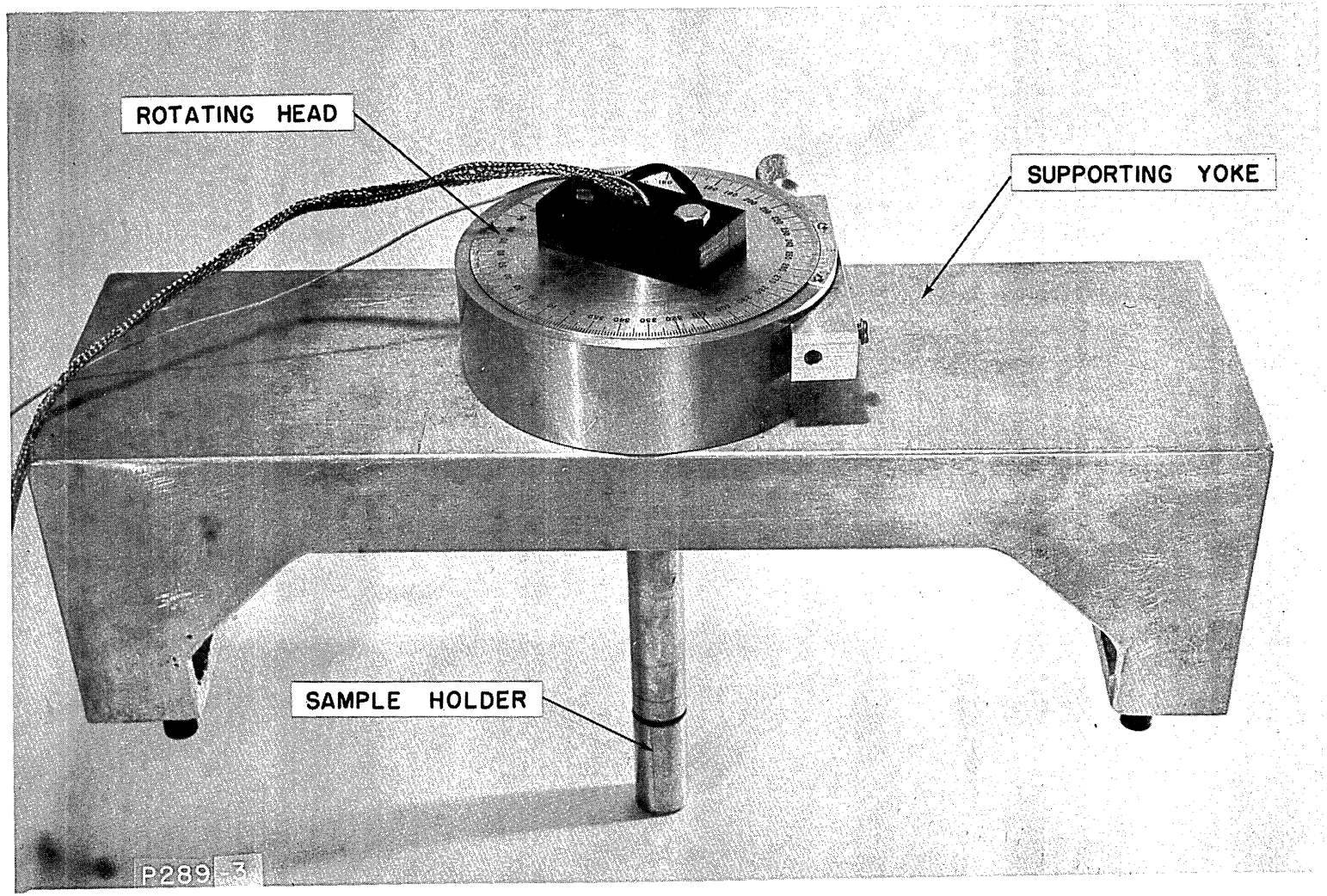

FIG. 4-7

MAGNETOSTRICTION SAMPLE HOLDER,
ROTATING HEAD AND SUPPORTING YOKE

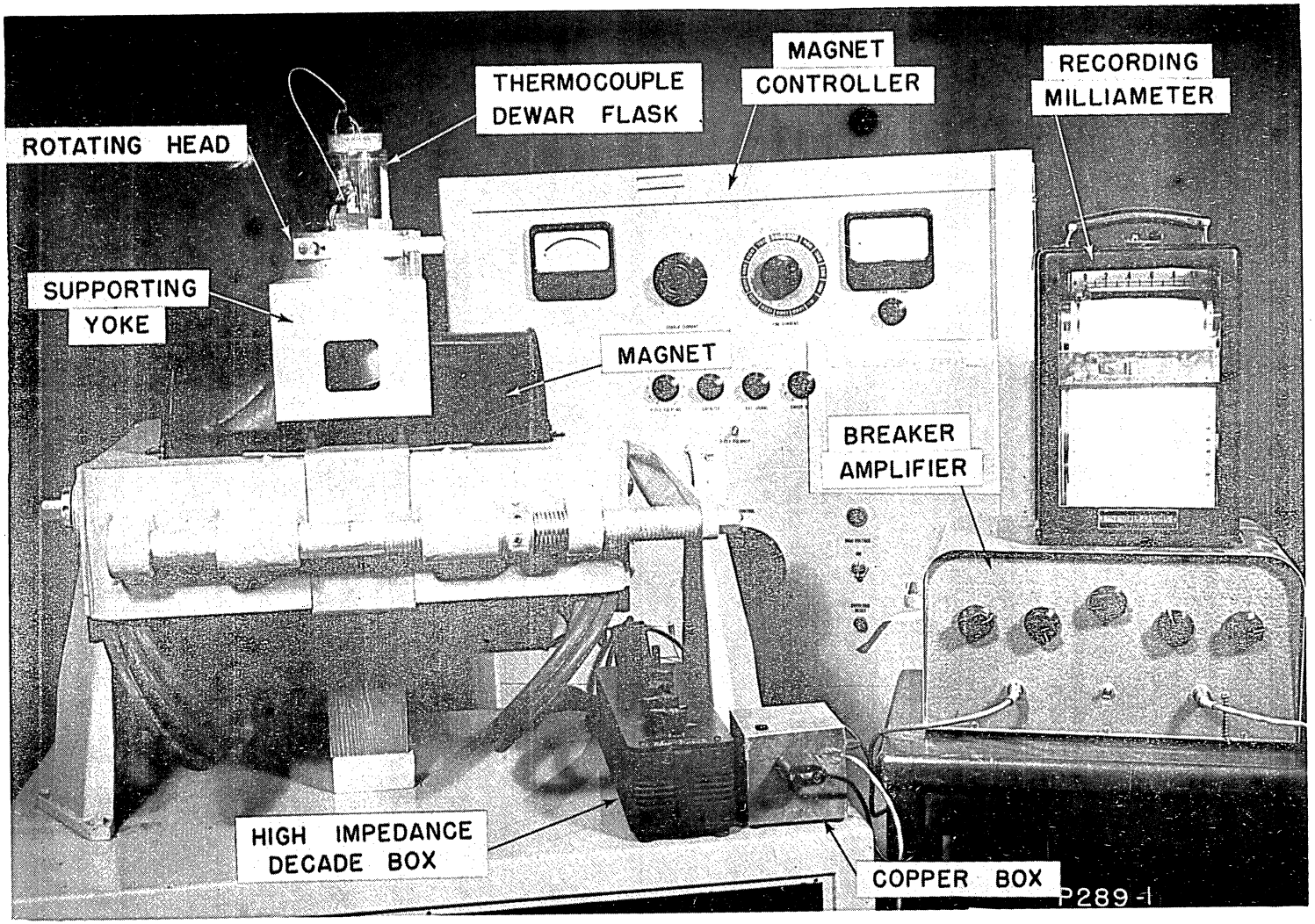

FIG. 4-8

EXPERIMENTAL SET-UP

3 percent of $\overline{\lambda}_{\parallel(S)}$.

3. By noting the dial readings on the rotating head for maximum deflections, it was possible to determine when the measured direction was parallel or perpendicular to the applied field since $\frac{\delta \ell}{\ell} = \frac{3}{2} \overline{\lambda}_{\parallel(S)} (\cos^2\theta - \frac{1}{3})$.

4. The sample was next placed so that the measuring direction was parallel to the applied field, then perpendicular to the field, and then parallel to the field. The excursion recorded on the meter was a measure of $\frac{3}{2} (\delta \ell / \ell)_{\text{isotropic}}$ for this field. This process was repeated for successively lower fields. This procedure provided data for an isotropic relative change in length, $(\delta \ell / \ell)_{\text{isotropic}}$, as a function of the external field. When the material is saturated, $(\delta \ell / \ell)_{\text{isotropic}} = \overline{\lambda}_{\parallel(S)}$. Therefore, examination of the data as a function of field determines whether, at the maximum field used, $(\delta \ell / \ell)_{\text{isotropic}} = \overline{\lambda}_{\parallel(S)}$.

The equipment was calibrated for each temperature and for each sample. This was necessary because the sensitivity of the equipment was adjusted to suit the saturation magnetostriction for each case. Calibration was carried out in the following manner: With the initial state that for bridge balance, the decade box was varied a sufficient extent to produce a deflection of the milliammeter of the same order as the measurements being made. The relative change in resistance of a bridge arm due to a change ΔR in the decade resistance R can be shown to be $\Delta r/r = (r \text{ gage}) \Delta R/R^2$. Therefore, the deflection of the meter can be calibrated for the change in resistance of the strain gage. For the conditions and over the range of measurements specified, it was found experimentally that the meter deflection was a linear function of the $\Delta r/r$ of a bridge arm. The calibration of the measurement, as derived

in Appendix C, is given by

$$S = \left(\frac{\Delta R}{d}\right)\left(\frac{r}{R^2}\right)\left(\frac{1}{G}\right) \text{ per milliampere deflection,}$$

where d is the deflection of the meter in milliamperes corresponding to the change in decade resistance ΔR, r is the gage resistance, and G is the gage factor.

The magnetostriction parallel to the saturating field was measured as a function of field as follows: the field was decreased from the maximum value to the field under consideration, and the corresponding strain parallel to the field measured. Return to a maximum field between measurements at lower fields permits any thermal drift present to be eliminated from the measurement. The measured value of $\overline{\lambda}_{\parallel (S)}$ was then added to the above data to obtain $\overline{\lambda}_{\parallel}$ as a function of field.

Data have been obtained from each sample in three coolants: (1) CO_2 + Acetone mixture (-78 C), (2) ice water (0 C), and (3) room temperature water (20 C). It had been hoped to obtain data at liquid-nitrogen temperature (-200 C). However, at these temperatures the Duco glue recommended by the strain-gage manufacturer for fastening the gage to the sample apparently froze. Since the glue has a different thermal coefficient of expansion than the sample, the bond was broken. Some experimentation was made with Teflon cement without success. If a satisfactory glue had been found, an extensive calibration experiment using this new adhesive at these temperatures would have been necessary. Because of time limitations, further attempts to obtain magnetostriction data at this temperature were not made.

E. Sample Preparation

As discussed in Chapter II a compositional series of the general formula $(MgOFe_2O_3)_{1-\gamma}(Mn_3O_4)_{\gamma}$ was prepared. Thirteen compositions were

made for $0 \leqslant \gamma \leqslant 0.6$ in steps of 0.05. For each value of γ both toroidal and disc samples were fired. Because of the complex chemistry involved, the firing cycle that produces optimum square-hysteresis characteristics would not, in general, be constant over a compositional series. Therefore, for each value of γ eight different firing conditions were used to fire both toroids and disc samples. To provide ten discs and two toroids for each compositional and firing condition, it was necessary to initially fire 1300 samples for this compositional series.

The toroids were all given a hysteresis test to ascertain the maximum B-H loop squareness R_s. Analysis of these data made it possible to determine the optimum firing condition for each value of γ. It was found that, except for $\gamma = 0$, a sintering temperature of 1450 C and a later anneal at 1100 C in a nitrogen atmosphere was the optimum firing condition. In the case of $\gamma = 0$, the as-mixed composition is completely $MgOFe_2O_3$. Since there are no Mn ions present which are oxidized in an air firing, there is no need for a nitrogen anneal to make the sample homogeneous. In fact a nitrogen anneal tends to reduce some of the Fe^{3+} ions to Fe^{2+} and therefore to make this composition less homogeneous. For $\gamma = 0$ the best firing condition was an air fire only at 1350 C; there was no subsequent anneal in nitrogen.

Discs, sintered according to the optimum firing conditions for the toroids, were then prepared for magnetostriction measurements. To evaluate these measurements, it is necessary to know the demagnetizing fields within the samples. Demagnetizing fields produced by samples not having a closed magnetic path are known only for the case of the ellipsoid. To permit a calculation of the demagnetizing field, it is necessary to approximate an ellipsoid by using a thin disc; the demagnetizing field is practically a linear function of the thickness of an oblate

spheroid of the dimensions used. After firing, the disc sample was approximately 0.75 cm in diameter and 0.2 cm thick. For the oblate spheroid of the same over-all dimension, the demagnetizing field along a diameter would be about 300 oersteds. To reduce the thickness of the disc both to approach the true ellipsoidal shape and to reduce the demagnetizing field, the fired discs were ground to about 0.02 cm, a thickness corresponding to a demagnetizing field of about 80 oersteds.

The grinding operation was also necessary from another aspect. A few compositions, notably those for $\gamma = 0.1$, 0.15, and 0.2, were consistently found containing large easily seen circumferential cracks inside the disc with radial cracks proceeding inward toward the center of the sample. It was therefore necessary to fire a new series; great pains were taken to insure a uniform temperature distribution throughout the sample while firing. Some difficulties with cracks were still found, but samples were finally obtained which showed no sign of cracks under a microscope. The difficulty has been narrowed down to effects caused by a varied density in the pressed samples before sintering. Magnetostriction data was then obtained on the ground-disc samples. Afterwards the central portions of the discs were cut out; hysteresis and switching-coefficient data were obtained on the cut toroids thus formed. The several stages of sample preparation are shown in Figure 4-9. The centers cut from some of the discs were also used for further tests. These small, cut discs were used to obtain saturation moments of some of these materials at very high field strengths, $H \simeq 10{,}000$ oersteds, for comparison with hysteresis data; the centers were also used for microstructure examination to ascertain if a second phase was present.

A-61504

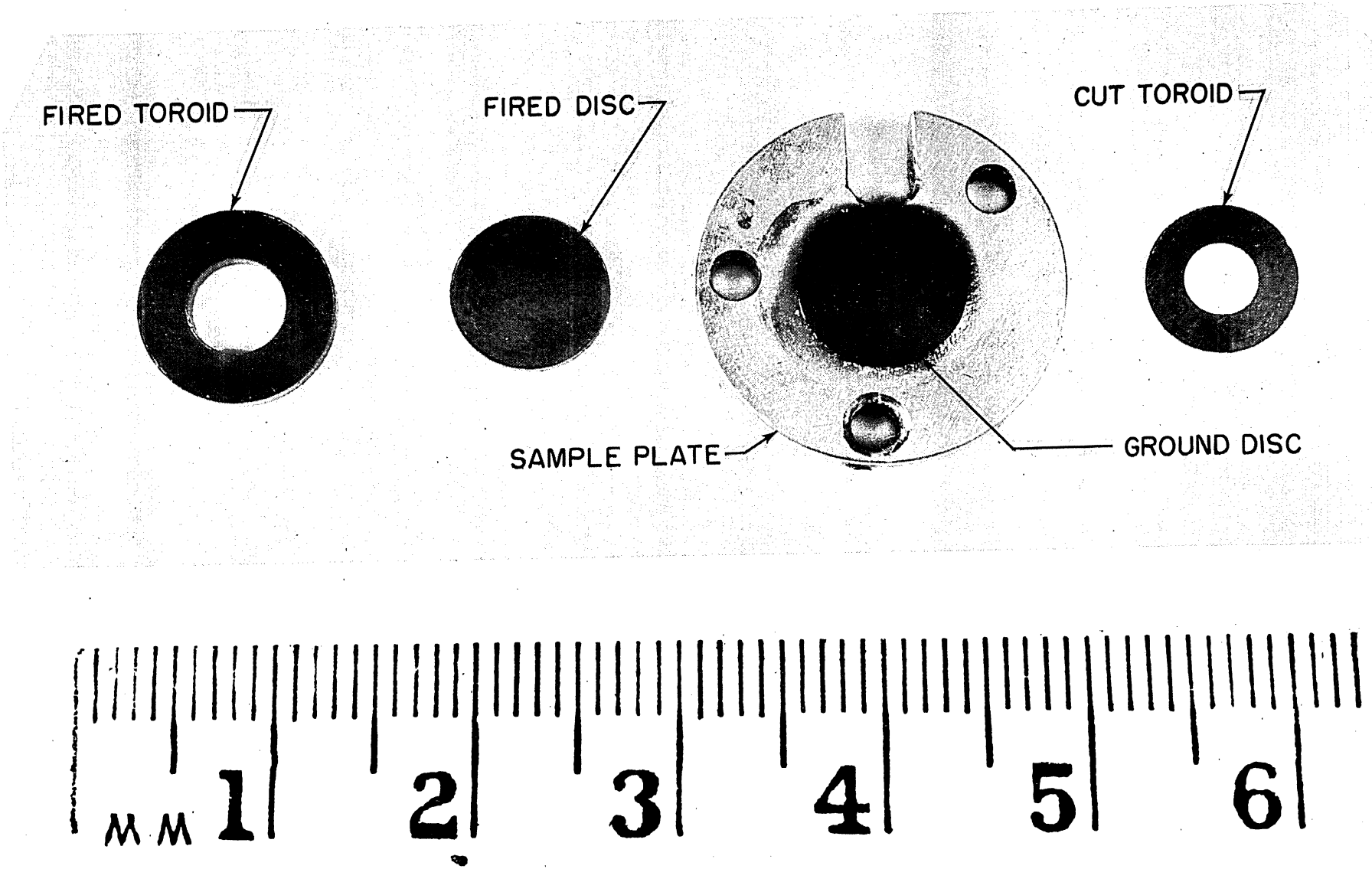

FIG 4-9
STAGES OF SAMPLE PREPARATION

CHAPTER V

EXPERIMENTAL RESULTS

A. Isotropic Magnetostriction

The isotropic magnetostriction was obtained as described in Chapter IV. The sample was held so that the direction of measurement was first parallel to the applied field and then perpendicular to the applied field, the difference in strain for these two cases being $\frac{3}{2}\left(\frac{\delta l}{l}\right)$ isotropic and $\frac{3}{2}\overline{\lambda}_{\parallel(S)}$ at saturating field strengths. These data were obtained for each sample at -78 C, 0 C, and 20 C and are shown in Figures 5-1 through 5-13.

The most significant part of these curves is the approach to saturation and the value at saturation, $\overline{\lambda}_{\parallel(S)}$. At low fields the material is not saturated, and the change in magnetization as the sample is rotated in the external field is due to domain-wall motion as well as domain-moment rotation. It is not possible to interpret the magnetostriction data in a meaningful way if an unknown amount of domain-wall motion is taking place.

The way that these data approach saturation is indicative of the strength of the effective anisotropy fields which tend to pull the magnetic moments within the material away from the the direction of the applied field. For all samples the magnitude of $\overline{\lambda}_{\parallel(S)}$ at -78 C is about 5/2 times (at $\gamma = 0$) to about 10 times (at $\gamma = 0.6$) greater than its value at room temperature. The most significant point of these data is the variation of $\overline{\lambda}_{\parallel(S)}$ with composition (see Figure 5-14). The irregular features of this plot are quite understandable as due to slight differences in the effective firing cycle received by each individual sample. The general trend is unmistakable; $\overline{\lambda}_{\parallel(S)}$ is negative and relatively

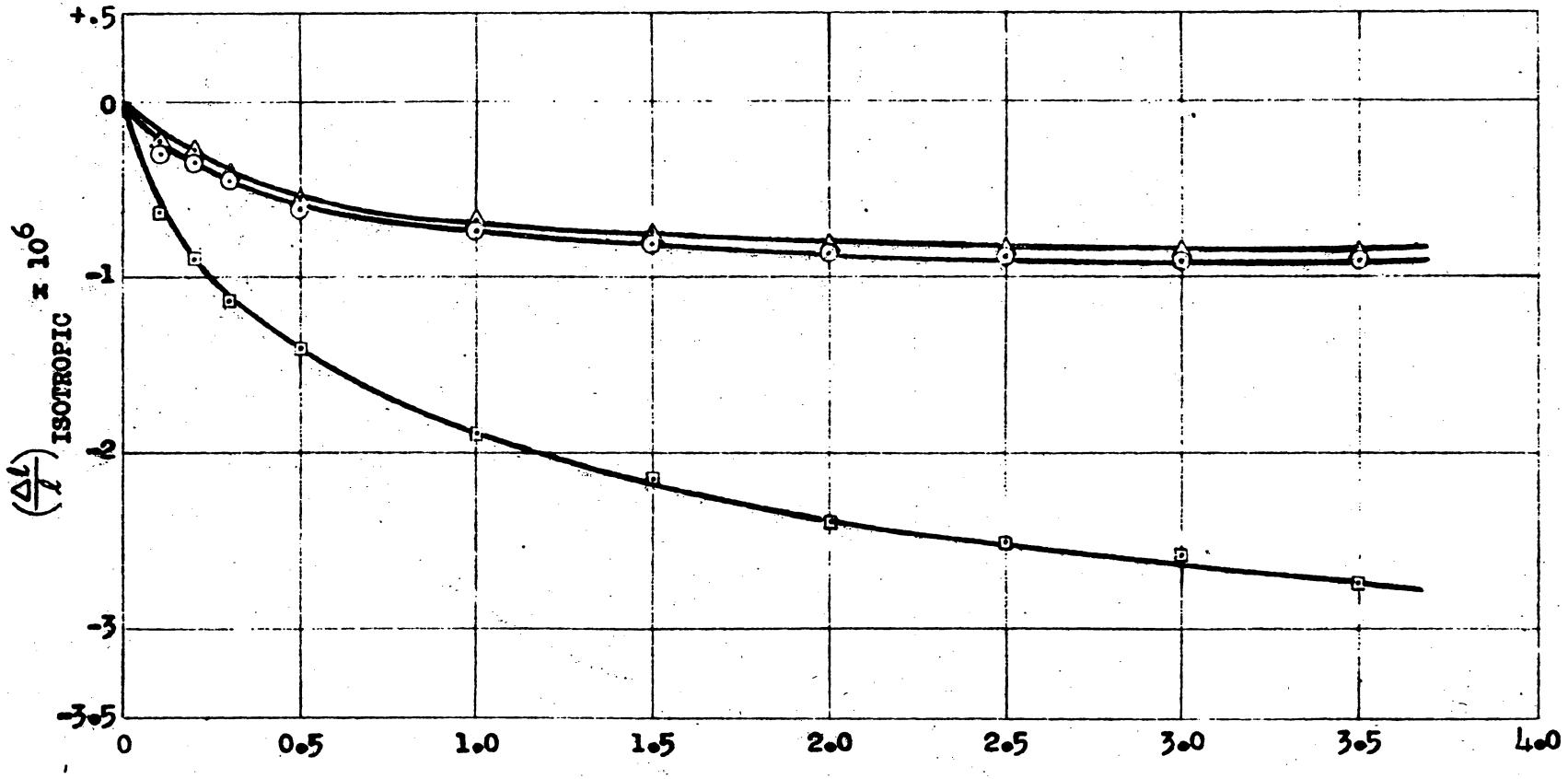

FIG. 5-1

ISOTROPIC MAGNETOSTRICTION
SAMPLE #1 ($\gamma = 0$)

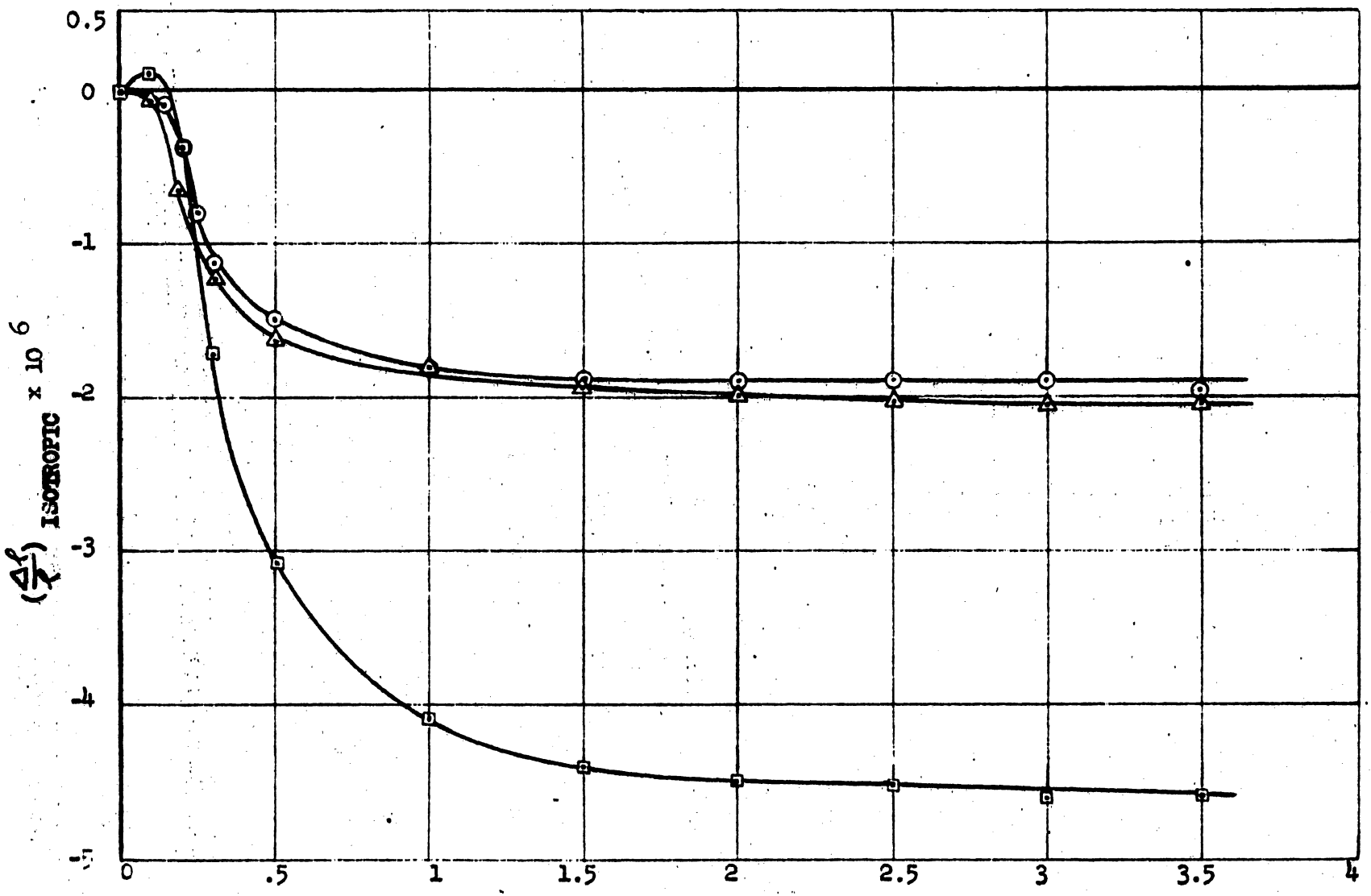

FIG. 5-2

ISOTROPIC MAGNETOSTRICTION

SAMPLE #2 (γ = .05)

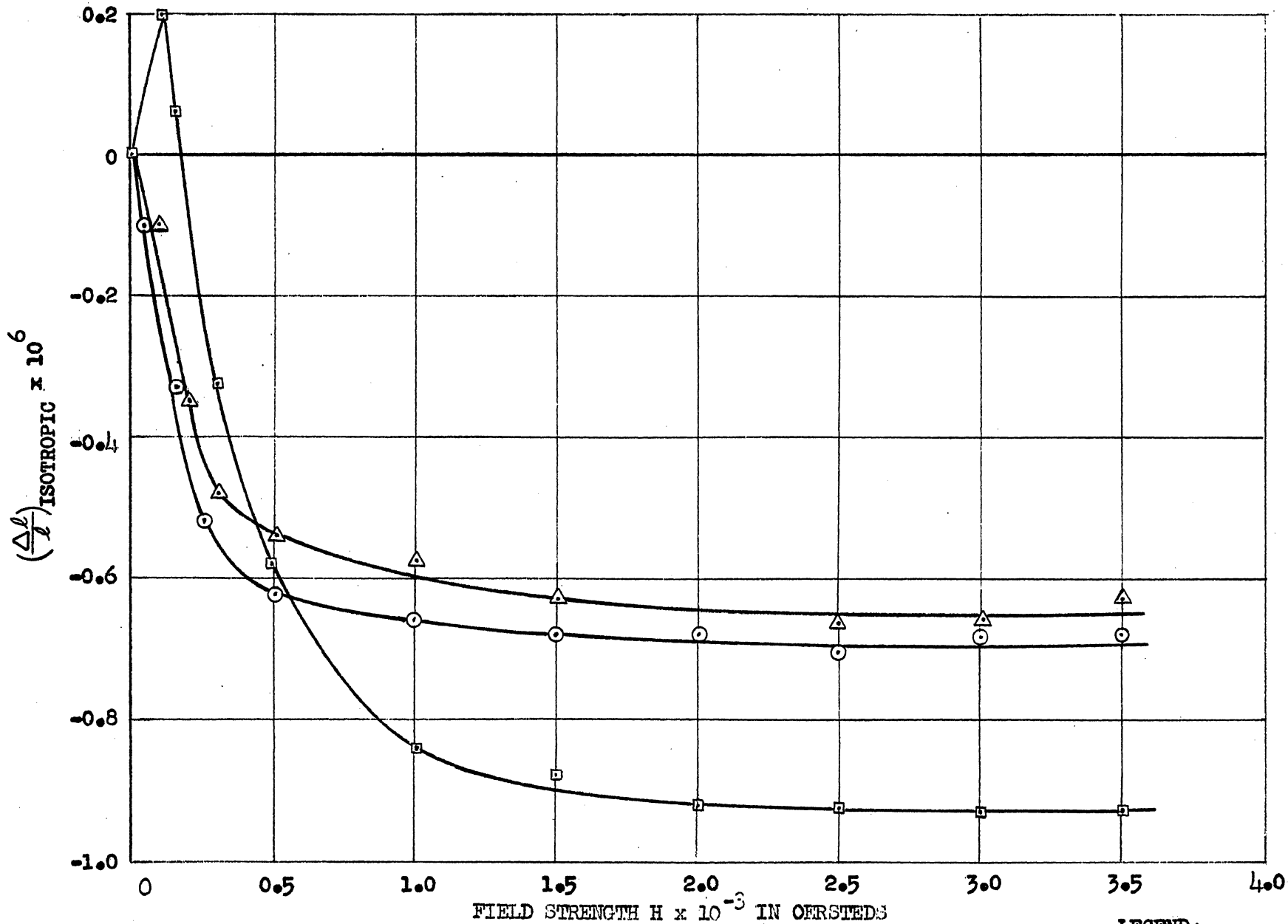

FIG. 5-3
ISOTROPIC MAGNETOSTRICTION SAMPLE 3(γ=0.1)

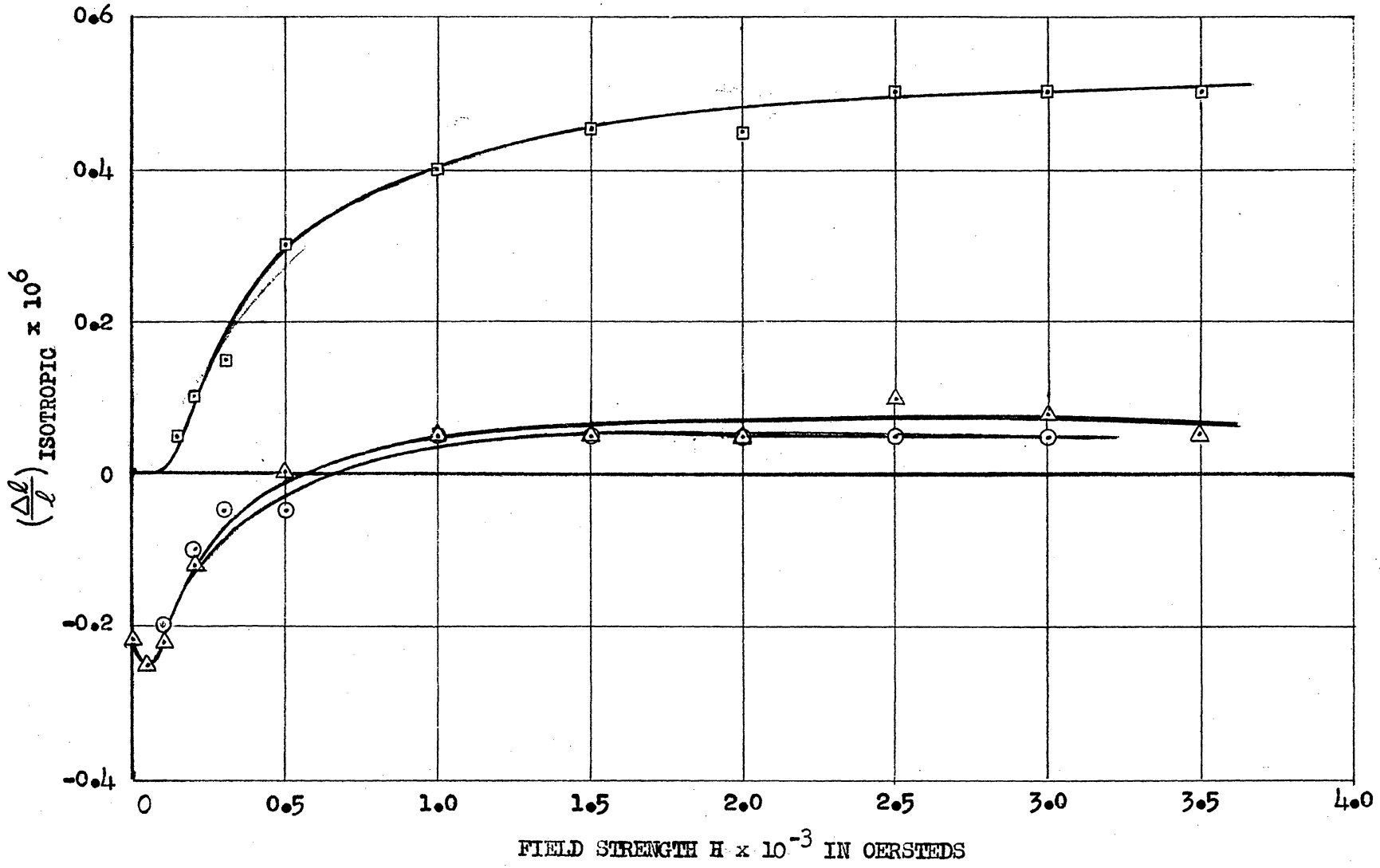

FIG. 5-4

ISOTROPIC MAGNETOSTRICTION
SAMPLE 4 (γ=0.15)

LEGEND:

⊡ -78 C
△ 0 C
⊙ 20 C

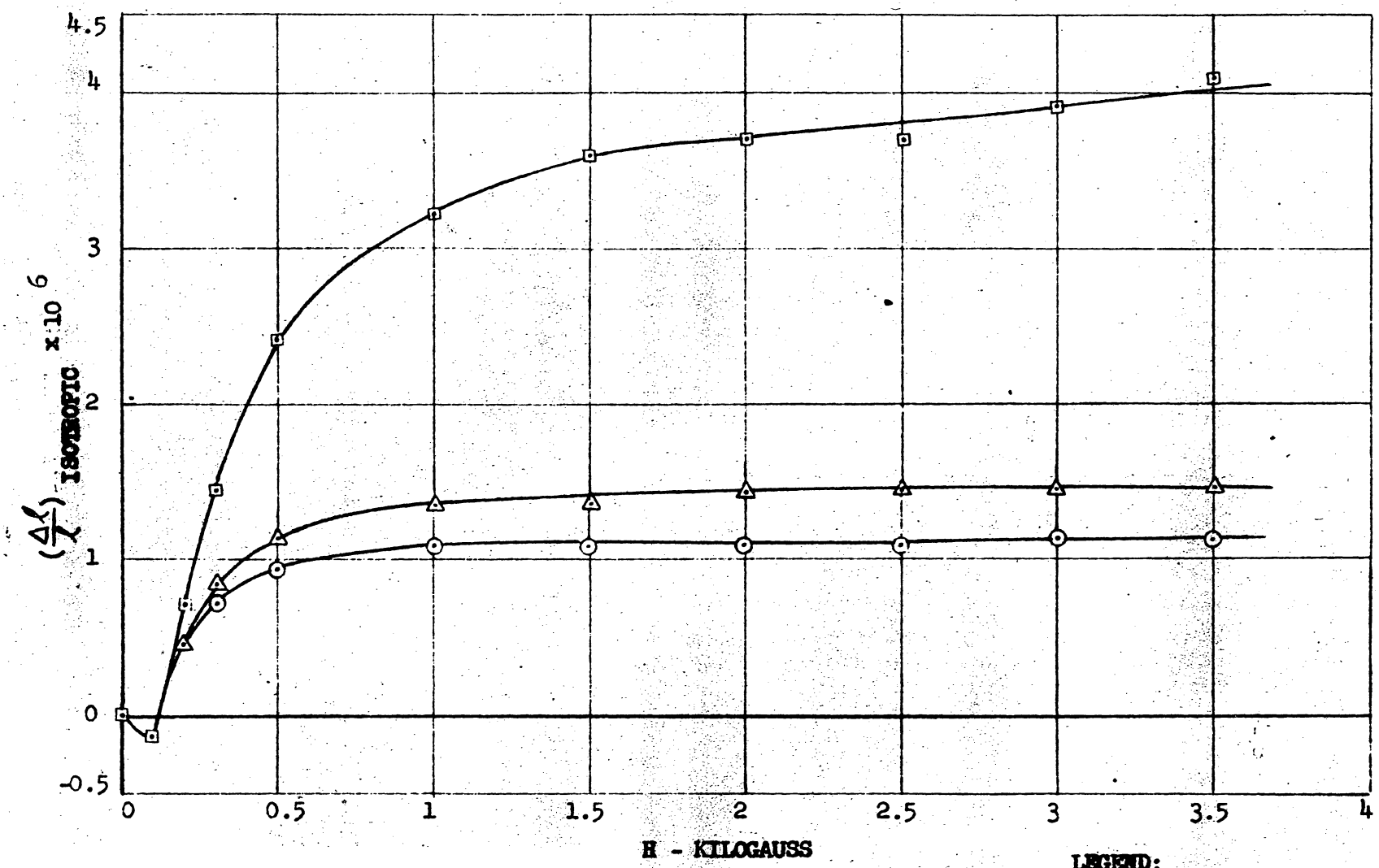

FIG. 5-5

ISOTROPIC MAGNETOSTRICTION

SAMPLE #5 (γ = 0.2)

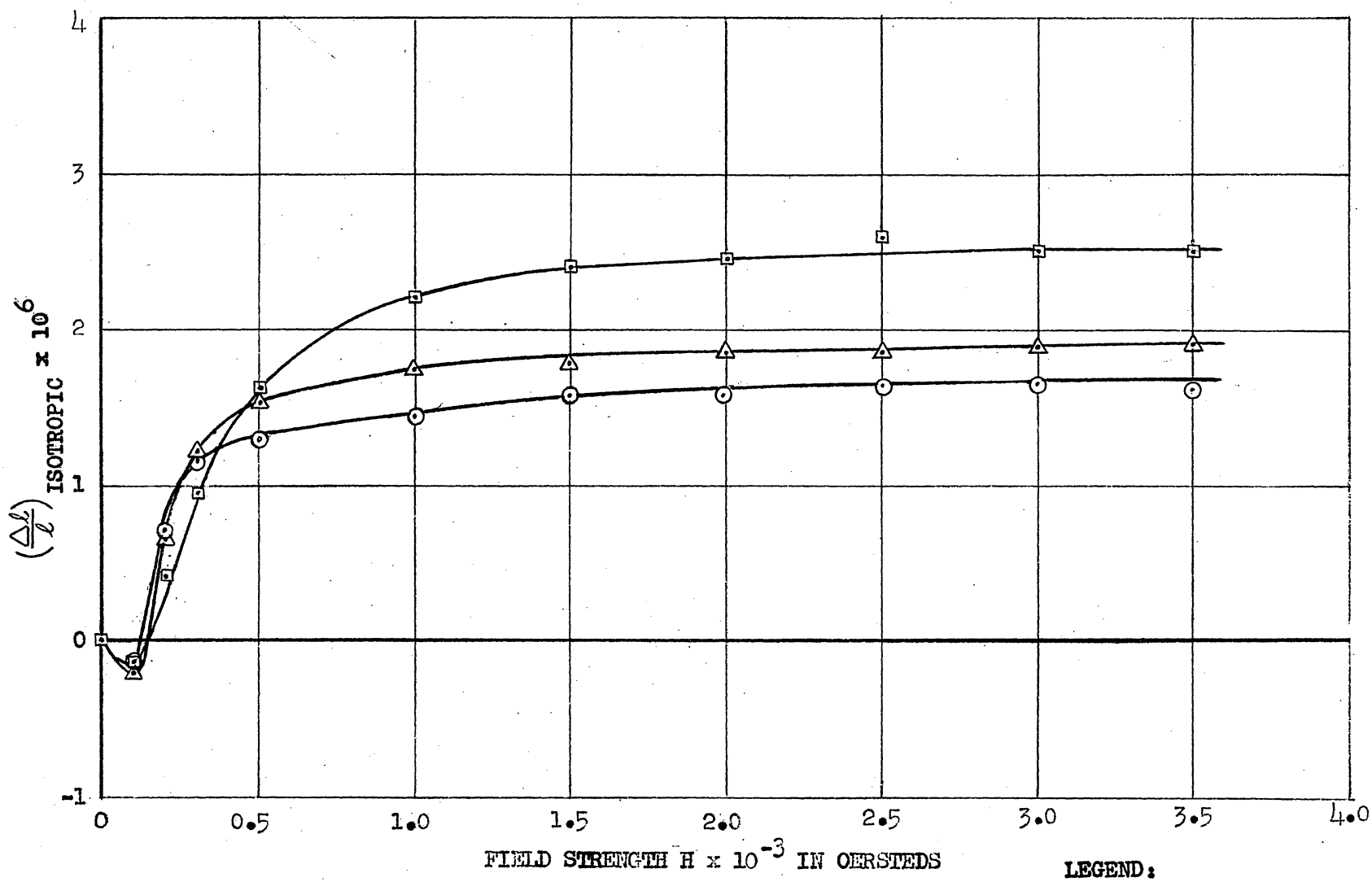

FIG. 5-6

ISOTROPIC MAGNETOSTRICTION
SAMPLE 6(γ=0.25)

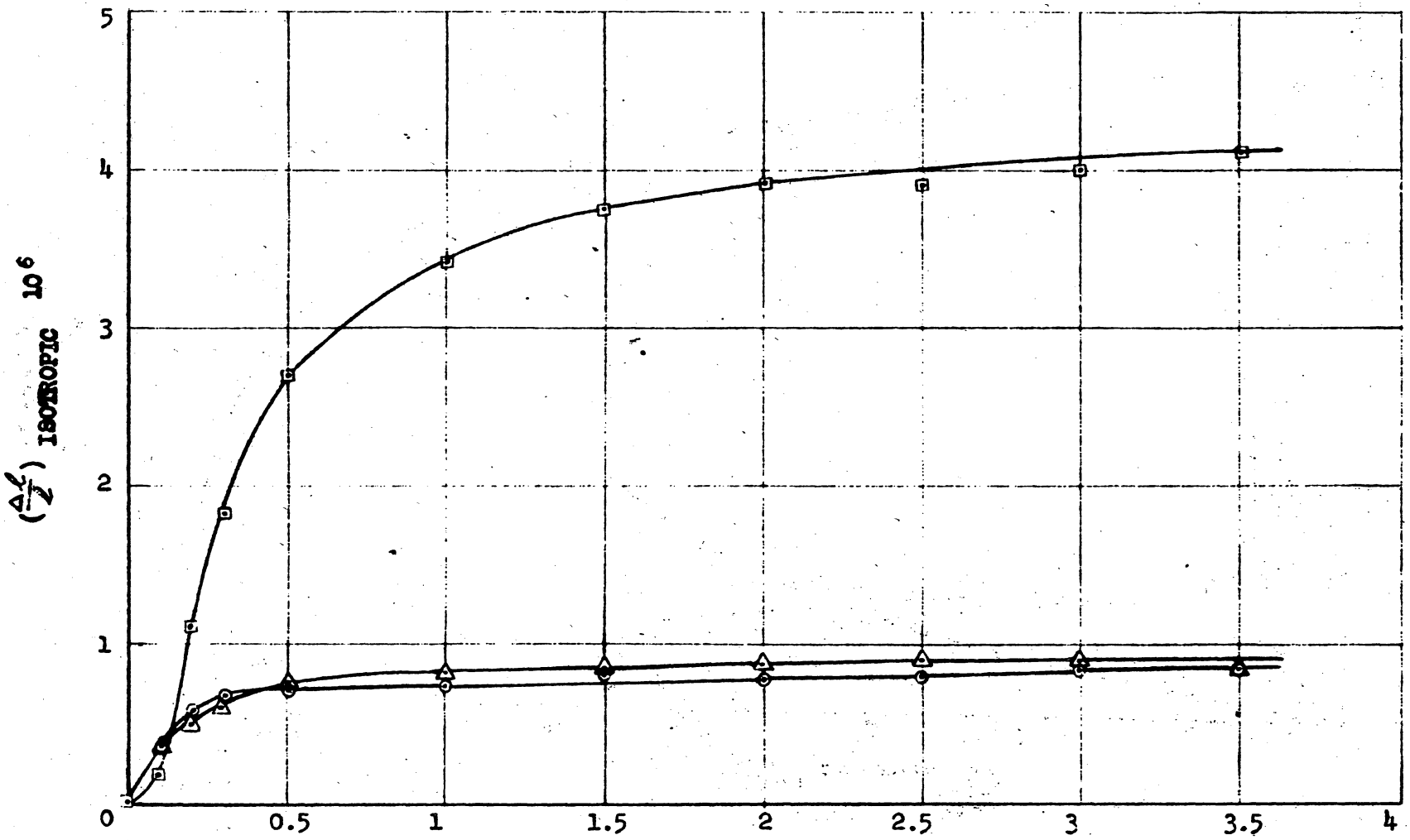

FIG. 5-7
ISOTROPIC MAGNETOSTRICTION

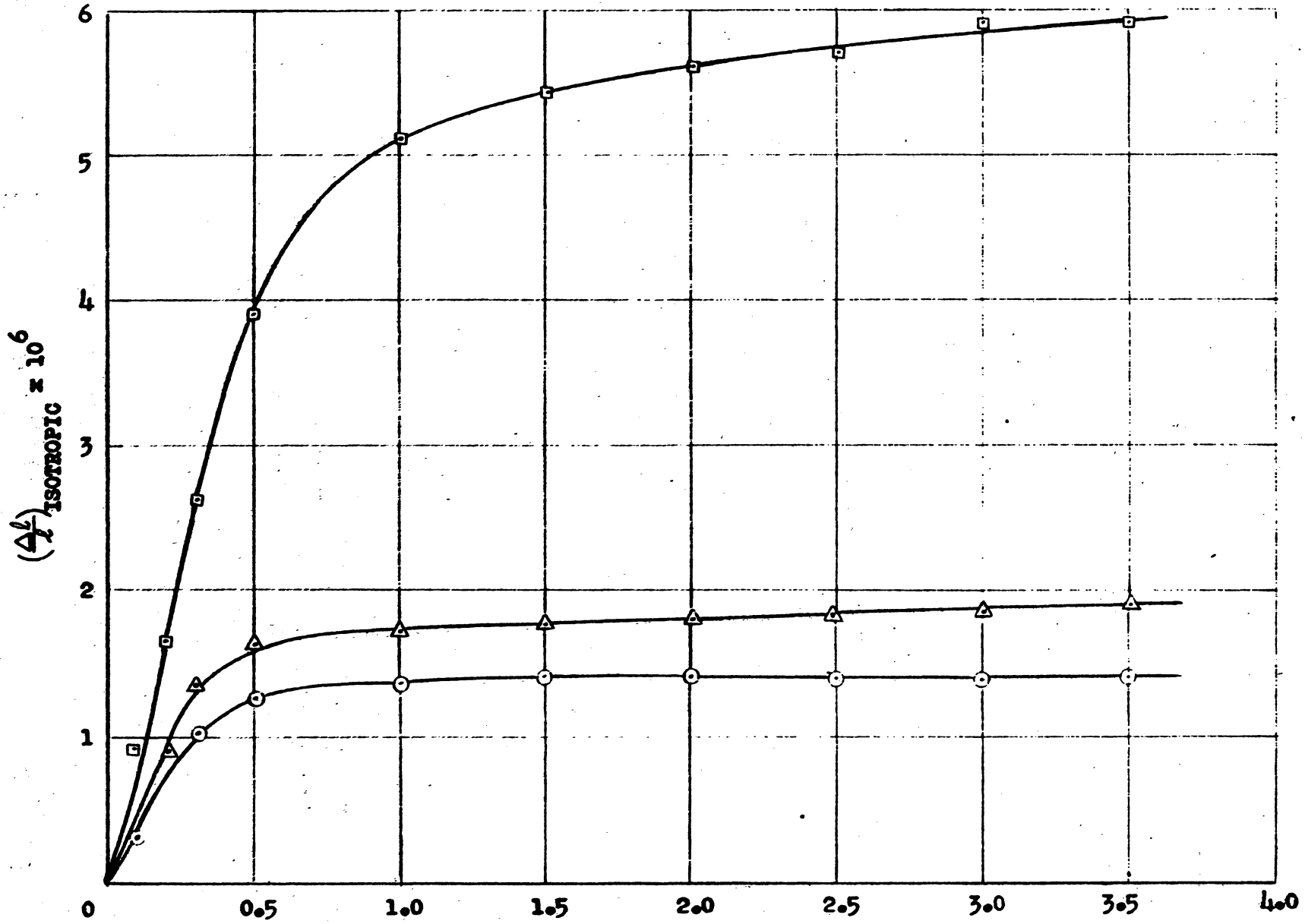

FIG. 5-8

ISOTROPIC MAGNETOSTRICTION SAMPLE #8 (X-.35)

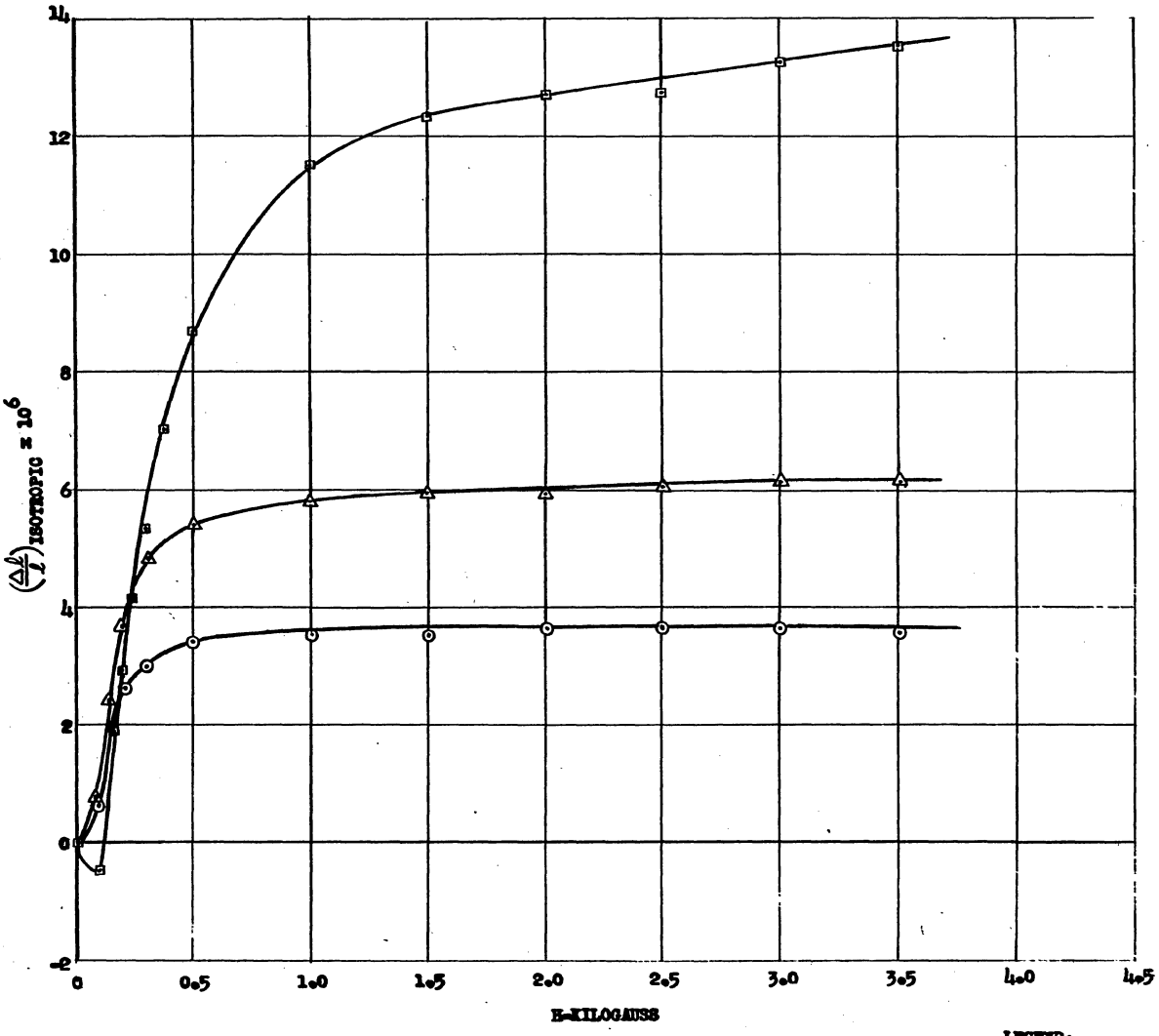

FIG. 5-9
ISOTROPIC MAGNETOSTRICTION, SAMPLE #9 (γ=.4)

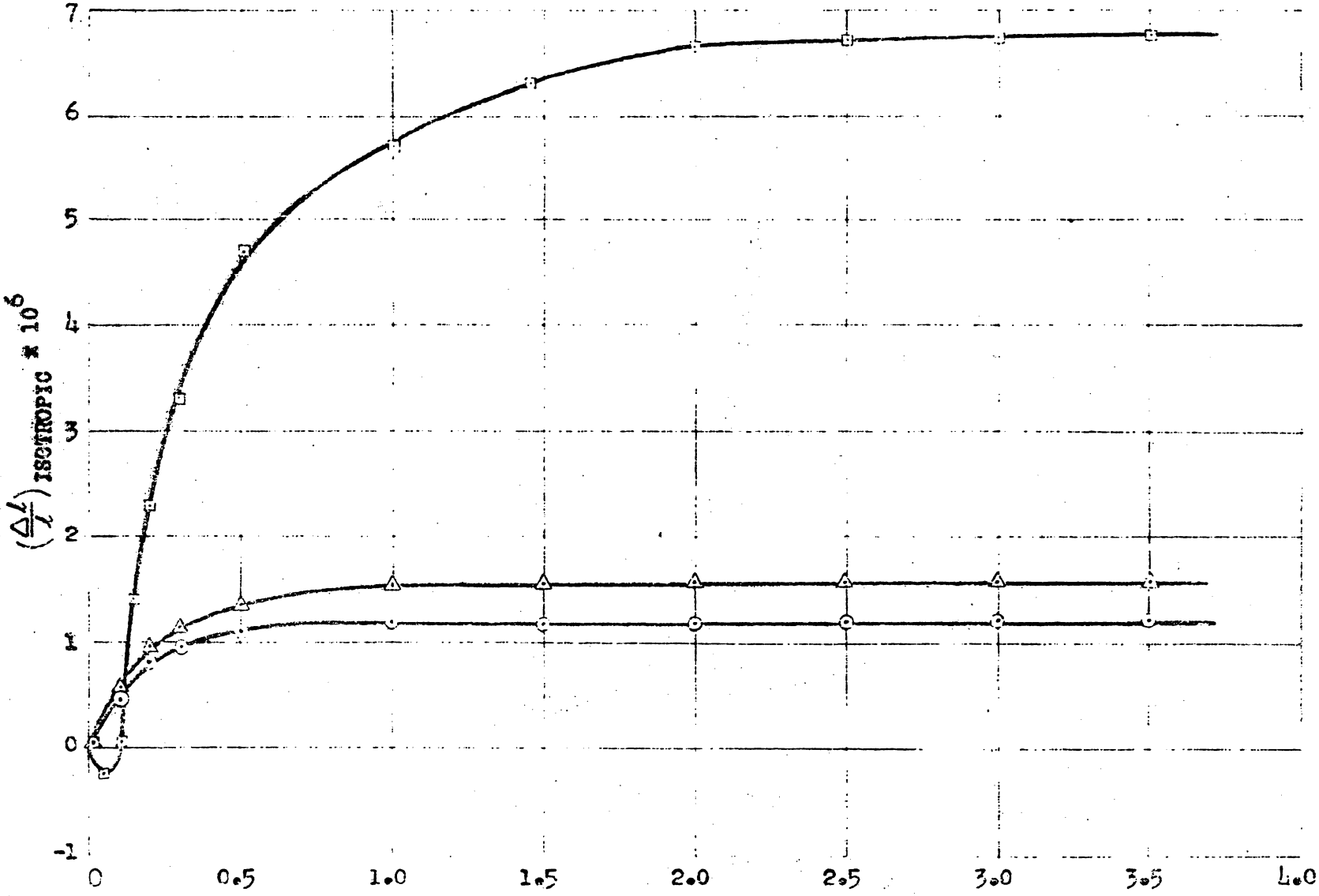

FIG. 5-10 ISOTROPIC MAGNETOSTRICTION, SAMPLE #10 (γ=.45)

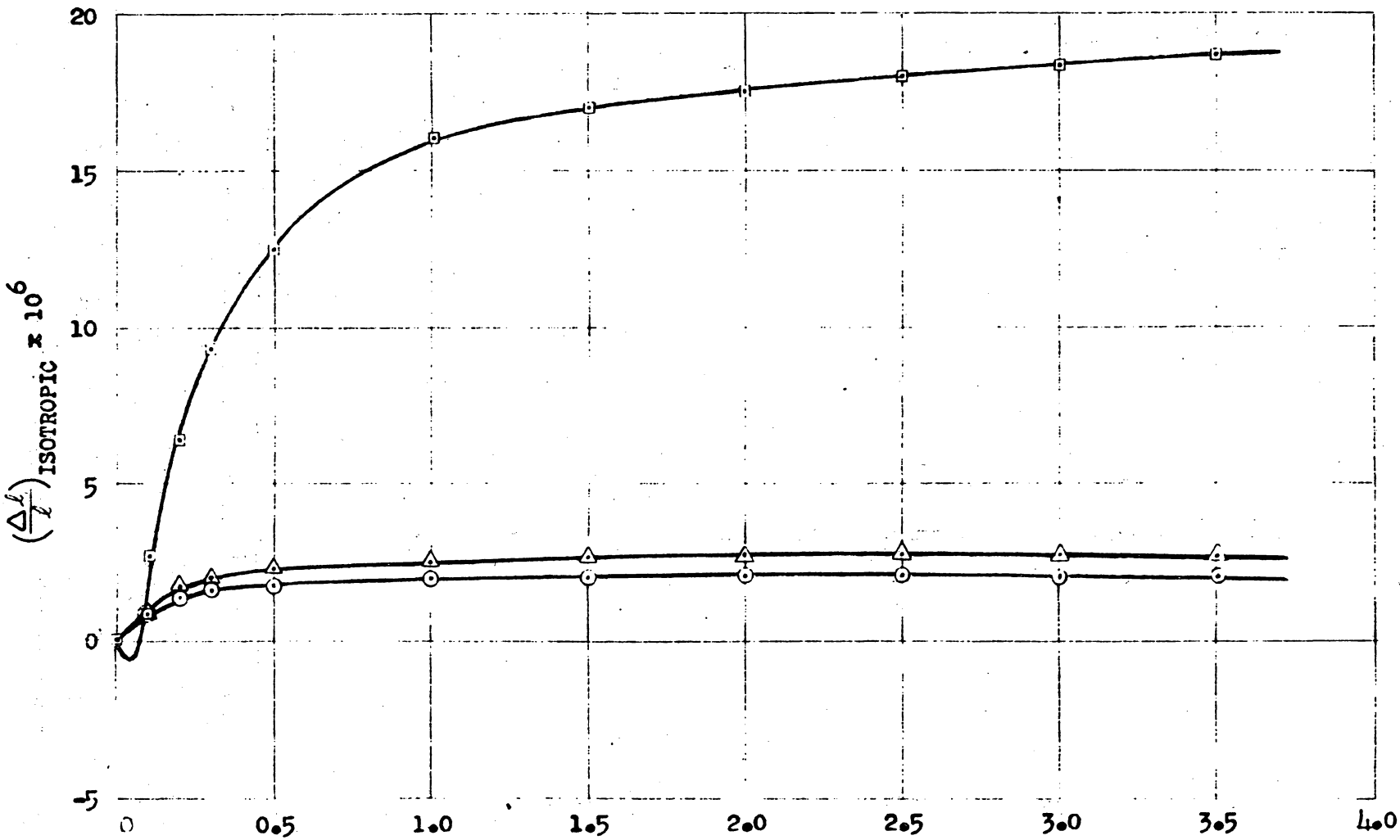

FIG. 5-11
ISOTROPIC MAGNETOSTRICTION
SAMPLE #11 (x=.5)

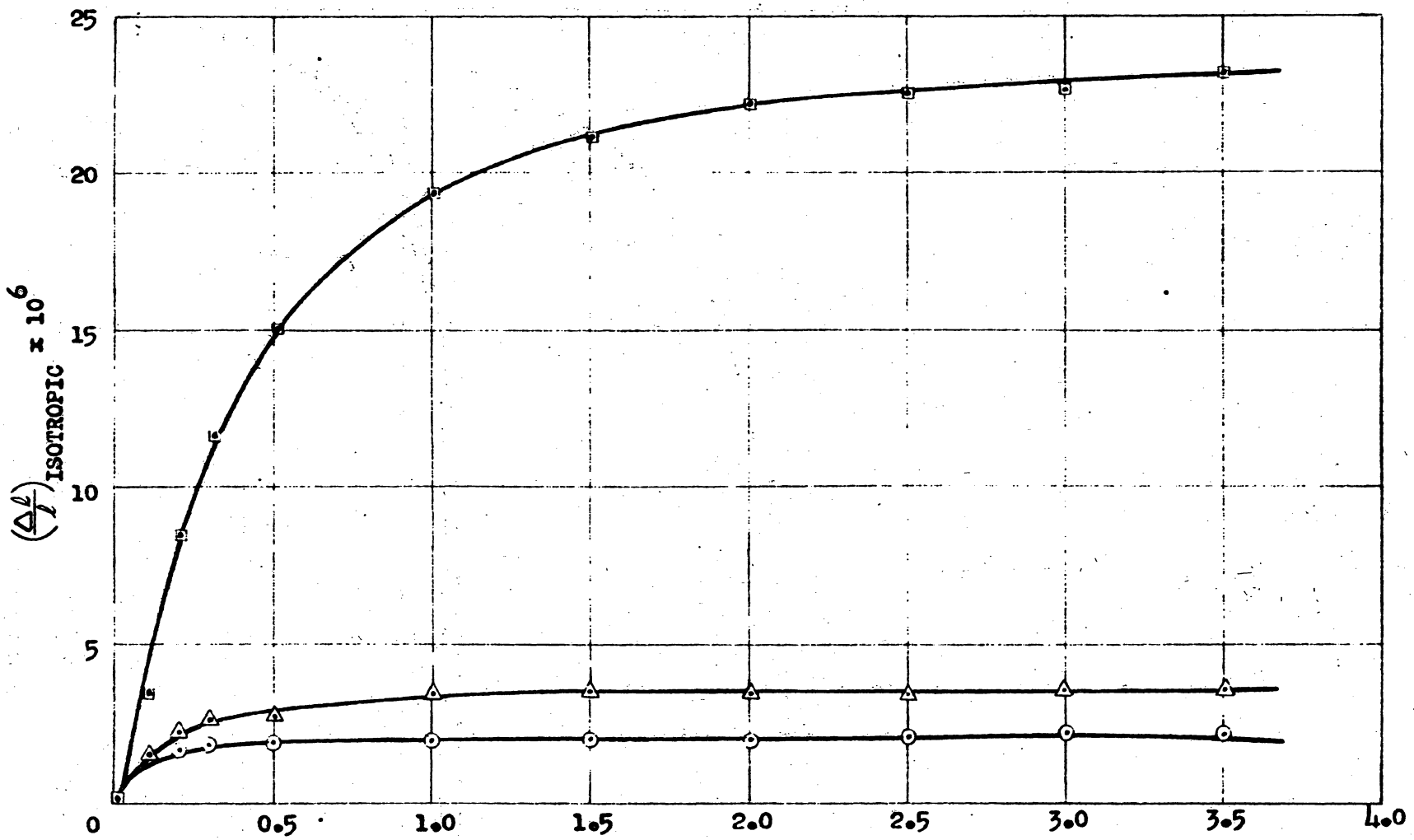

FIG. 5-12
ISOTROPIC MAGNETOSTRICTION
SAMPLE #12 (χ=.55)

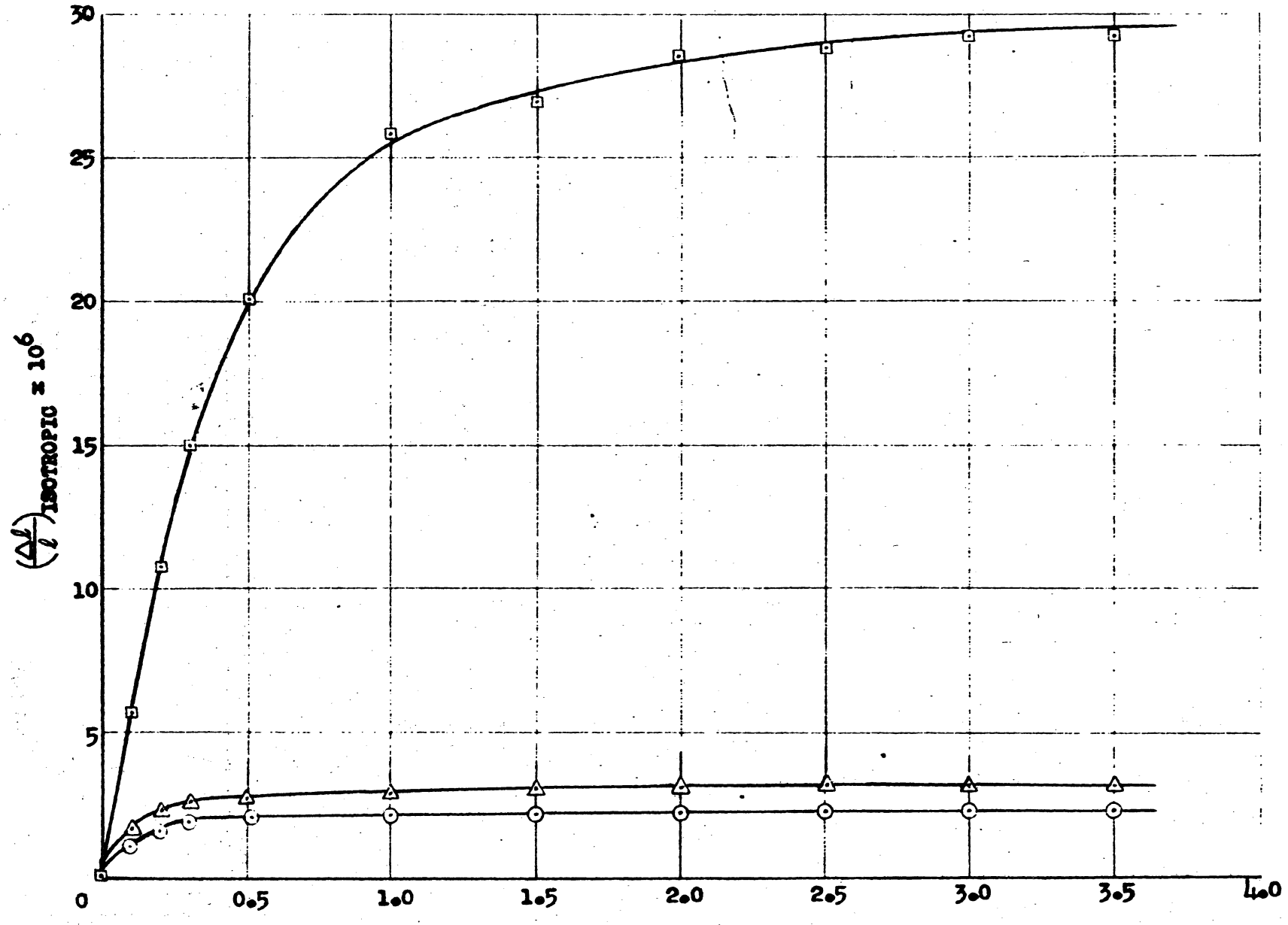

FIG. 5-13
ISOTROPIC MAGNETOSTRICTION SAMPLE #13 (γ=.6)

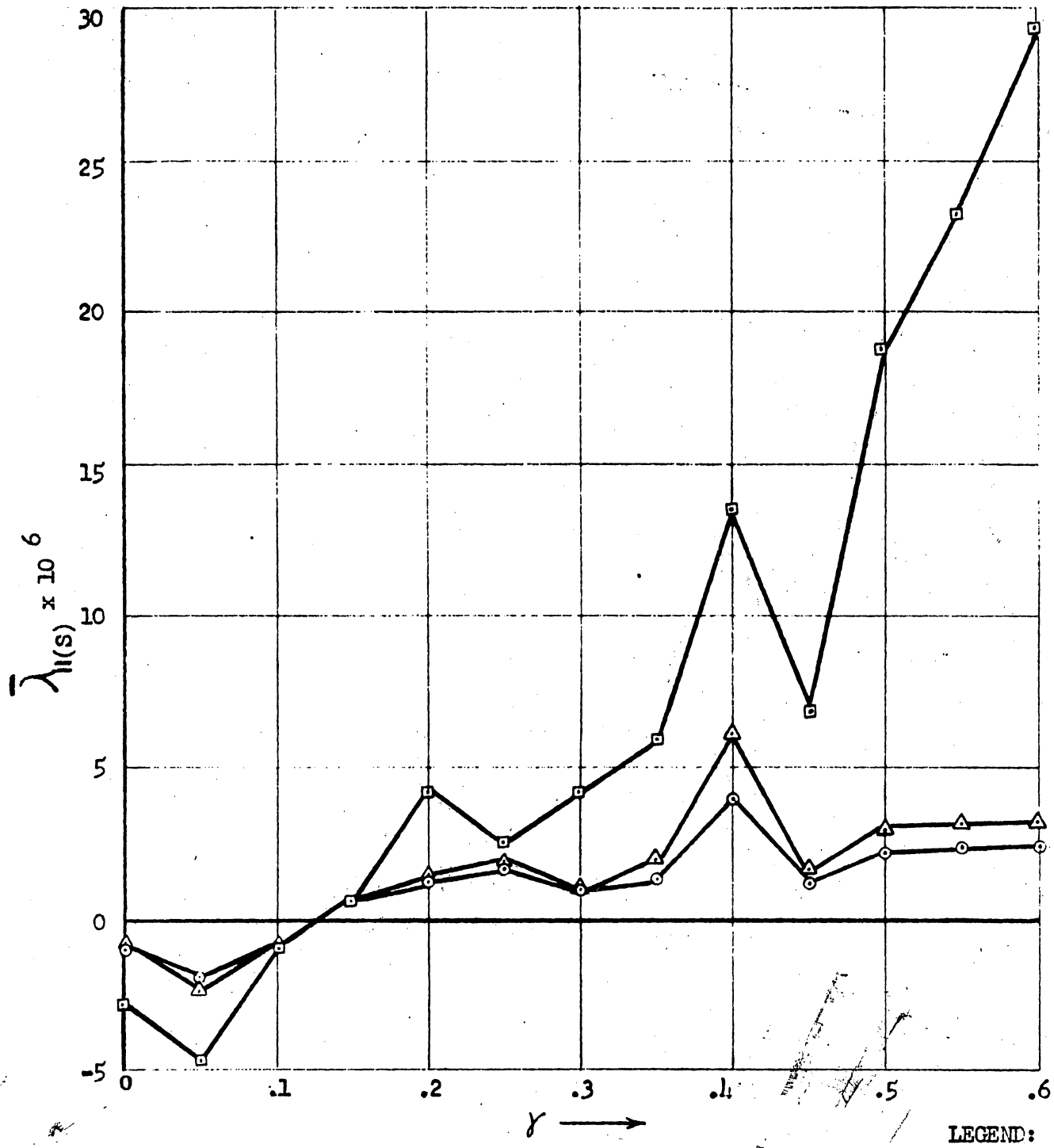

FIG. 5-14

SATURATION MAGNETOSTRICTION vs COMPOSITIONAL PARAMETER γ

low in magnitude for values of γ below $\gamma = 0.13$. Above $\gamma = 0.13$ the $\overline{\lambda}_{\parallel(S)}$ increases to positive values for 0 C and 20 C; at -78 C it increases to the relatively high value of 30×10^{-6} for $\gamma = 0.6$. It should be noted that $\gamma \approx 0.15$ was the critical value for squareness found in the compositional survey discussed in Chapter II.

B. Magnetostriction Parallel to Saturation Field

These data are obtained by measuring the change in strain parallel to field as the magnetic moments relax when the field is reduced from a saturation value; the $\overline{\lambda}_{\parallel(S)}$ obtained from the previously discussed data is added to obtain the correct zero reference. The individual data obtained for the 13 samples are shown in Figures 5-15 to 5-27.

Since the saturation value of these data have been determined from previously discussed data, the remaining significant feature is the field dependence relative to the value at saturation fields. The characteristic field dependence, with very few exceptions, is that the value of the magnetostriction goes through zero and reverses in sign as the field is reduced from saturating values. This reversal phenomenon has been observed on iron and other materials. It is called the Villari reversal after E. Villari who first observed the effect in 1865.[23]

The Villari reversal remains when the saturation value changes sign from that for $0 \leqslant \gamma \leqslant 0.13$ to that for $0.13 \leqslant \gamma \leqslant 0.6$. Also the reversal generally becomes more marked at lower temperatures.

C. B-H and S_w Data

These data were obtained to supplement the magnetostriction data. Data were obtained on fired toroids at 20 C and on toroids cut from discs at -78 C, 0 C and 20 C.

In Figure 5-28 the maximum squareness for the hysteresis loop is plotted versus the compositional parameter γ. The hysteresis charac-

9-61359

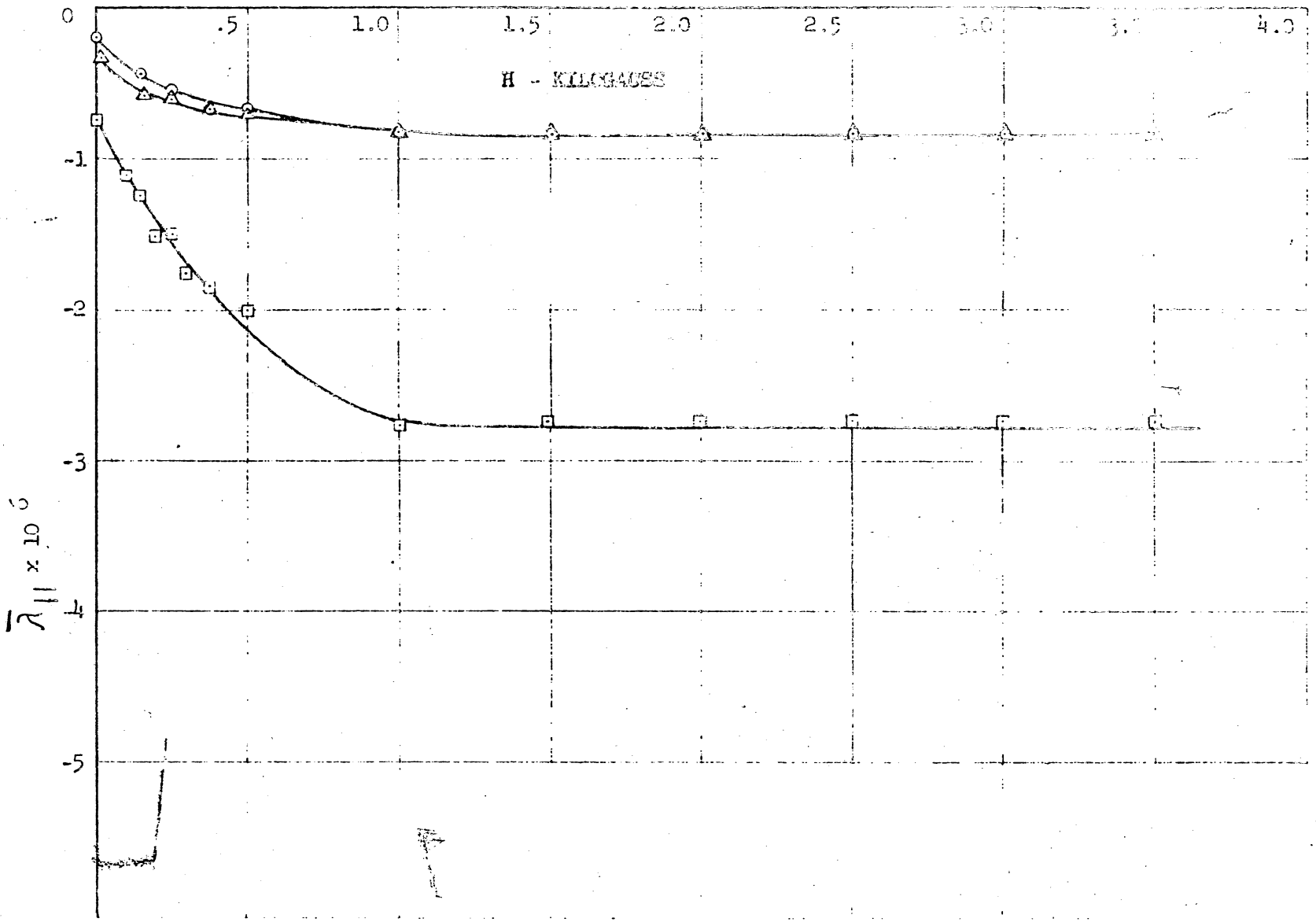

FIG. 5-15
MAGNETOSTRICTION IN DIRECTION OF SATURATING FIELD
SAMPLE # 1 ($\gamma = 0$)

LEGEND:
○ -70° C
△ 0° C
□ 20° C

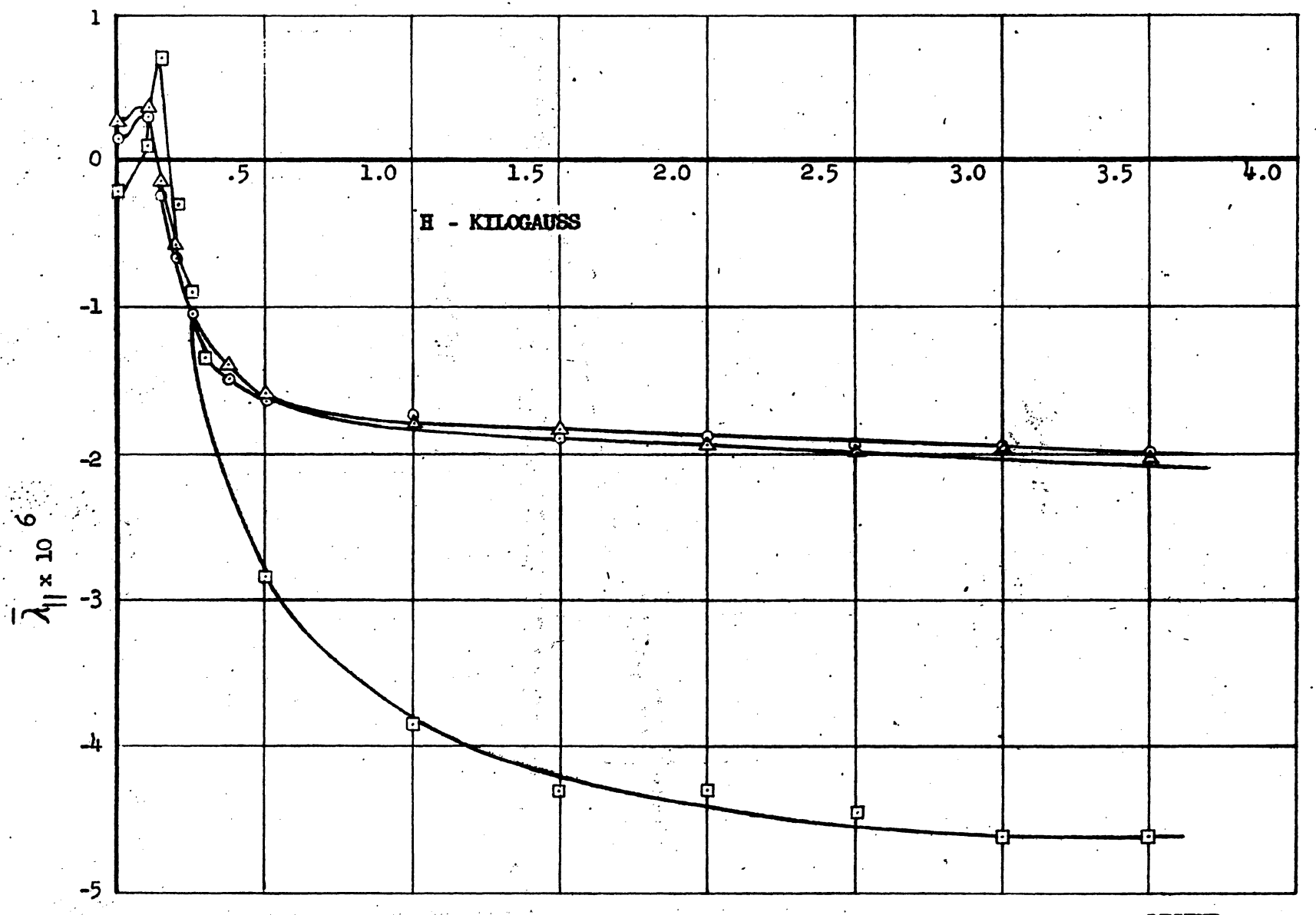

FIG. 5-16
MAGNETOSTRICTION IN DIRECTION OF SATURATING FIELD
SAMPLE #2 (γ = .05)

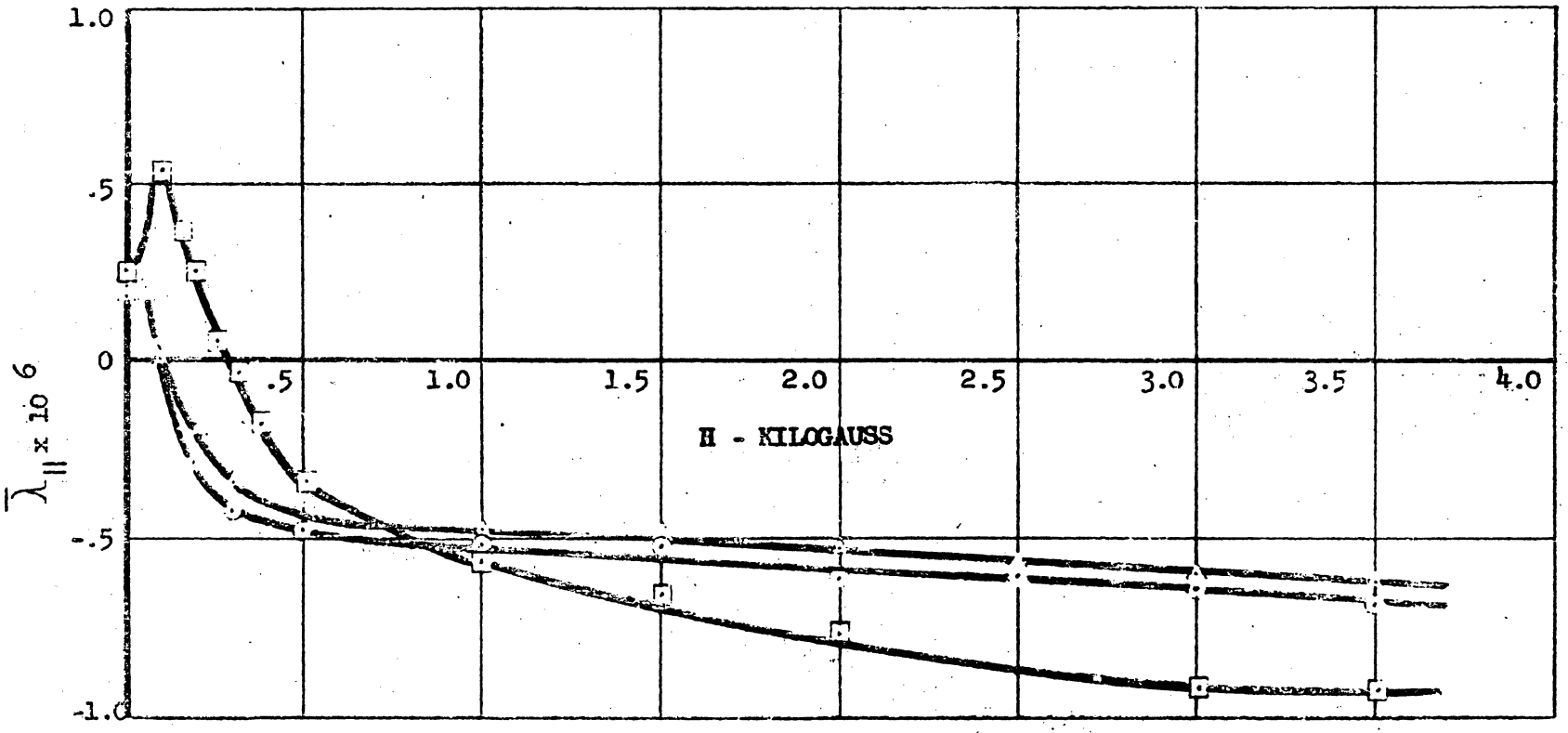

FIG. 5-17
MAGNETOSTRICTION IN DIRECTION OF SATURATING FIELD
SAMPLE #3 (γ = .1)

LEGEND:
□ 78° C
△ 0° C
○ 20° C

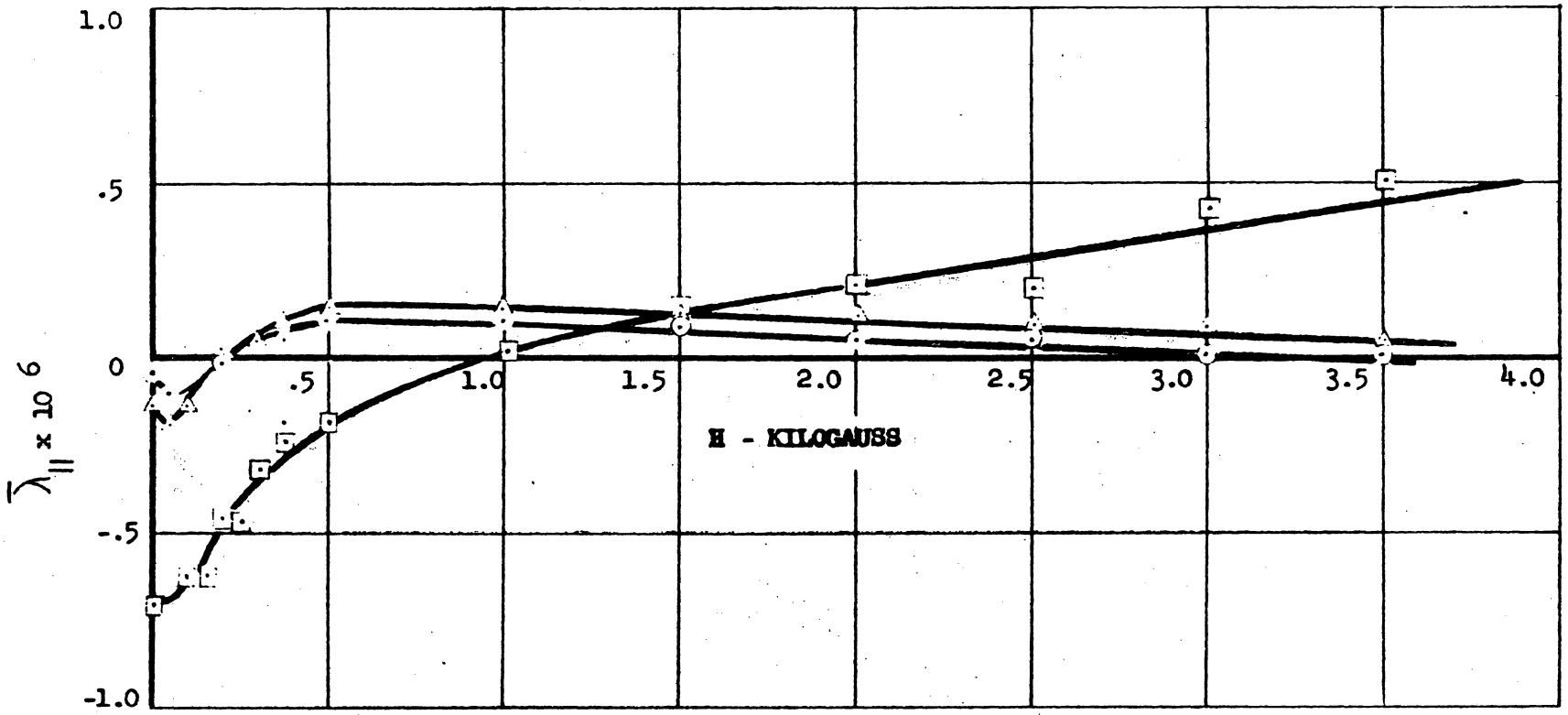

FIG. 5-18
MAGNETOSTRICTION IN DIRECTION OF SATURATING FIELD
SAMPLE #4 (γ = .15)

LEGEND:
⊡ -78° C
△ 0° C
⊙ 20° C

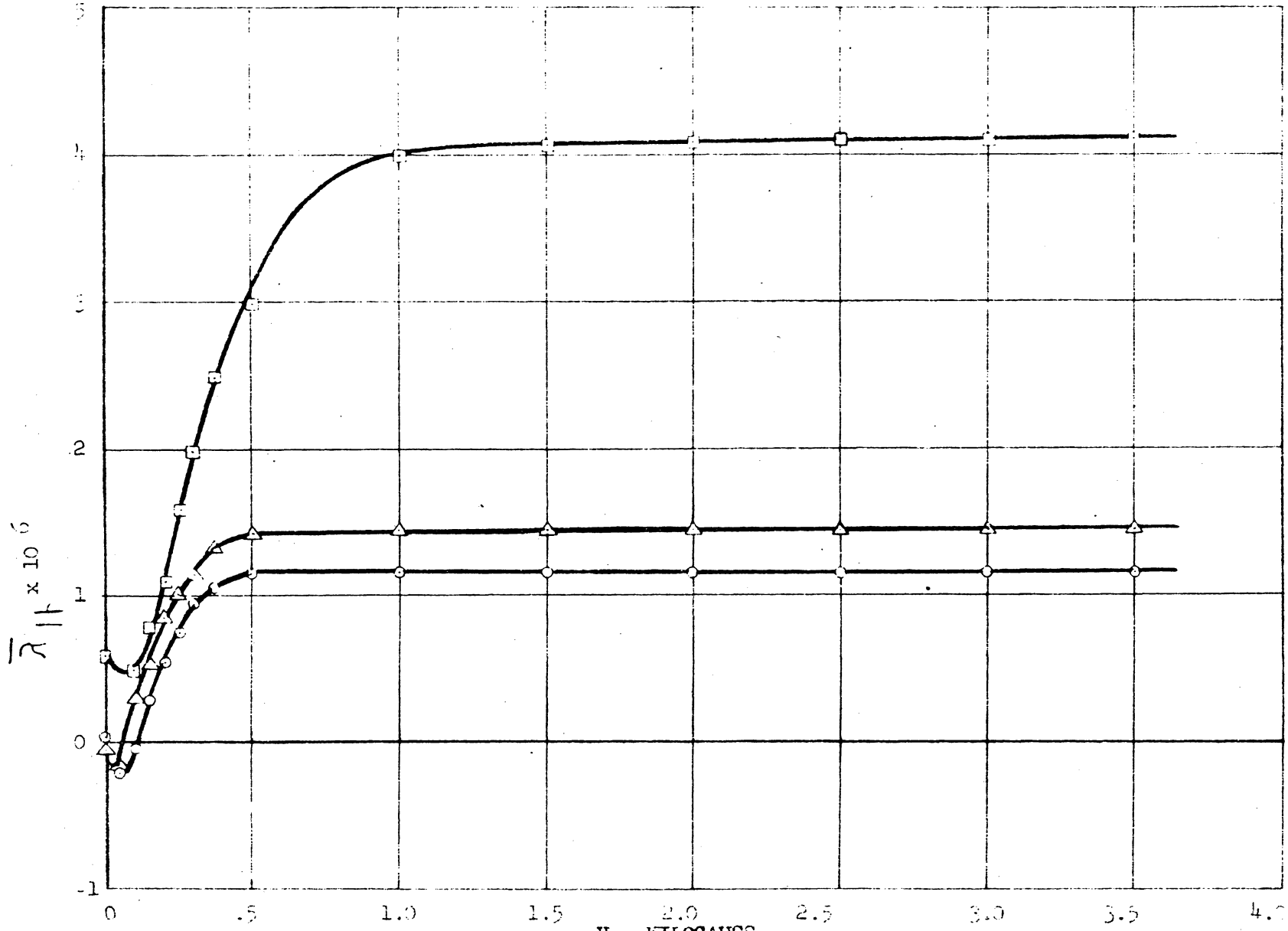

FIG. 5-19 MAGNETOSTRICTION IN DIRECTION OF SATURATING FIELD
SAMPLE #5 (γ = .2)

LEGEND:

□ -78° C
△ 0° C
○ 22° C

A-61355

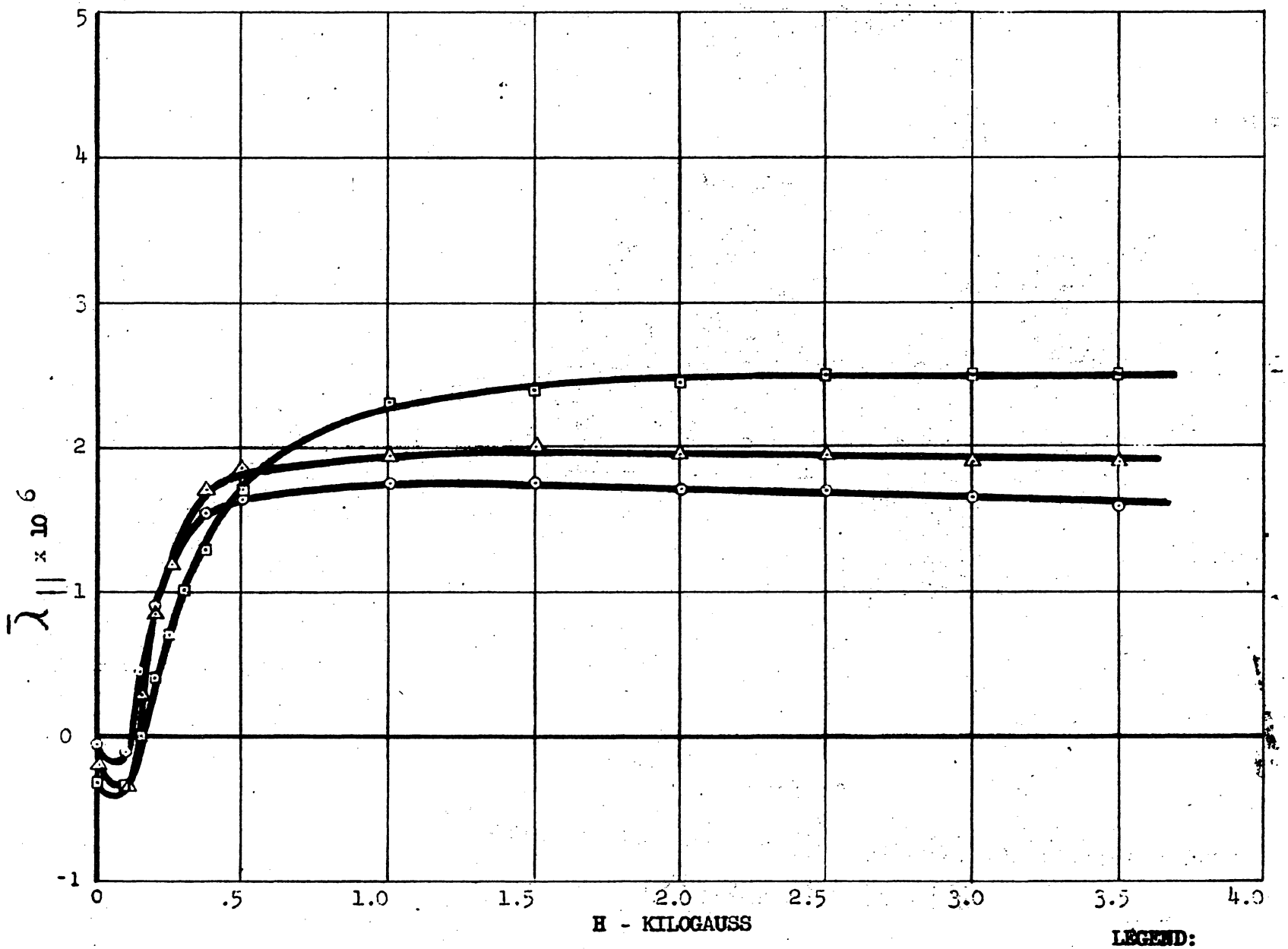

FIG. 5-20 MAGNETOSTRICTION IN DIRECTION OF SATURATING FIELD
SAMPLE #6 (γ = .25)

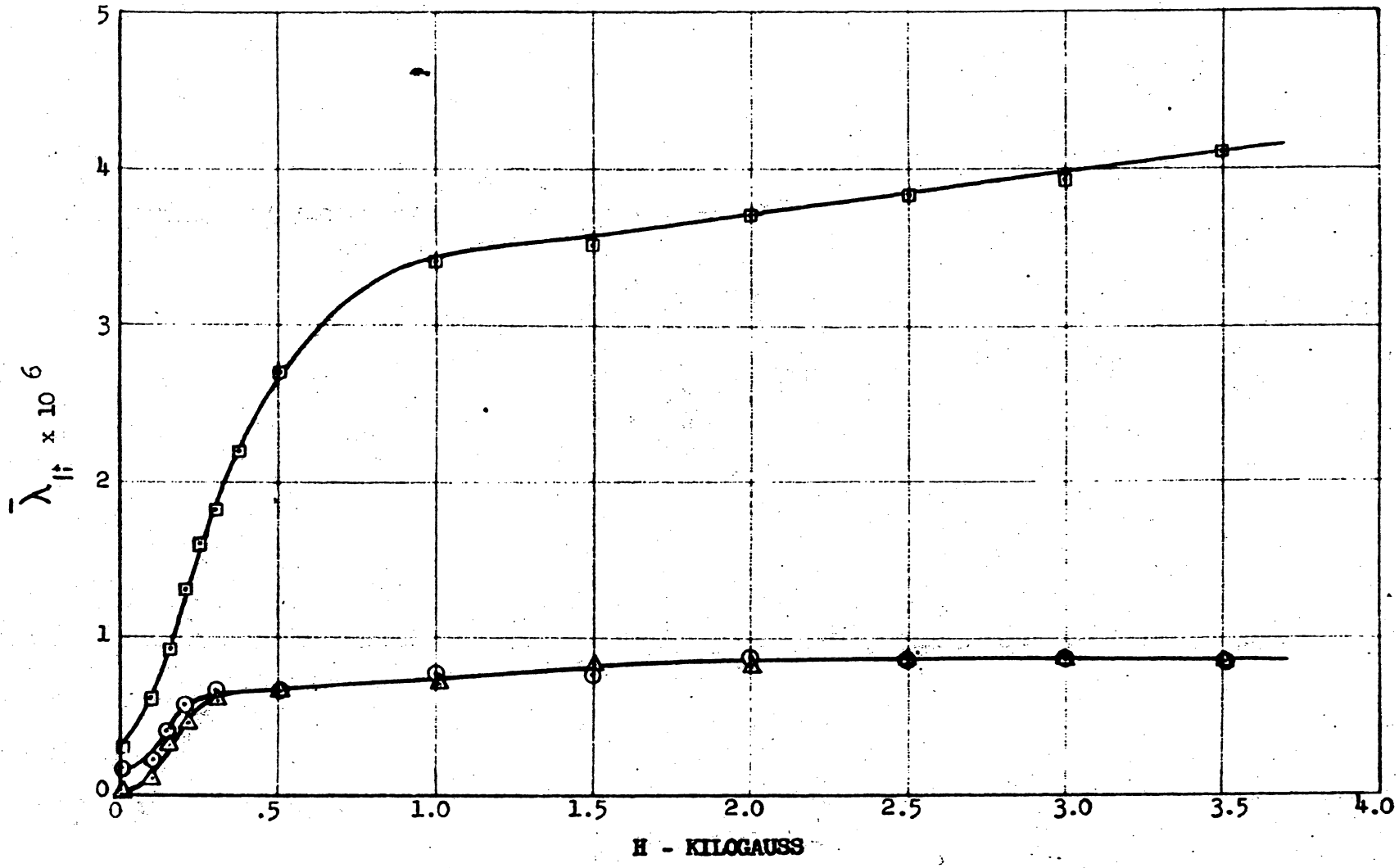

FIG. 5-21

MAGNETOSTRICTION IN DIRECTION OF SATURATING FIELD

SAMPLE #7 (γ = .3)

A-61357

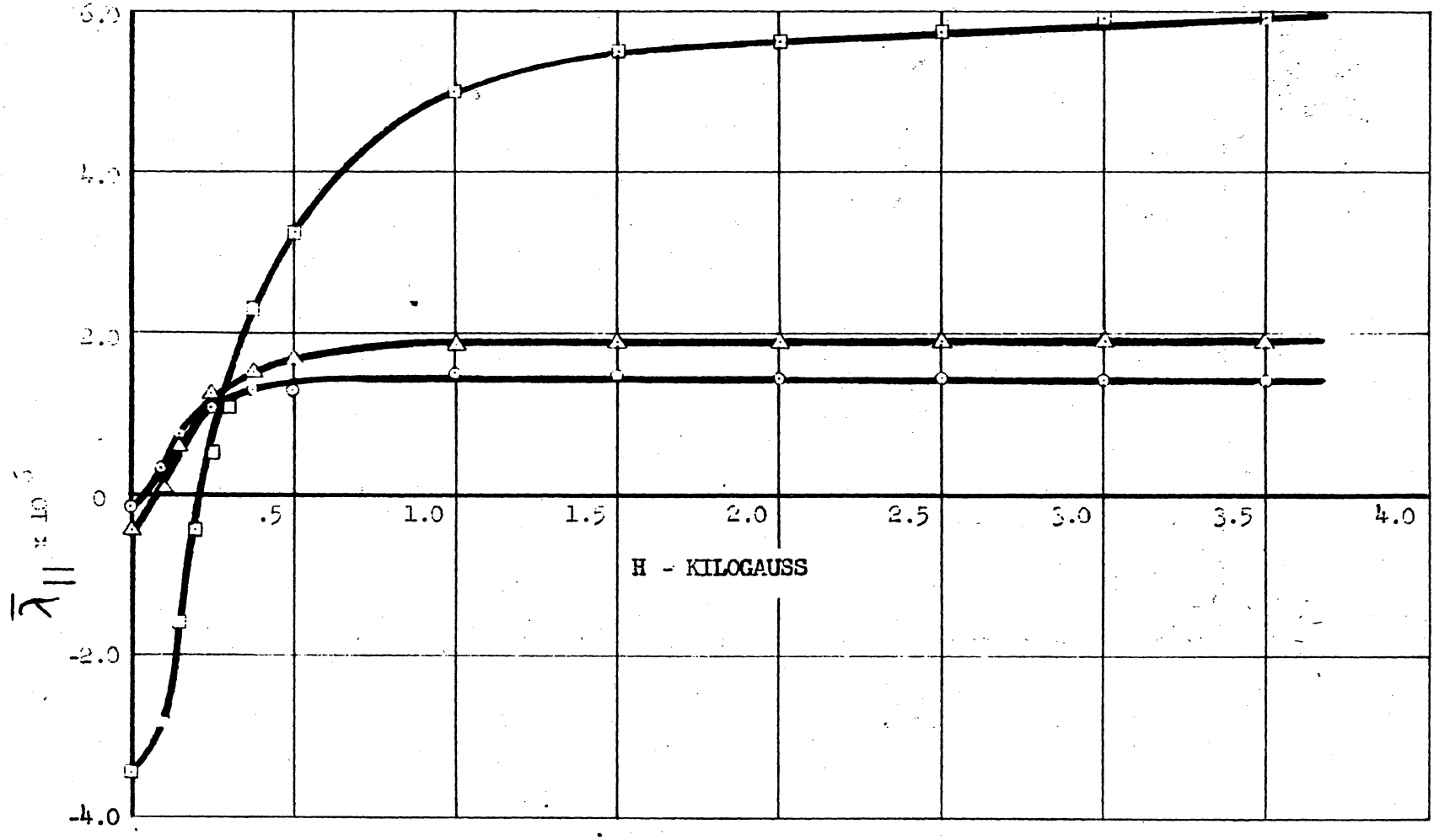

FIG. 5-22
MAGNETOSTRICTION IN DIRECTION OF SATURATING FIELD
SAMPLE #8 (γ = .35)

LEGEND:
□ -78°C
△ 0°C
○ 25°C

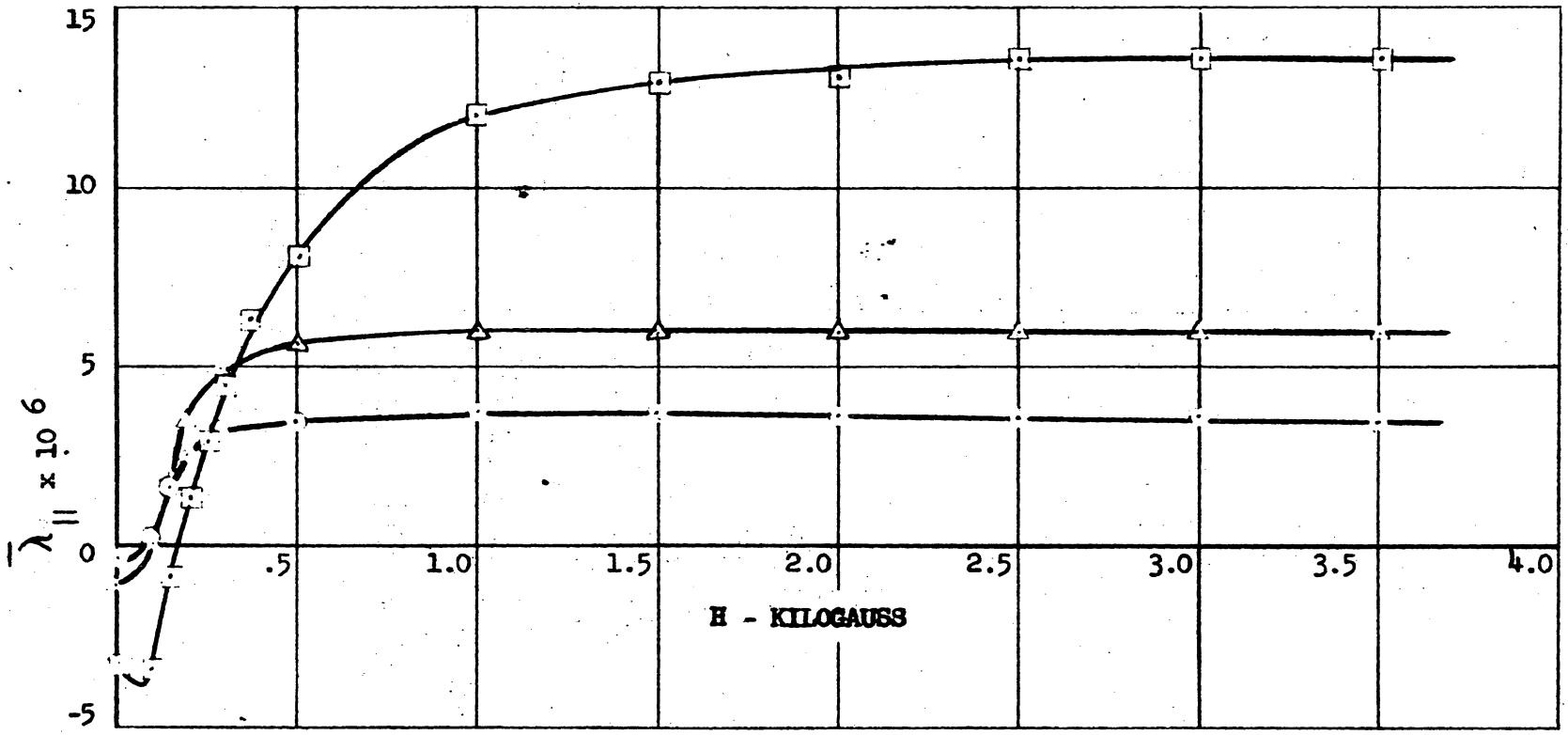

FIG. 5-23
MAGNETOSTRICTION IN DIRECTION OF SATURATING FIELD

SAMPLE #9 (γ = .4)

LEGEND:
⊡ 78° C
△ 0° C
⊙ 20° C

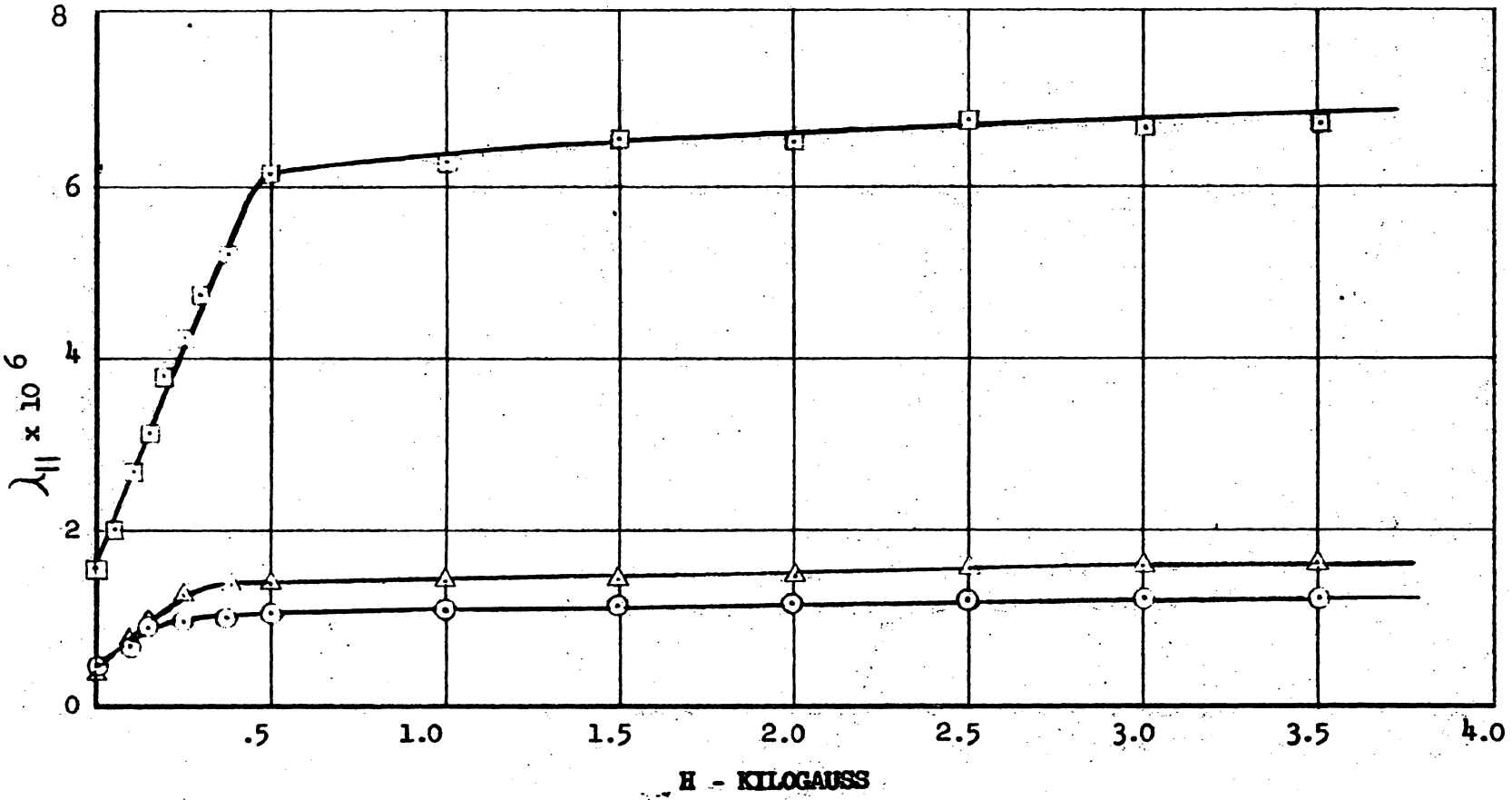

FIG. 5-24 MAGNETOSTRICTION IN DIRECTION OF SATURATING FIELD
SAMPLE #10 (γ = .45)

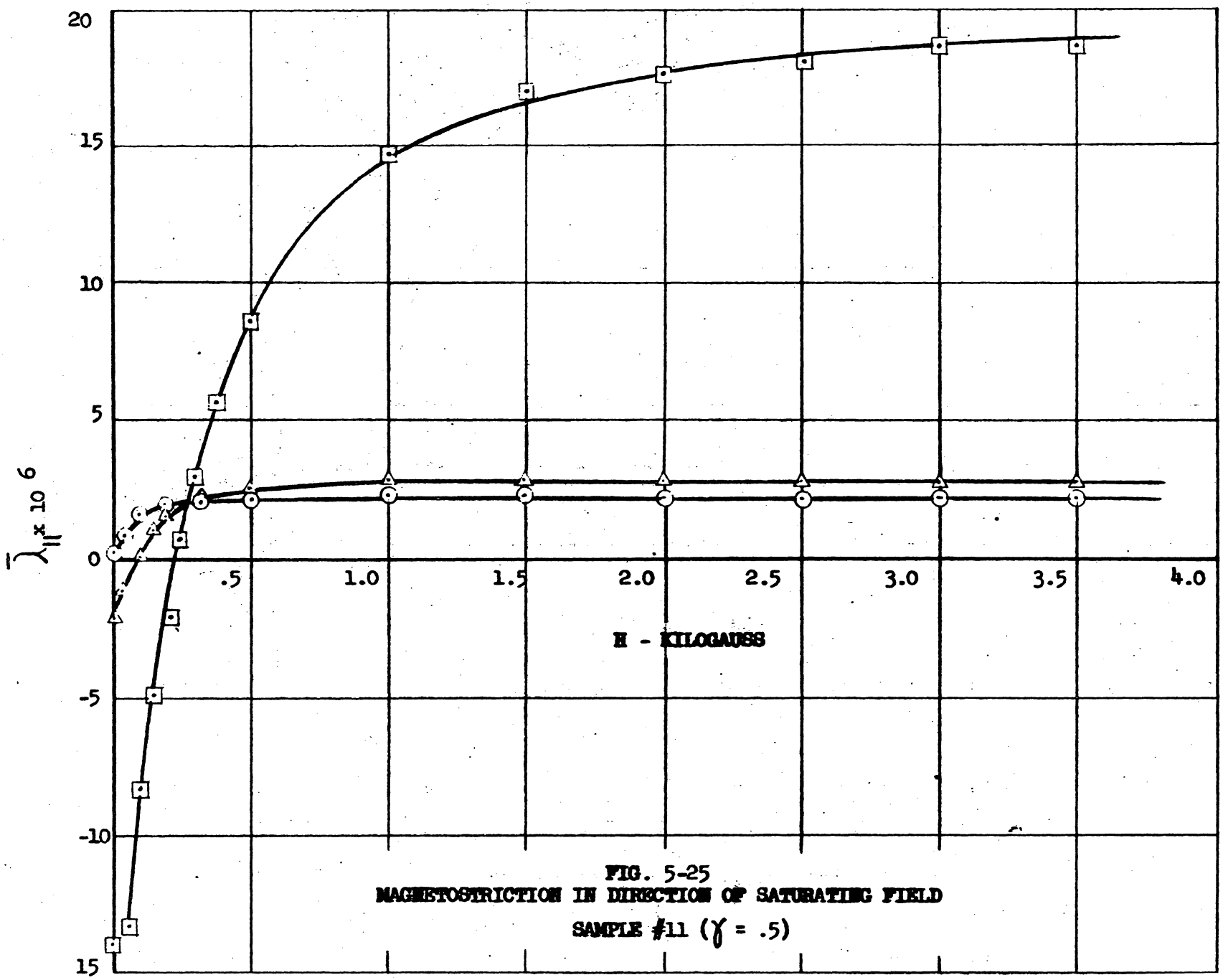

FIG. 5-25
MAGNETOSTRICTION IN DIRECTION OF SATURATING FIELD
SAMPLE #11 (γ = .5)

LEGEND:
⊡ -78° C
△ 0° C

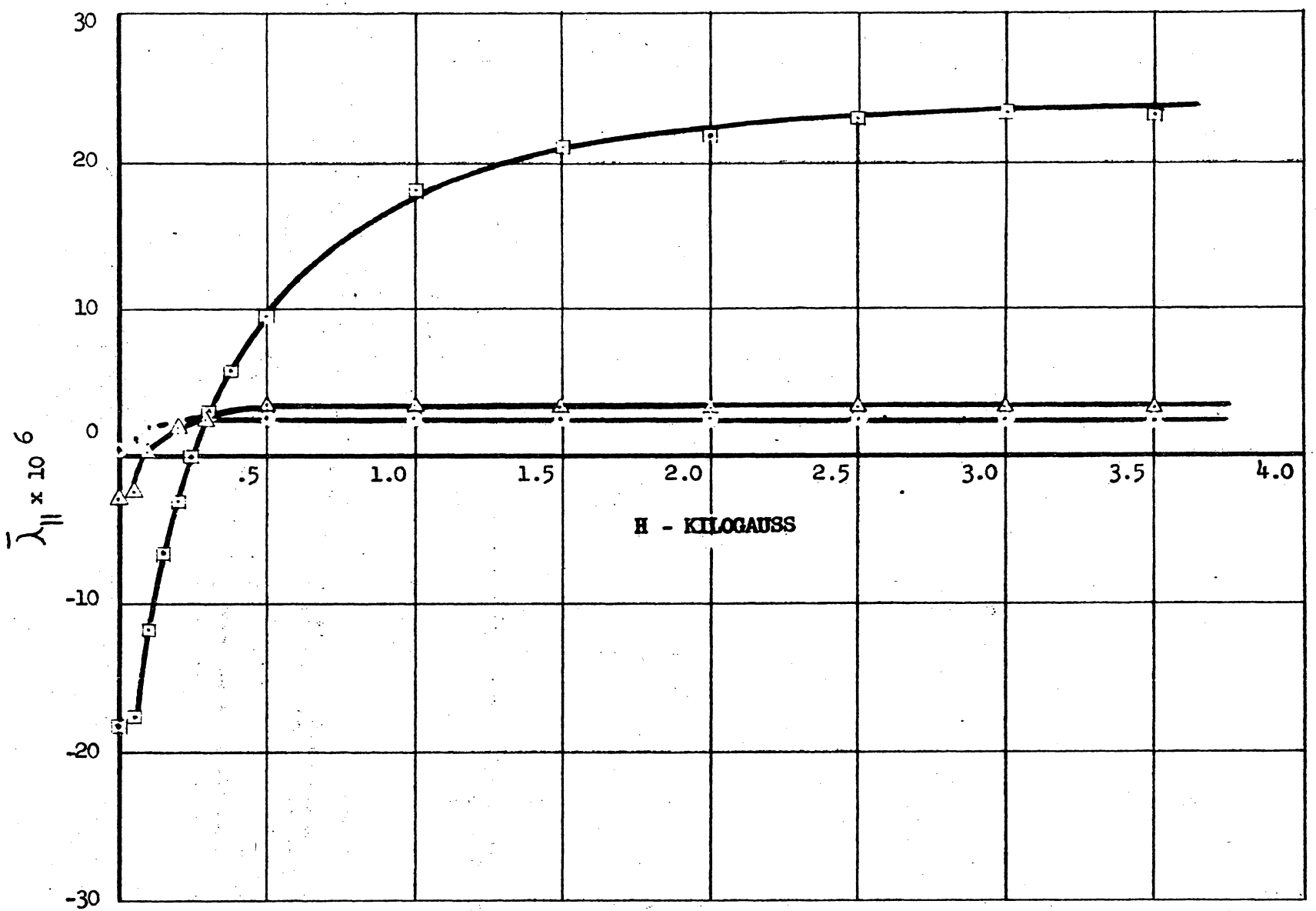

FIG. 5-26
MAGNETOSTRICTION IN DIRECTION OF SATURATING FIELD

SAMPLE #12 (γ = .55)

LEGEND:
⊡ -78° C
△ 0° C
⊙ 20° C

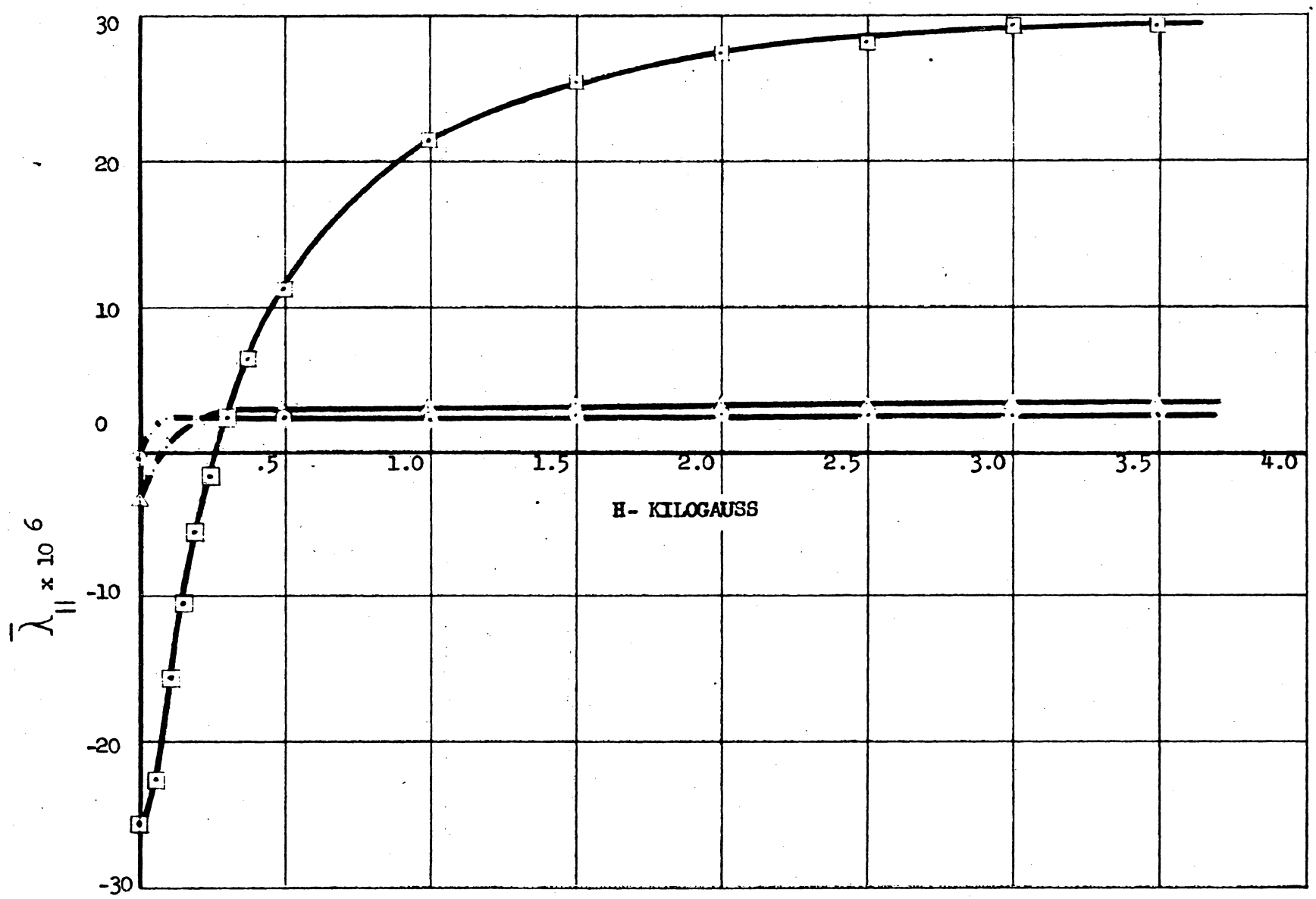

FIG. 5-27

MAGNETOSTRICTION IN DIRECTION OF SATURATING FIELD

SAMPLE #13 ($\gamma = .6$)

LEGEND:

⊡ -78° C

△ 0° C

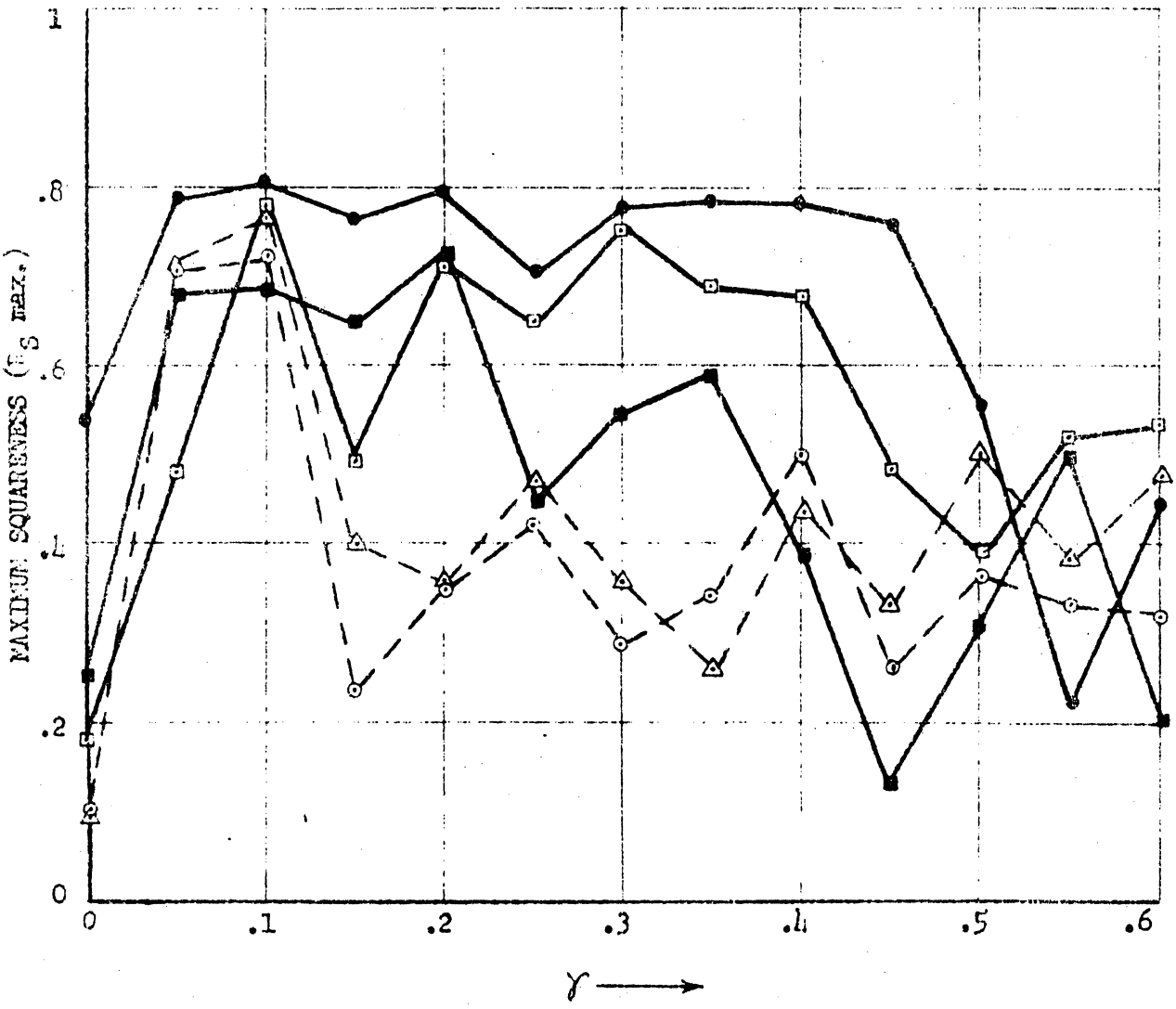

LEGEND:

CUT TOROIDS
- -200° C ■
- -78° C ⊡
- 0° C △
- 20° C ⊙

FIRED TOROIDS 20° C ●

FIG. 5-28
MAXIMUM SQUARENESS **vs.** COMPOSITONAL PARAMETER γ

teristics are very sensitive to the chemical homogeneity, grain size, and void density. Therefore, the rather wide dispersion found for the cut toroids is quite understandable owing to difficulties in controlling the firing conditions for the disc samples. The data shown for the fired toroids is much more indicative for the optimum squareness for each value of γ, but even for these samples slight variations in the crystalline structure are very apparent in the maximum-squareness data. In general, however, there exists a broad maximum of $R_s \lesssim 0.8$ from $\gamma = 0.05$ to $\gamma = 0.45$; this is consistent with the data of Figure 2-1 which was obtained on a general compositional survey.

The saturation flux density B_s that is shown in Figure 5-29 is that measured for fields of about 20 oersteds in the cut toroidal samples. These data are less sensitive to chemical homogeneity, grain size, and void density than R_s. The general variation of B_s with γ is in complete agreement with the data obtained on a general compositional survey. A saturation-moment measurement has also been made, at H = 10,000 oersteds, on the disc center of samples No. 3, 6, and 11. The room-temperature flux densities calculated for these samples are:

Sample	γ	B_s (H=10,000 oe.)	$\frac{B_s(H= 20 \text{ oe.})}{B_s(H= 10{,}000 \text{ oe.})}$
3	0.1	2.9 kilogauss	0.86
6	0.25	2.9	0.96
11	0.5	2.1	0.81

The switching coefficient S_w was obtained from dynamical measurements in the following way: By definition $S_w = \tau (H-H_o)$, where τ is the time for a complete flux reversal, H is the applied field, and H_o is the average threshold field for domain-wall motion. Therefore, $1/\tau$

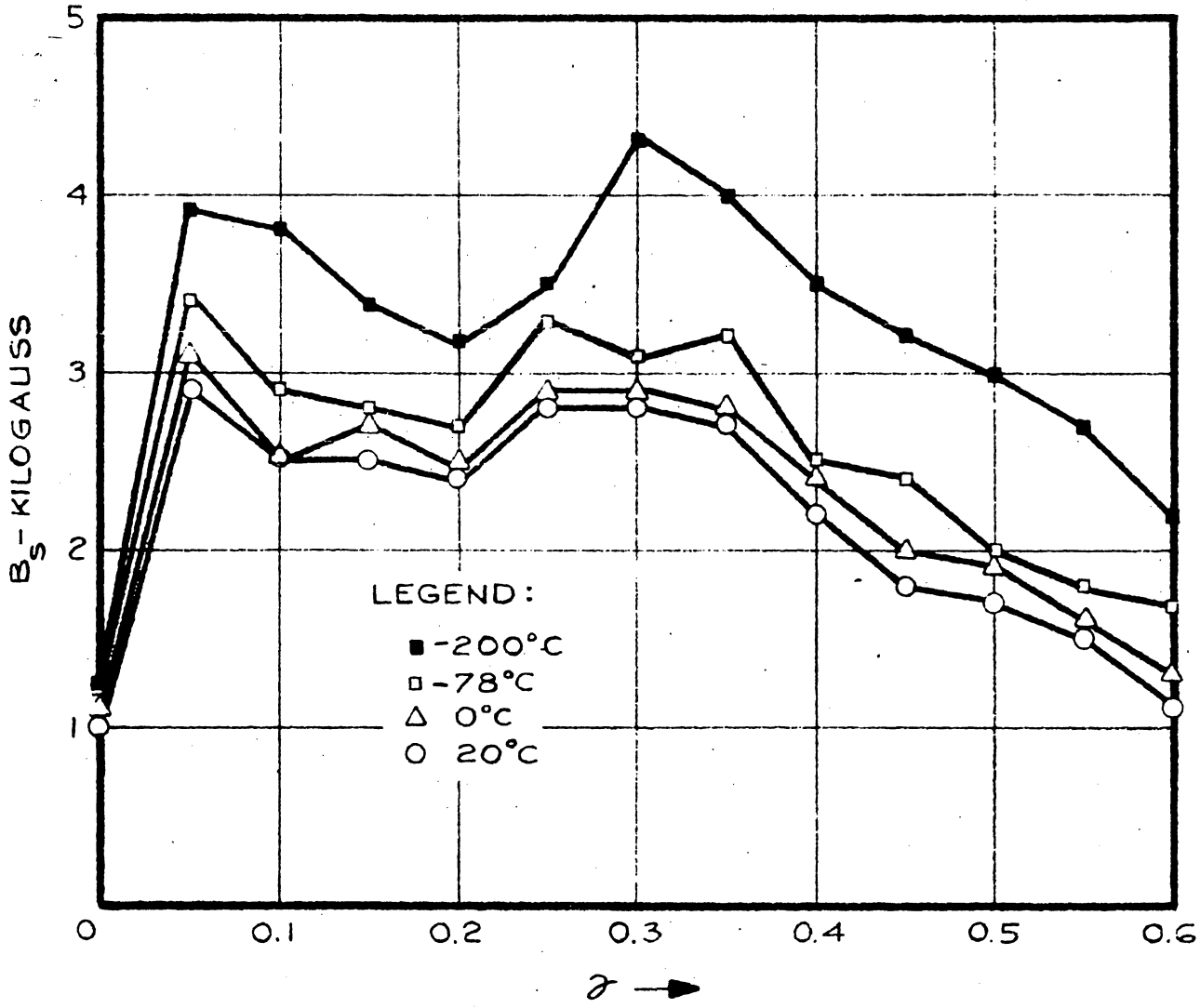

FIG. 5-29

SATURATION FLUX DENSITY vs COMPOSITIONAL PARAMETER γ

is plotted versus H as shown in Figure 5-30. The switching coefficient S_w therefore is the reciprocal slope of the linear portion of this plot.

The switching coefficient S_w versus the compositional parameter γ is shown in Figure 5-31. S_w does not vary significantly with composition; there is only a gradual increase with γ. However, a very strong variation is found as the temperature is changed to - 200 C; S_w increases to about three times its room-temperature value for most values of γ.

The Curie temperature T_c is that temperature at which the thermal energy overcomes the magnetic-exchange energy. At this point the material becomes paramagnetic as the temperature is increased further. Therefore, the value of T_c is indicative of the magnitude of the magnetic-exchange energy in the material. The permeability of square-loop ferrites has a sharp discontinuity at T_c. Therefore, T_c was determined using a 1000-cycle permeammeter. A typical output plot from the permeammeter is shown in Figure 5-32. The arithmetic average between the discontinuity found for increasing temperature and that for decreasing temperature was used for the value of T_c. In Figure 5-33 T_c is plotted versus the compositional parameter γ. A monotonic decrease in T_c is found as γ increases.

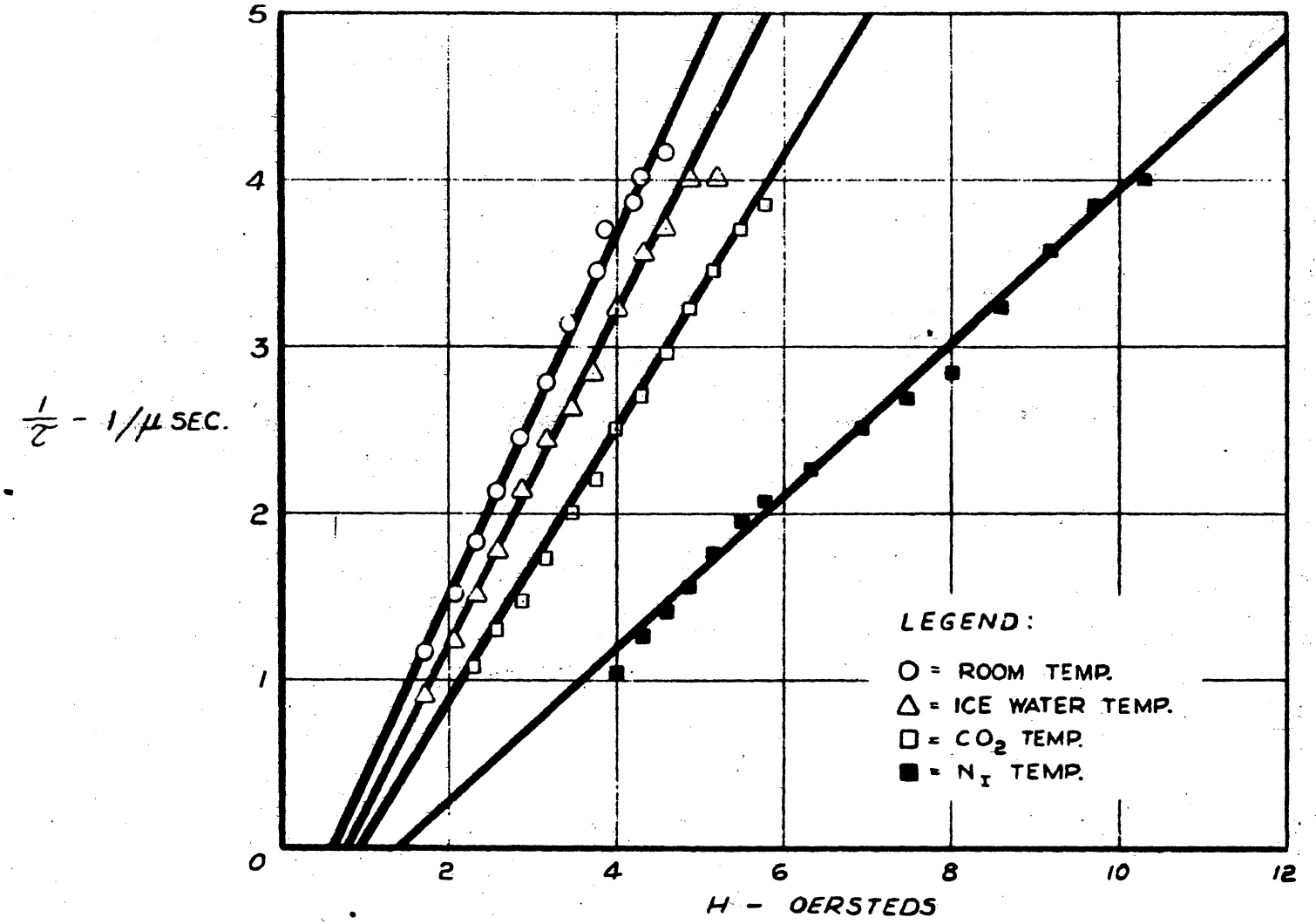

FIG. 5.30

TYPICAL PLOT FOR THE DETERMINATION OF THE SWITCHING COEFFICIENT S_w.

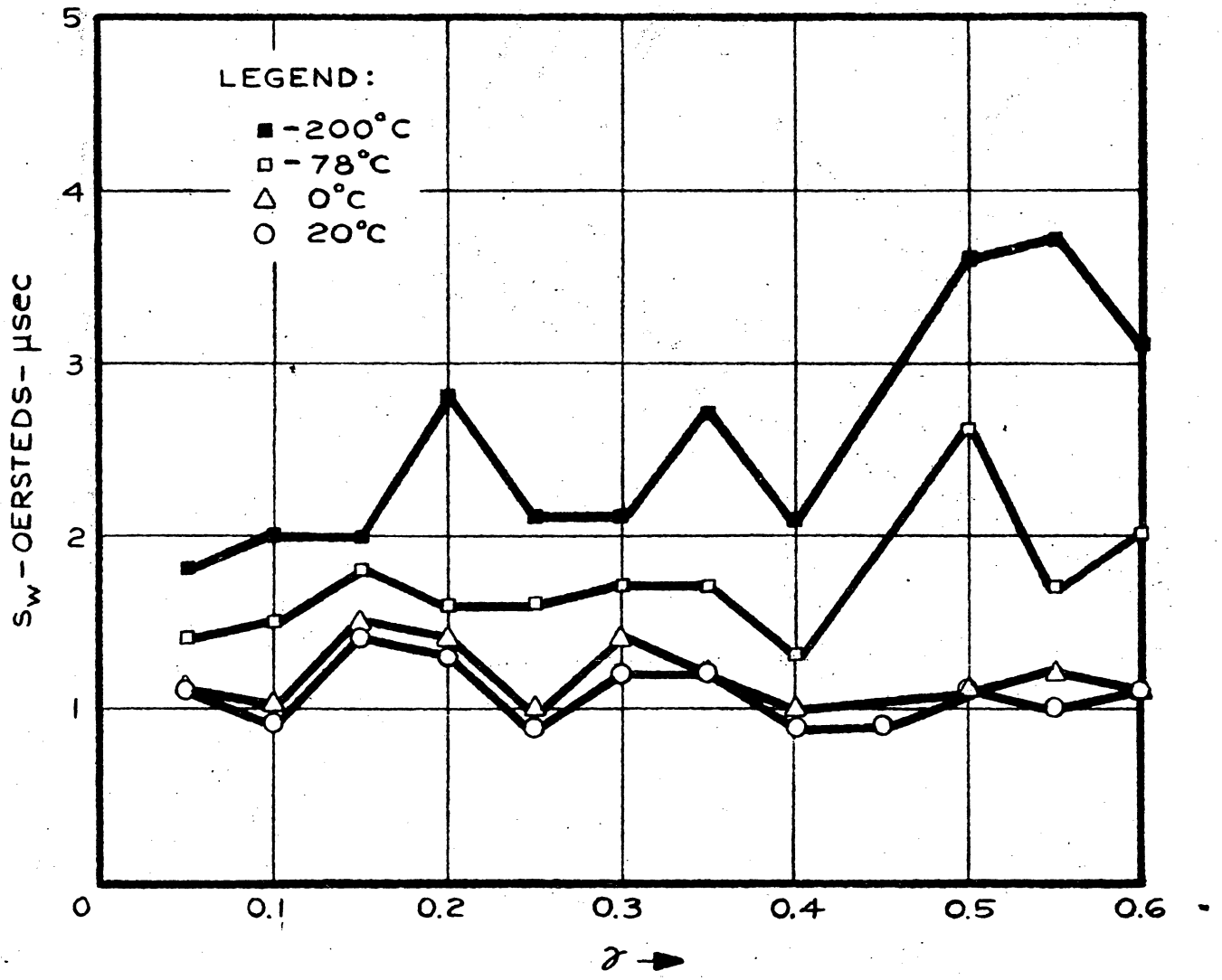

FIG. 5-31

SWITCHING COEFFICIENT vs COMPOSITIONAL PARAMETER γ

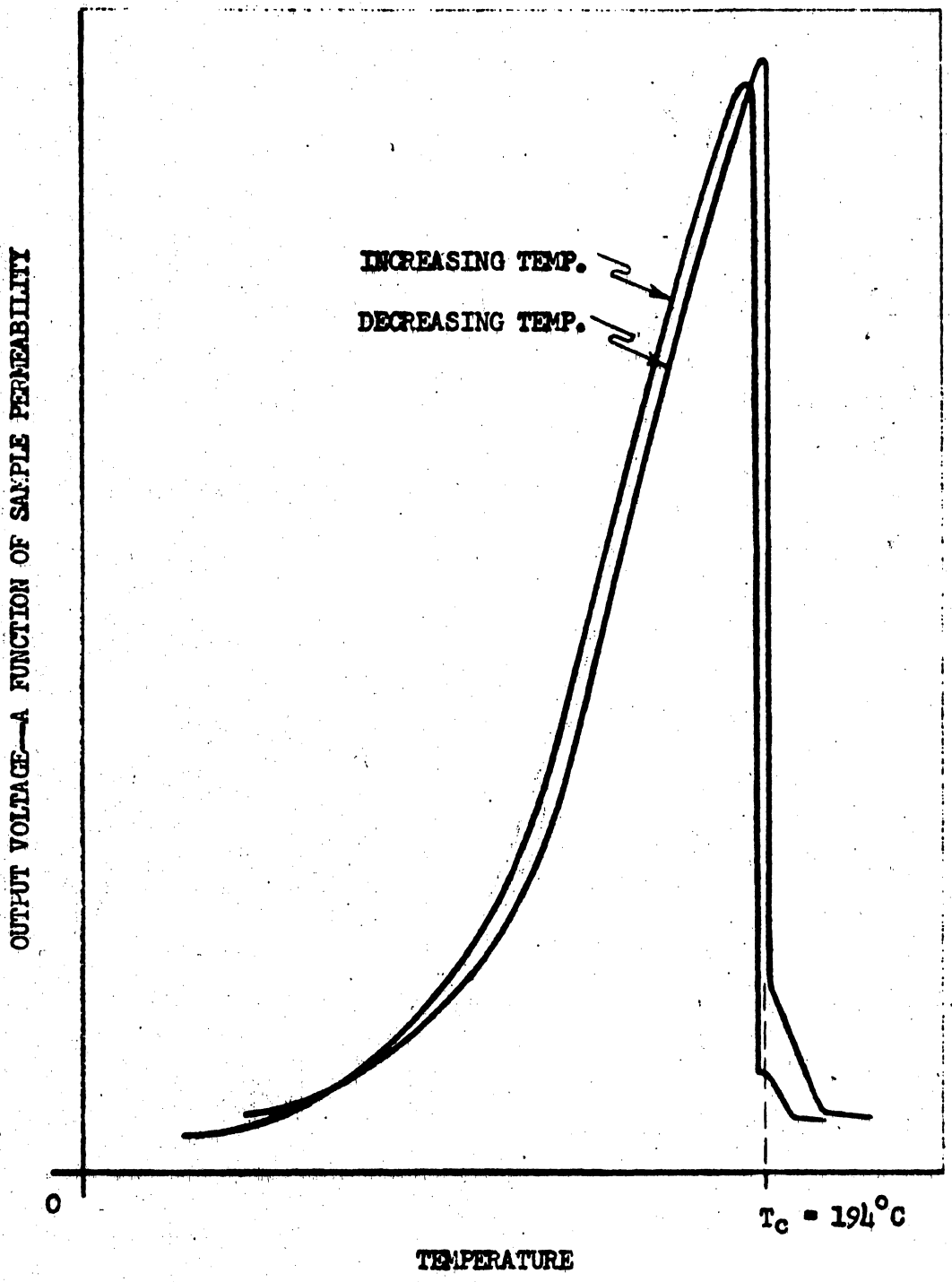

FIG. 5-32

TYPICAL CURIE POINT DETERMINATION

SAMPLE #7, (γ = .3)

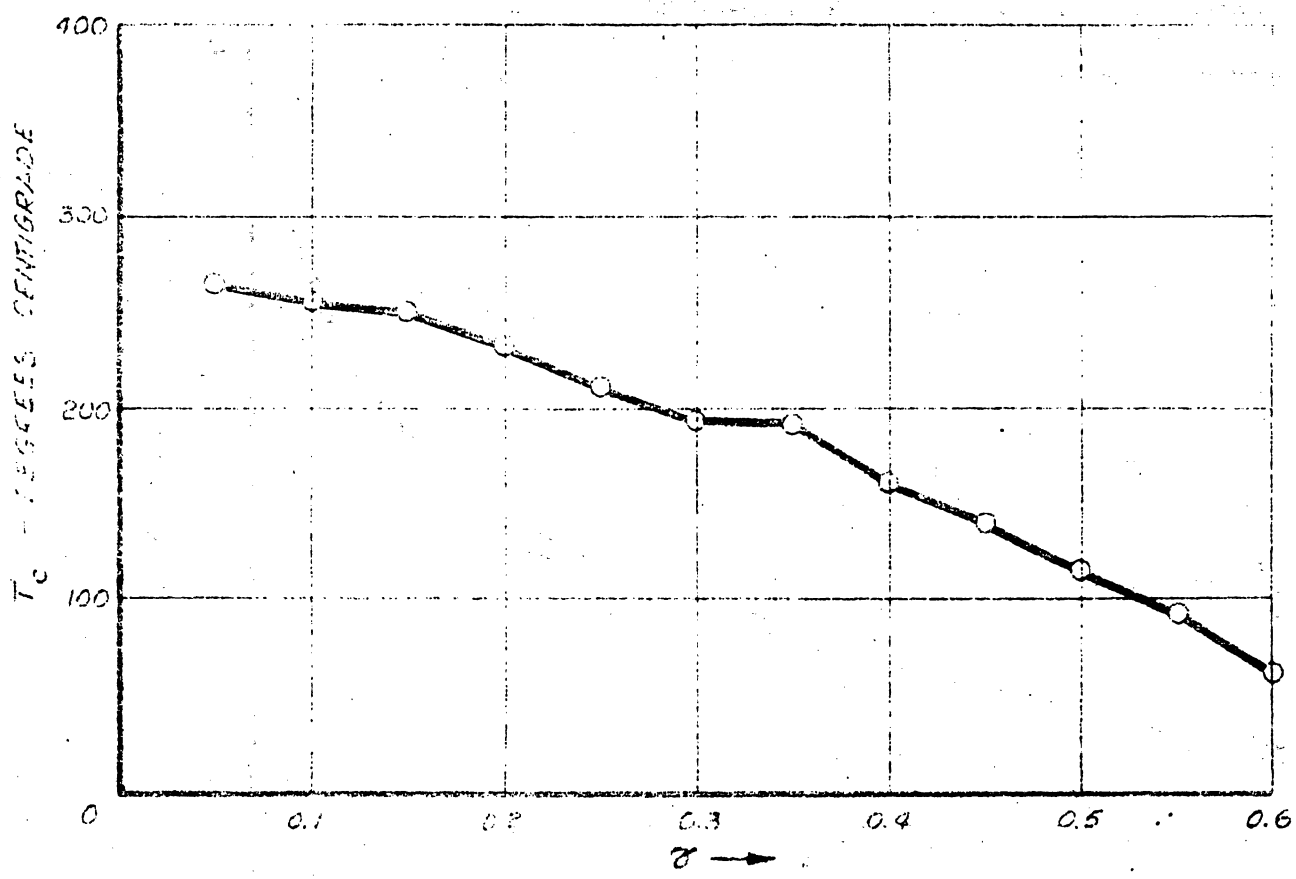

FIG. 5-33

CURIE TEMPERATURE vs. COMPOSITIONAL PARAMETER σ

CHAPTER VI

INTERPRETATION OF RESULTS

A. Effective Anisotropy

The magnetostriction data in Figures 5-14 to 5-27, inclusive, permit a qualitative interpretation of the fundamental mechanisms involved in producing the observed effects. These interpretations must then be compatible with the supplementary B-H, S_w, and T_c measurements.

The effective domain anisotropy energy K_d describes the energy potential producing the actual angular dependence of the magnetization of any domain relative to the externally applied field. Although K_d is affected by the local demagnetizing fields and the shape effects of the individual crystallites, in polycrystals it is mainly the result of the crystalline anisotropy energy K and the magnetoelastic energy due to magnetostrictive effects; the magnetic poles associated with the grain boundaries are relatively weak, and the grains are approximately spherical. When the applied field just equals the demagnetizing field $H \simeq 100$ oerseteds, the effective field is zero. When the effective field is zero, the crystallite moments are along equilibrium directions determined by K_d.

The sign of K_d will be considered to have the same general meaning as that given the sign of the crystalline anisotropy K. If $K_d \simeq K$ the directions of easy magnetization would be the $\langle 100 \rangle$ or the $\langle 111 \rangle$ directions for $K_d > 0$ or $K_d < 0$, respectively. For the more general case in which $K_d \neq K$, the direction of the crystallite moments will be near the $\langle 100 \rangle$ or the $\langle 111 \rangle$ directions for $K_d > 0$ or $K_d < 0$, respectively. When $K_d = 0$, the crystallite moments will not turn from

the direction of saturation when the effective field is zero.

If a saturation field is applied and removed, the magnetostriction measured parallel to the saturation field in a zero effective field is defined as $\overline{\lambda}_{\parallel(H=0)}$. Examination of the data shows that $\overline{\lambda}_{\parallel(H=0)}$ changes sign from positive to negative values as γ increases through 0.13, while $\overline{\lambda}_{\parallel(S)}$ also changes sign from negative to positive for the same compositional variation. This indicates an apparent change in the sign of K_d as will be shown. First, however, these data will be analyzed for three assumed values of K_d as γ increases through the critical value $\gamma = 0.13$.

Case I: $K_d = K$ and is large and negative. For this condition $\overline{\lambda}_{\parallel(H=0)} = \overline{\lambda}_{\parallel(111)} = 0.64\varepsilon\,\lambda_{100}$. Therefore, to satisfy the data, either ε or λ_{100} must go through 0, from positive to negative.

Case 2: $K_d = K$ and is large and positive. For this condition $\overline{\lambda}_{\parallel(H=0)} = \overline{\lambda}_{\parallel(100)} = 0.55\,\lambda_{100}$. Therefore, in this case λ_{100} must go through 0 from a positive to a negative value.

Case 3: $K_d = 0$ at $\gamma = 0.13$. For this case $\overline{\lambda}_{\parallel(H=0)} = \overline{\lambda}_{\parallel(S)} = \frac{3\varepsilon + 2}{5}\lambda_{100} = 0$. For this relation to hold, either λ_{100} must go through 0 or ε go through the value $\varepsilon = -\frac{2}{3}$ at $\gamma = 0.13$.

The results of this analysis must now be compared with interpretations of other features of the magnetostriction data.

B. The Villari Reversal

A Villari reversal in the magnetostriction is observed for all compositions whether γ is greater or less than its critical value $\gamma = 0.13$. This reversal is the result of an anisotropy in the magnetostriction of the crystallites and may be analyzed in terms of the ratio:

$$\chi = \overline{\lambda}_{\parallel(H=0)} / \overline{\lambda}_{\parallel(S)}.$$

Since the actual angular configuration of the crystallite moments is responsible for producing $\overline{\lambda}_{\parallel(H=0)}$, angular configurations must be assumed corresponding to the three cases of K_d considered above.

Case 1: $K_d = K$ and is large and negative. For this condition $\overline{\lambda}_{\parallel(H=0)} = \overline{\lambda}_{\parallel(111)}$. Therefore,

$$\chi = \frac{\overline{\lambda}_{\parallel(111)}}{\overline{\lambda}_{\parallel(S)}} = \frac{10\,\varepsilon}{\pi\,(3\varepsilon + 2)}, \qquad (6\text{-}1)$$

where $\varepsilon = \lambda_{111} / \lambda_{100}$.

Expressing ε in terms of χ, one obtains

$$\varepsilon = \frac{2\pi\,\chi}{10 - 3\pi\,\chi}. \qquad (6\text{-}2)$$

Since the experimental data has, in general, shown $\chi < 0$, it follows from Equation 6-2 that $-2/3 \leq \varepsilon \leq 0$.

Case 2: $K_d = K$ and is large and positive. For this case $\overline{\lambda}_{\parallel(H=0)} = \overline{\lambda}_{\parallel(100)}$. Therefore,

$$\chi = \frac{\overline{\lambda}_{\parallel(100)}}{\overline{\lambda}_{\parallel(S)}} = \frac{2\sqrt{3}}{\pi(3\varepsilon + 2)}. \qquad (6\text{-}3)$$

Expressing ε in terms of χ, one obtains

$$\varepsilon = \frac{2\sqrt{3} - 2\pi\,\chi}{3\pi\,\chi}. \qquad (6\text{-}4)$$

Since the experimental data has, in general, shown $\chi < 0$, it follows from Equation 6-4 that $-\infty \leq \varepsilon \leq -2/3$.

Case 3: $K_d = 0$. In this case $\overline{\lambda}_{\parallel(H=0)} = \overline{\lambda}_{\parallel(S)} = 0$, and χ is undefined.

C. Summary of Magnetostriction Data

The saturation magnetostriction, $\overline{\lambda}_{\parallel(S)} = \frac{3\varepsilon + 2}{5}\,\lambda_{100}$, goes through zero as the compositional parameter γ increases through the critical value $\gamma = 0.13$. Therefore, the final condition that must be fulfilled is that either ε must go through the value $\varepsilon = -2/3$ or λ_{100} go through zero for the same compositional variation. The necessary conditions for fulfilling the observed data for the three assumed values of

K_d are summarized for the composition $\gamma = 0.13$ in the chart below.

Cases	Condition on K_d	$\bar{\lambda}_{\parallel}(H = 0) = 0$	Villari Reversal	$\bar{\lambda}_{\parallel}(S) = 0$
1	$K_d = K < 0$ and large	$\varepsilon = 0$ or $\lambda_{100} = 0$	$-2/3 \leqslant \varepsilon \leqslant 0$	$\varepsilon = -2/3$ or $\lambda_{100} = 0$
2	$K_d = K > 0$ and large	$\lambda_{100} = 0$	$-\infty \leqslant \varepsilon \leqslant -2/3$	$\varepsilon = -2/3$ or $\lambda_{100} = 0$
3	$K_d = 0$	$\varepsilon = -2/3$ or $\lambda_{100} = 0$	———	$\varepsilon = -2/3$ or $\lambda_{100} = 0$

Since the conditions imposed on ε and λ_{100} for each assumed variation must be entirely compatible, the data on the chart can be reduced to the following four cases for $\gamma = 0.13$.

I. $K_d = 0$, $\lambda_{100} = 0$

II. $K_d > 0$, $-\infty \leqslant \varepsilon \leqslant -2/3$, $\lambda_{100} = 0$

III. $K_d < 0$, $-2/3 \leqslant \varepsilon \leqslant 0$, $\lambda_{100} = 0$

IV. $K_d = 0$, $\varepsilon = -2/3$

Cases I through IV are the conditions necessary at $\gamma = 0.13$. If $\gamma \neq 0.13$, however, some of these cases must be further divided into different conditions. This has been done in Table 6-I.

Table 6 - I. Physical conditions necessary to explain observed magnetostriction data

Case	$\gamma < 0.13$	$\gamma = 0.13$	$\gamma > 0.13$
Ia	$K_d \geq 0, -\infty \leq \varepsilon \leq -2/3,$ $\lambda_{100} > 0$	$K_d = 0,$ $\lambda_{100} = 0$	$K_d \leq 0, -2/3 \leq \varepsilon \leq 0,$ $\lambda_{100} > 0$
Ib	$K_d \leq 0, -2/3 \leq \varepsilon \leq 0,$ $\lambda_{100} < 0$	$K_d = 0,$ $\lambda_{100} = 0$	$K_d \geq 0, -\infty \leq \varepsilon \leq -2/3,$ $\lambda_{100} < 0$
Ic	$K_d \geq 0, -\infty \leq \varepsilon \leq -2/3,$ $\lambda_{100} > 0$	$K_d = 0,$ $\lambda_{100} = 0$	$K_d \geq 0, -\infty \leq \varepsilon \leq -2/3,$ $\lambda_{100} < 0$
Id	$K_d \leq 0, -2/3 \leq \varepsilon \leq 0,$ $\lambda_{100} < 0$	$K_d = 0,$ $\lambda_{100} = 0$	$K_d \leq 0, -2/3 \leq \varepsilon \leq 0,$ $\lambda_{100} > 0$
II	$K_d > 0, -\infty \leq \varepsilon \leq -2/3,$ $\lambda_{100} > 0$	$K_d > 0,$ $-\infty \leq \varepsilon \leq -2/3$ $\lambda_{100} = 0$	$K_d > 0, -\infty \leq \varepsilon \leq -2/3,$ $\lambda_{100} < 0$
III	$K_d < 0, -2/3 \leq \varepsilon \leq 0$ $\lambda_{100} < 0$	$K_d < 0, -2/3 \leq \varepsilon \leq 0,$ $\lambda_{100} = 0$	$K < 0, -2/3 \leq \varepsilon \leq 0,$ $\lambda_{100} > 0$
IVa	$K_d > 0, -\infty \leq \varepsilon \leq -2/3,$ $\lambda_{100} > 0$	$K_d = 0,$ $\varepsilon = -2/3,$ $\lambda_{100} > 0$	$K_d < 0, -2/3 \leq \varepsilon \leq 0,$ $\lambda_{100} > 0$
IVb	$K_d < 0, -2/3 \leq \varepsilon \leq 0,$ $\lambda_{100} < 0$	$K_d = 0$ $\varepsilon = -2/3,$ $\lambda_{100} < 0$	$K_d > 0, -\infty \leq \varepsilon \leq -2/3,$ $\lambda_{100} < 0$

In all cases considered $\varepsilon < 0$. Therefore, the cases where $\lambda_{100} = 0$ at $\gamma = 0.13$ (Cases Ia,Ib,Ic,Id, II, and III) require also that $\lambda_{111} = 0$ and that λ_{111} be of opposite sign to λ_{100} when $\gamma \neq 0.13$. It should be noted at this point that the formalism involving ε does not of itself force both λ_{100} and λ_{111} to go to zero together. It is the additional requirement due to the Villari reversal which forces λ_{111} to go simultaneously to zero with λ_{100}.

The way in which λ_{100} and λ_{111} go through zero would be determined by the crystal structure and the magnetic configuration in the structure. Ferrites possess a spinel structure in which there are two types of crystallographic sites occupied by magnetic ions. One type of site has tetrahedral coordination, and the other has octahedral coordination. It has already been pointed out that magnetostriction may be caused by the spin-orbit coupling; it was also noted that the orbital angular momentum should be closely associated with the crystal structure. The sites having tetrahedral coordination have crystallographic bonds in $\langle 111 \rangle$ directions, and the sites with octahedral coordination have bonds in $\langle 100 \rangle$ directions. Therefore, the magnetostriction coefficients for the $\langle 111 \rangle$ and $\langle 100 \rangle$ directions may well be associated with the ions in the tetrahedral or octahedral crystallographic sites, respectively. If this is the case, although the moments in the two types of sites are coupled together, it would be a very special case for both λ_{100} and λ_{111} to go through zero together.

In Cases Ia through Id, both the anisotropy K_d and magnetostriction λ_{100} are zero at $\gamma = 0.13$. It is conceivable that this could happen at some critical composition. However, it is well known that for this case the initial permeability of a material is extremely high.

Since this is not the case with a square B-H loop, Cases Ia through Id do not exist.

In Cases II and III, K_d remains of the same sign over the compositional variation whereas λ_{100} and λ_{111} must go through zero simultaneously and in an opposite sense. The unlikelihood that λ_{100} and λ_{111} approach zero simultaneously was discussed above. If such were the case, however, one would expect a similar effect on the crystalline anisotropy K near $\gamma = 0.13$, since K also depends on the spin-lattice coupling. However, Cases II and III require that K_d remain of the same sign while λ_{100} and λ_{111} reverse their sign. It is felt that this situation is unlikely to exist.

In Cases IVa and IVb the effective domain anisotropy K_d must change sign, going through zero at $\gamma = 0.13$, while the parameter $\varepsilon = \lambda_{111} / \lambda_{100}$ must go through $\varepsilon = -2/3$ for the same value of γ. In these cases λ_{100} and λ_{111} are not required to go through zero simultaneously, nor are they limited in magnitude. The requirement that $\varepsilon = -2/3$ at some critical value puts no restrictive constraints on the λ's, since ε may be expected to take any value less than zero. The requirement that $K_d = 0$ at the critical composition for which $\varepsilon = -2/3$ is more severe; however, it is shown in Sec. D. below that this requirement is entirely feasible provided the λ's are large. It is to be noted that $K_d \neq K$ so that the requirement $K_d = 0$ at $\varepsilon = -2/3$ does not necessarily place restrictions on K. It is concluded that Case IV represents the most likely physical situation. It will be shown in Sec. D. that this case not only explains the magnetostrictive data but, more important, that it also correlates these data with hysteresis-loop squareness.

Finally, the single-crystal magnetostrictive data for the ferrites (see page 24) indicates that $\lambda_{100} < 0$ for most ferrites. This

indicates that Case IVb is more likely to hold for the system studied than Case IVa.

There are independent, supplementary data which confirm the possibility that λ_{100} and λ_{111} may be very high at $\gamma = 0.13$ even though $\overline{\lambda}_{\parallel(S)} = 0$.

1. Mechanical properties indicate that high local stresses, such as would be the case for large λ_{100} and λ_{111}, are present, causing excessive cracking and brittleness for $\gamma = 0.13$.

2. The data for the switching coefficient S_w are relatively independent of composition, indicating that, other factors remaining constant, the domain-wall anisotropy energy K_w does not vary with composition. In general, $K_w \neq K_d$, K_w depends on local magnetostriction effects, as shown in Chapter IB, and could be large and relatively independent of composition if λ_{100} and λ_{111} were large and reasonably constant over the same compositional variation.

There are also independent supplementary data which confirm that $K_d = 0$ at the critical composition.

1. The relative magnitude of the flux density at H = 20 oersteds with respect to the value at H = 10,000 oersteds was obtained for samples numbered 3, 6 and 11 as shown on page 76. For all of these samples the ratio was above 0.8 and in one case was 0.96. These data indicate that even at low fields there is a high degree of alignment of the moments with respect to the direction of the applied field; this implies a low value of K_d.

2. Measurements of μ_{rem}/μ_i have been made by others[11] on square-looped ferrites, where μ_{rem} is the reversible permeability at remanence and μ_i is the initial permeability. The value of μ_{rem}/μ_i is very low

for materials possessing high loop squareness, whereas nonsquare loops have a $\mu_{rem}/\mu_i \lesssim 1$. A low value of μ_{rem}/μ_i is shown in Appendix D to indicate high alignment of the magnetic moments so that the major contributions to the permeability are due to domain-wall motion.

D. Proposed Alignment Mechanism

In order to justify the conclusion that Case IV of Chapter VIC is the most likely physical situation in the square-looped ferrites, it is necessary to show that the effective anisotropy energy K_d goes through zero at the critical composition $\gamma = 0.13$ for which $\varepsilon = \lambda_{111}/\lambda_{100} = -2/3$. If $K_d = 0$, the individual magnetic moments remain in the same direction after a saturating field is removed; the alignment of the magnetic moments by the saturating field is maintained. The existence of a grain-to-grain alignment is a major factor responsible for the square hysteresis loops which have been observed in other materials. The discussion of the mechanism which forces K_d through zero at $\varepsilon = 2/3$ gives further insight into the alignment effects due to magnetostriction.

The influence of magnetostriction on the equilibrium direction of the magnetic moment of a crystallite is the result of constraints which are placed on the physical dimensions of a crystallite by its environment. The value $\bar{\lambda}_{\parallel(S)} = 0$, which is observed at $\gamma = 0.13$, indicates that the environment seen by each crystallite in this case tends to inhibit any distortion due to magnetostriction. This inhibition of crystalline distortion means that if the λ's are not zero, the crystallites are under stress. The resulting magnetoelastic anisotropy energy must be added to K to give the effective anisotropy energy K_d. It should be noted that although the resultant stresses and strains over the entire material are zero, internal stresses and strains can be present precisely because the magnetostriction is not isotropic.

The magnetoelastic energy is proportional to $E \sum_{ij} a_{ij} \lambda_i \lambda_j$, where E is Young's modulus and the λ_i are the magnetostriction coefficients. If $\lambda_{100} = 0$ and $\lambda_{111} \neq 0$, the magnetoelastic energy would, with the constraint of zero distortion, produce minimum-energy positions for the magnetic moment along $\langle 100 \rangle$ directions. Therefore, if the crystalline anisotropy energy K is small compared to the magnetoelastic anisotropy energy, the result would be $K_d > 0$ regardless of the sign of K. Similarly if $\lambda_{100} \neq 0$ and $\lambda_{111} = 0$, $K_d < 0$ for the same relative magnitude of K and the magnetoelastic anisotropy energy.

Since $\varepsilon = \lambda_{111} / \lambda_{100}$, the above cases for $K_d > 0$ and $K_d < 0$ correspond to $\varepsilon = \pm \infty$ and $\varepsilon = 0$, respectively. These values of K_d and ε are compatible with the conditions required for Cases IVa and IVb when $\gamma \neq 0.13$.

Since these extreme relationships between K_d and ε may exist, there is some value of $\varepsilon < 0$ which will cause the magnetoelastic anisotropy energy to be equal and opposite to the crystalline anisotropy energy K, thus making $K_d = 0$. The magnitude of the magnetoelastic anisotropy energy would depend both on the magnitude of λ_{100} and ε; whereas the sign would depend only on the magnitude of ε for $\varepsilon < 0$. A formal theory has not been developed. However, since there are six $\langle 100 \rangle$ directions and eight $\langle 111 \rangle$ directions, zero magnetoelastic anisotropy would occur for $\varepsilon \lesssim -1/3$. For the case where the crystalline anisotropy energy $K < 0$, the magnetoelastic anisotropy must be positive. The condition necessary for $K_d = 0$ could thus be established if λ_{100} is large and $\varepsilon < -1/3$. The values $K_d = 0$ and $\varepsilon = -2/3$ are compatible with this proposed alignment because the experimental magnetostriction data do not require a low λ_{100} if $\varepsilon = -2/3$.

E. Critique of a Recent Publication

A paper on the same general subject as this investigation has recently been published by others.[11] These workers investigated the correlation between magnetostriction and B-H loop squareness for the ferrite system $(NiOFe_2O_3)_{1-x} + (Fe_3O_4)_x$. Although their conclusions and arguments are in complete opposition with those of this paper, their experimental data can be shown to be completely compatible with the ideas outlined above. Hence a critique of their work is necessary.

They concluded that the necessary conditions for B-H loop squareness are as follows:

1. The magnetostriction in the preferred direction must be zero. Therefore, since $K < 0$, it is necessary to have $\lambda_{111} = 0$.

2. The crystalline anisotropy energy must be large compared to the magnetoelastic energy.

These conclusions were based on arguments which do not appear to be valid for the case under consideration.

The heart of their argument is that magnetostriction in polycrystalline materials causes a random distribution of strains so that the magnetoelastic energy is minimized by a disorientation of the moments. If the magnetoelastic energy predominates the effective anisotropy, the crystalline anisotropy has no orienting influence, and the moments relax to a completely random distribution at remanence. Since magnetostriction can only have a disorienting effect, according to their model, a necessary, but not sufficient, condition for a square B-H loop is that the magnetoelastic energy be much smaller than the crystalline anisotropy energy.

The difficulty with this argument is their assumption of a random distribution of strains as a result of magnetostriction. The

magnetostriction effects can only alter the direction of easy magnetization in a grain if that grain is physically constrained. These constraints are presumably those which are imposed by the neighboring grains; but this paper has attempted to show that these are just the constraints which have an orienting, not a disorienting, effect on the magnetic moments. Consequently this paper argues that the observed condition between loop squareness and $\overline{\lambda}_{11\,(S)} = 0$ is due to a magnetoelastic anisotropy energy which is equal in magnitude but opposite in sign to the crystalline anisotropy energy so that $K_d = 0$; their argument, on the other hand, requires that the magnetoelastic anisotropy energy is much smaller than the crystalline anisotropy energy in a material with a square B-H loop. To show that this assumption of a random distribution of strains is open to serious question, the following hypothetical situation is cited: If the magnetostriction in each of the grains of a polycrystal is isotropic, a saturation field will produce an alignment of magnetostrictive strains as well as of the magnetic moments. If the saturation field is removed and the magnetoelastic energy is greater than the crystalline anisotropy energy, the moments should remain aligned as any disorientation would require work against the elastic energy of the crystal which is minimized by the orientation of the strains. Since the magnetostrictive strain is not random and has an orienting rather than a randomizing influence on the moments in this example, the assumption of random magnetostrictive strains is not generally valid.

The magnetostriction data that were reported is shown in Figure 6-1. They were obtained on polycrystalline rods in a manner similar to those techniques discussed in Chapter IVA* and are therefore open to the criticisms made in Chapter IV. The zero reference was

* These experimental details were kindly provided the author by Dr. Gorter in a private communication.

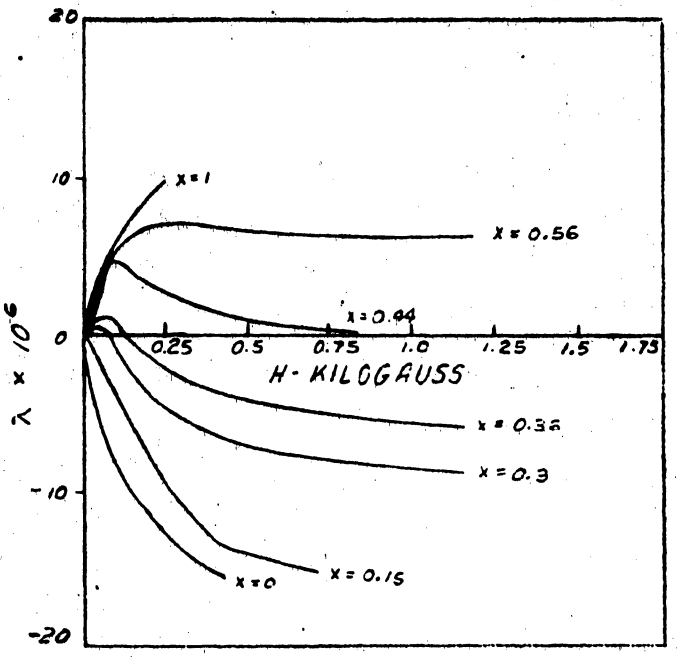

FIG. 6-2

MAGNETOSTRICTION OF MIXED POLYCRYSTALS OF NICKEL FERRITE AND MAGNETITE, $(Ni\ O\ Fe_2\ O_3)_{1-X} + (Fe_3\ O_4)_X$

(AFTER H.P.J. W.I.J.N. et al.)

arbitrarily taken at H = 0 and may not be valid. However, with this reservation, their data will be given an interpretation in terms of the conclusions of this paper.

The compositional series which they have investigated can be expressed in the following general formula: $(NiOFe_2O_3)_{1-x} + (Fe_3O_4)_x$, where the compositional parameter x may be $0 \leqslant x \leqslant 1$. Since single-crystal magnetostriction and anisotropy data exist for both of these components (see Page 24), it is much easier to interpret the polycrystalline magnetostriction data for a mixed series of these components.

The shape of the magnetostriction versus field data, which were obtained for several compositions for which the compositional parameter x was increased from 0 to 0.3, is very similar to that observed in the compositional series studied in this paper for $0 \leqslant \gamma \leqslant 0.1$. A Villari reversal is observed for $0 \leqslant x \leqslant 0.3$. There is a reversal of the saturation magnetostriction for $0.36 < x < 0.44$. However, for $0.44 \leqslant x$, a Villari reversal is not observed. The magnetostriction increases in magnitude as the field is reduced for $x > 0.44$.

The corresponding hysteresis data for these series indicate an increase in squareness with an increase in x for $x < 0.36$. For $x > 0.44$ hysteresis data were not presented; it is implied that the loop squareness is low in this region of x.

The single-crystal data show that $\varepsilon > -2/3$ and $\varepsilon < -2/3$ for $x = 0$ and $x = 1$, respectively. Since there is a reversal of the saturation magnetostriction in the region $0.36 < x < 0.44$ while, judging from its values at $x = 0$ and $x = 1$, λ_{100} does not change sign, it is concluded that ε must pass through $\varepsilon = -2/3$. This variation of ε with x would produce a magnetoelastic anisotropy energy which would be negative

and positive for low and high values of x, respectively. However, since the crystalline anisotropy energy K is $K < 0$ and large, the composition for which $K_d = 0$ may never be obtained. The fact that a Villari reversal is not found for high x is indicative of the fact that K_d does not go through zero. In this case the increase in squareness is attributed to a minimization of K_d; whereas in the case of the series investigated in this paper K_d was made to change sign.

The minimum effective domain anisotropy K_d will occur at a value of ε which is not necessarily $\varepsilon = -2/3$. Therefore, the maximum squareness does not necessarily occur for $\overline{\lambda}_{\parallel (S)} = 0$.

Since their data can be explained by the same arguments as were developed in this paper for the other compositional series, further weight is given to the conclusions of this study which were drawn without the aid of single-crystal data for any compositions in the compositional series.

CHAPTER VII

SUMMARY

A. Experimental Results

Magnetostriction data have been obtained for the compositional series $(MnOFe_2O_3)_{1-\gamma} + (Mn_3O_4)_\gamma$. These data were obtained at three different temperatures as a function of field by using a new technique.

A definite correlation was found between the hysteresis and the magnetostriction data. A fundamental mechanism has been proposed which not only interprets the magnetostriction data observed but also its correlation with the B-H loop data.

The positive isotropic saturation magnetostriction which was found for samples with large Mn_3O_4 content is significant since magnetite is the only other known ferrite to possess this property.

B. Conclusions

It is concluded from this investigation that magnetostriction plays a major role in square B-H loop ferrites. Although the saturation polycrystalline magnetostriction may be small, large single-crystal magnetostriction may be responsible for an internal orientation mechanism. This orientation mechanism would produce the high squareness obtained for these materials.

The orientation mechanism produces a very low effective domain anisotropy without reducing the effective anisotropy for a domain wall. This means that domain walls can exist in these materials even though the macroscopic anisotropy is zero.

C. Further Investigation

As indicated in the compositional survey, other compositional series must be investigated in much the same manner as that in this work.

This will confirm any extrapolation of the information obtained in this series into more complicated ternary systems. The sharp variation in squareness observed in other systems indicates that the effects noted here may be even more pronounced in other compositional series.

Low-temperature studies of magnetostriction should also be very informative, since there are apparently important changes in hysteresis data at -200 C; at -200 C the squareness for some compositions decreases, for others increases, relative to its value at room temperature and -78 C.

Single crystals are still not available for most ferrite compositions. However, until single-crystal measurements are made, it will not be known whether λ_{111} and λ_{100} go simultaneously through zero at optimum-squareness compositions, or whether they are large with $\varepsilon = -2/3$ and $K_d = 0$.

BIBLIOGRAPHY

1. Bozorth, R. M., "Ferromagnetism," D. Van Nostrand Company, Inc., New York (1951)

2. Forrester, J. W., "Digital Information Storage in Three Dimensions Using Magnetic Cores," J. Appl. Phys. 22, 44 (1951)

3. Kittel, C., "Physical Theory of Ferromagnetic Domains," Revs. Mod. Phys. 21, 541 (1949)

4. Galt, J. K., Andrus, J., and Hopper, H. G., "Motion of Domain Walls in Ferrite Crystals," Revs. Mod. Phys. 25, 93 (1953)

5. Williams, H. J., Sherwood, R. C., Goertz, M., and Schnettler, F. J., "Stressed Ferrites Having Rectangular Hysteresis Loops," Communications and Electronics 9, 531 (1953)

6. Baltzer, P. K., unpublished research, Lincoln Laboratory

7. Williams, H. J., Goertz, M., "Domain Structure of Perminvar Having a Rectangular Hysteresis Loop," J. Appl. Phys. 23, 316 (1952)

8. Brown, D. R., and Albers-Schoenburg, E., "Ferrites Speed Digital Computers," Electronics 26, 146 (1953)

9. Goodenough, J. B., "A Theory of Domain Creation and Coercive Force in Polycrystalline Ferromagnetics," Phys. Rev. 95, 917 (1954)

10. Menyuk, N., and Goodenough, J. B., "A Theory of Flux Reversal in Polycrystalline Ferromagnetics," J. Appl. Phys. - to be published

11. Wijn, H. P. J., Gorter, E. W., Esveldt, C. J., Geldermans, P., "Conditions for Square Hysteresis Loops in Ferrites," Philips Tech. Rev. 16, 49 (1954)

12. Joule, J. P., "On a New Class of Magnetic Forces," Ann. Electr. Magn. Chem. 8, 219 (1842)

13. Becker, R., Doring, W., "Ferromagnetismus," Berlin, Springer (1939)

14. Van Vleck, J. H., "On the Anisotropy of Cubic Ferromagnetic Crystals," Phys. Rev. 52, 1178 (1937)

15. Vonsovsky, S. V., "On the Quantum Theory of Magnetostriction of Ferromagnetic Single Crystals," J. Phys. USSR III, No. 3, 181 (1940)

16. Love, A. E. H., "A Treatise on the Mathematical Theory of Elasticity," Dover Publications, New York (1944)

17. Bozorth, R. M., Walker, J. G., "Magnetostriction of Single Crystals of Cobalt and Nickel Ferrites," Phys. Rev. 88, 1209 (1952)

BIBLIOGRAPHY (CONTINUED)

18. Vautier, R., "Contribution A L'Etude Du Phenomene De Magnetostriction," Ann. phys. (Paris) 9, 322 (1954)

19. Burgt, C. M. van de, "Dynamical Physical Parameters of the Magnetostrictive Excitation of Extensional and Torsional Vibrations in Ferrites," Philips Research Repts. 8, 91 (1953)

20. Bickford, L. R., Jr., Pappis, J., Stull, J. L., "Permeability and Magnetostriction of Cation-Substituted Magnetite," Phys. Rev. 94, 1433 (1954)

21. Goldman, J. E., "New Techniques and Results in the Measurement of Magnetostriction," J. phys. radium 12, 471 (1951)

22. Page, L., Adams, N. I., "Principles of Electricity," D. Van Nostrand Company, Inc., New York (1949)

23. Villari, E., "Change of Magnetization by Tension and by Electric Current," Ann. Phys. Chem. 126, 87 (1865)

24. Calhoun, B. A., Tech. Rep. 68, Lab. for Ins. Res., M.I.T. (July 1953)

APPENDIX A

DERIVATION OF THE EQUATION OF MOTION FOR A CYLINDRICAL 180° DOMAIN WALL

The motion of planar-180°-domain walls has been investigated by J. K. Galt.[4] The equation of planar-180°-domain-wall motion is $m\ddot{z} + \beta\dot{z} + \alpha z = 2I_s H$ for a unit area of 180° Block wall; m is equivalent mass per unit area, β is the damping coefficient, α is the stiffness coefficient, and z is the linear displacement of the wall. I_s is the saturation magnetization, and H is the applied field.

To derive the equation of motion for a cylindrical wall, the Lagrangian formulation is used. The Lagrangian $= \mathcal{L} = T - V$ where T is the kinetic energy of the system and V is the total potential energy. The dissipation function is $G(\dot{\rho})$ where ρ is the radial displacement of the wall. From the Lagrangian formulation the equation of motion is:

$$\frac{\partial}{\partial t}\left(\frac{\partial \mathcal{L}}{\partial \dot{\rho}}\right) + \frac{\partial G}{\partial \dot{\rho}} - \frac{\partial \mathcal{L}}{\partial \rho} = 0$$

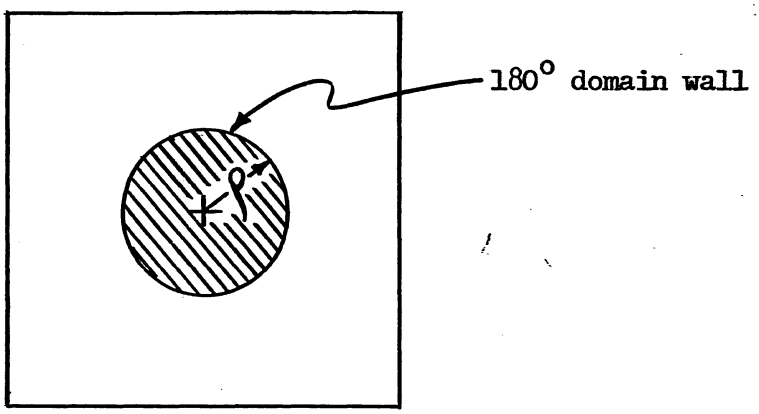

Cross Section of a Unit Area of Material

Note: Saturation magnetization of shaded domain is perpendicular to paper and toward reader, and that for the unshaded domain is away from reader.

Wall motion is considered for a wall of the configuration shown where the domain enclosed by the wall is magnetized in opposition to that outside and is ℓ units long. The applied field will be parallel to the domains, favoring one of the two directions, thus causing the wall to move radially in such a direction as to enlarge the domain magnetized in the direction of the applied field.

The kinetic energy is

$$T = \frac{(2\pi\rho\ell)m\dot{\rho}^2}{2}$$

The total potential energy is

$$V = E_{mutual} + E_{wall} + E_{magnetostatic}$$
$$= (1-\pi\rho^2)\ell\, 2HI_s + (2\pi\rho\ell)\,\sigma_\omega + \frac{(2\pi\rho\ell)\alpha\rho^2}{2}$$

and the dissipative function is

$$G(\dot{\rho}) = \frac{(2\pi\rho\ell)\,\beta\dot{\rho}^2}{2}$$

where σ_w is the wall energy per unit area, all other constants being the same as those in the equation of motion used for a planar wall.

Hence substituting these values in the equation of motion,

$$\frac{\partial}{\partial t}\left(\frac{\partial \mathcal{L}}{\partial \dot{\rho}}\right) + \frac{\partial G}{\partial \dot{\rho}} - \frac{\partial \mathcal{L}}{\partial \rho} = 0$$

one obtains for the motion of a cylindrical 180° Bloch wall (per unit wall area),

$$m\ddot{\rho} + \frac{m\dot{\rho}^2}{2\rho} + \beta\dot{\rho} + \frac{3}{2}\alpha\rho + \frac{\sigma_\omega}{\rho} = 2\,HI_s,$$

the equation of motion for a planar wall being

$$m\ddot{z} + \beta\dot{z} + \alpha z = 2\,HI_s.$$

In general, since $m \gtrsim 10^{-10}$, the normal inertial term can be neglected. For low fields where $\dot{\rho}$ would not be excessively large, the additional inertial term can also be neglected. However, the additional nonlinear term, $\frac{\sigma_\omega}{\rho}$, is of the same order as the driving force and cannot be neglected in calculations involving the motion of a cylindrical wall. This term enters here since the total wall area, and thus also the total wall energy, varies as the wall moves.

APPENDIX B

DERIVATION OF POLYCRYSTALLINE MAGNETOSTRICTION WHEN CRYSTALLITE MOMENTS ARE ALONG ⟨111⟩ DIRECTIONS

A polycrystalline model has been defined in Chapter III B, which enables the polycrystalline phenomena to be derived from the single-crystal formalism. Polycrystalline effects are derived by averaging the single crystal effects. However, the angular distribution of crystallite magnetic moments must be known or assumed before the averaging process can be properly done.

It is desired to derive the polycrystal magnetostriction for the following angular configuration. The magnetostriction is measured parallel to the axis of symmetry for the magnetic moments, which lie along the crystallite ⟨111⟩ direction nearest to the axis of symmetry, and is called $\bar{\lambda}_{\parallel\,(111)}$ in the text.

The single-crystal phenomenon can be expressed by:

$$\frac{\delta\ell}{\ell} = \lambda_{100}\left[\frac{3}{2}\left(\alpha_1^2\beta_1^2 + \alpha_2^2\beta_2^2 + \alpha_3^2\beta_3^2 - \frac{1}{3}\right) + 3\varepsilon\left(\alpha_1\alpha_2\beta_1\beta_2 + \alpha_1\alpha_3\beta_1\beta_3 + \alpha_2\alpha_3\beta_2\beta_3\right)\right],$$

where $\varepsilon = \lambda_{111}/\lambda_{100}$ and the α_i's are the direction cosines of the magnetization and the β_i's are the direction cosines of the measuring direction. When the moment is along a ⟨111⟩ direction $\alpha_1 = \alpha_2 = \alpha_3 = \frac{1}{\sqrt{3}}$ and this equation reduces to

$$\frac{\delta\ell}{\ell} = \varepsilon\lambda_{100}\left(\beta_1\beta_2 + \beta_1\beta_3 + \beta_2\beta_3\right).$$

The β_i will be expressed in the angular polar coordinates θ and ϕ to facilitate calculations:

$$\beta_1 = \cos\theta,\ \beta_2 = \sin\theta\sin\phi,\ \beta_3 = \sin\theta\cos\phi.$$

Since the crystallites can be considered to be randomly oriented, an average over single-crystal directions is equivalent to an average over the crystallite orientations.

Since the moment is along a $\langle 111 \rangle$ direction this can be expressed as $\theta' = \cos^{-1} \frac{1}{\sqrt{3}}$, $\phi = \frac{\pi}{4}$ in spherical coordinates. The direction cosines β_i need only be averaged over the octant, defined

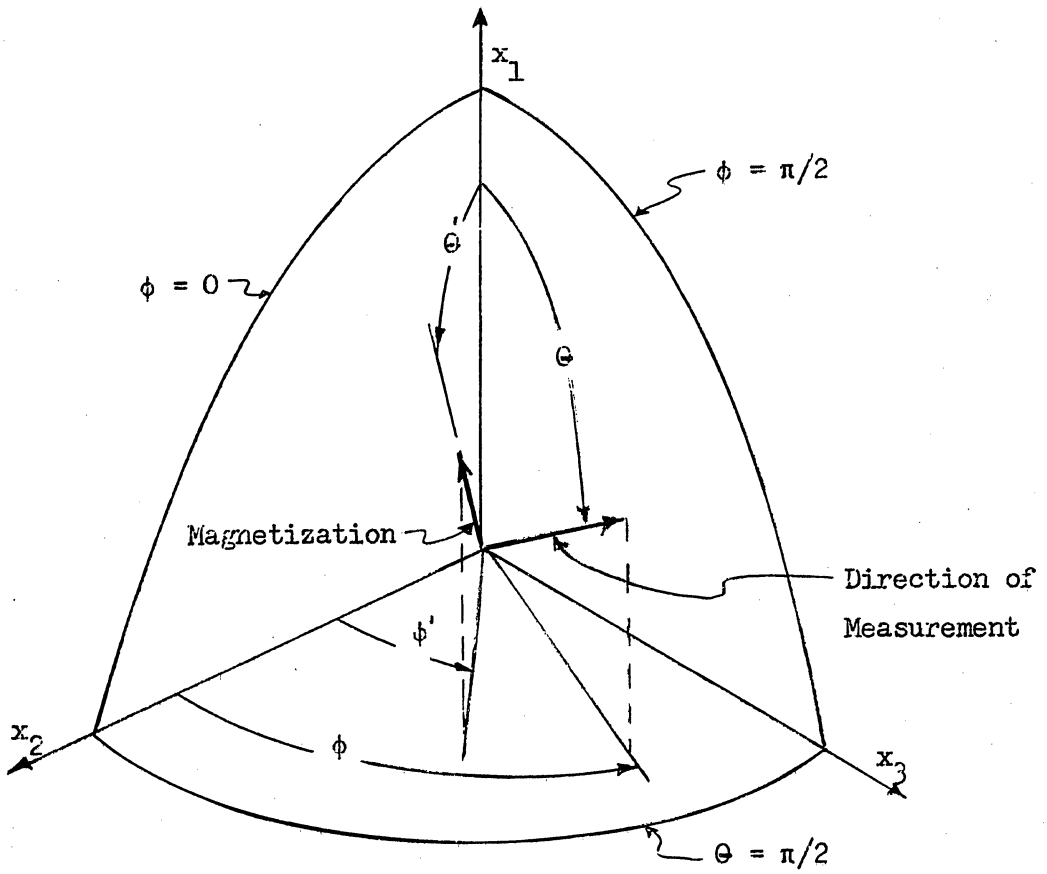

Octant of Integration

by the planes $\phi = 0$, $\phi = \pi/2$, and $\theta = \pi/2$ since all the moments are along the $\langle 111 \rangle$ direction nearest to the measuring direction. The octant of integration is a solid angle of $\pi/2$; therefore, the polycrystal magnetostriction can be expressed as:

$$\overline{\lambda}_{\parallel(111)} = \left(\overline{\frac{\delta \ell}{\ell}}\right) = \frac{2\varepsilon\lambda_{100}}{\pi} \int_0^{\pi/2} \int_0^{\pi/2} (\beta_1\beta_2 + \beta_1\beta_3 + \beta_2\beta_3) \sin\theta \, d\theta \, d\phi .$$

Each term integrated separately is:

$$\int_0^{\pi/2}\int_0^{\pi/2} \beta_1\beta_2 \sin\theta \, d\theta \, d\phi = \int_0^{\pi/2} \cos\phi \, d\phi \int_0^{\pi/2} \sin^2\theta \cos\theta \, d\theta$$

$$= \left[\sin\phi\right]_0^{\pi/2} \cdot \left[\frac{\sin^3\theta}{3}\right]_0^{\pi/2} = \frac{1}{3}$$

$$\int_0^{\pi/2}\int_0^{\pi/2} B_1\beta_3 \sin\theta \, d\theta \, d\phi = \int_0^{\pi/2} \sin\phi \, d\phi \int_0^{\pi/2} \sin^2\theta \cos\theta \, d\theta$$

$$= \left[-\cos\theta\right]_0^{\pi/2} \cdot \left[\frac{\sin^3\theta}{3}\right]_0^{\pi/2} = \frac{1}{3}$$

$$\int_0^{\pi/2}\int_0^{\pi/2} \beta_2\beta_3 \sin\theta \, d\theta \, d\phi = \int_0^{\pi/2} \sin\phi\cos\phi \, d\phi \int_0^{\pi/2} \sin^3\theta \, d\theta$$

$$= \left[\frac{\sin^2\phi}{2}\right]_0^{\pi/2} \cdot \left[\frac{\cos^3\theta}{3} - \cos\theta\right]_0^{\pi/2} = \frac{1}{3}$$

Therefore, when the separately integrated terms are added together the polycrystal magnetostriction for the specified conditions is determined:

$$\overline{\lambda}_{\parallel(111)} = \frac{2}{\pi} \varepsilon \lambda_{100} = .64 \, \varepsilon \lambda_{100}.$$

APPENDIX C

DERIVATION OF CALIBRATION FORMULA

The magnetostriction measurements were made with resistance-wire strain gages which are an active arm of a sensitive Wheatstone bridge. It is therefore desirable to derive a simple calibration formula for determining strain measurements from null detector outputs.

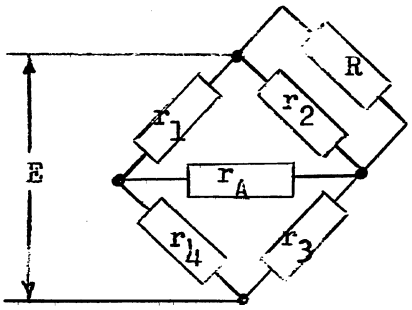

In the bridge circuit above r_1, r_2, r_3 and r_4 are resistance-wire strain gages; r_A is the input resistance of the detector and R is the resistance of the high impedance decade box used for obtaining bridge balance.

As an initial condition, the bridge will be considered at balance. To obtain a calibration it is only necessary to introduce a known change of resistance into one bridge arm for a null detector indication of the same order as that observed for the measurements. This is easily done by introducing a small change ΔR to the balancing decade-box resistance. The parallel combination of r_2 and R will be called r_2'.

$$r_2' = \frac{r_2 R}{R + r_2}, \text{ and } \Delta r_2' = \frac{(r_2)^2 \Delta R}{(R + r_2)^2}.$$

Therefore,

$$\frac{\Delta r_2'}{r_2'} = \frac{r_2 \Delta R}{R(R + r_2)}.$$

However, since $r_2/R \leq 10^{-2}$, $\frac{\Delta r'_2}{r_2'}$ may be written as $\frac{\Delta r_2'}{r_2'} \leq \frac{r_2 \Delta R}{H^2}$.

The proportionality between a relative change in resistance and the relative change in length of a strain gage is called the gage factor, $G = \frac{\delta r}{r} / \frac{\delta \ell}{\ell}$. The relative change in length is therefore $\frac{\delta \ell}{\ell} = \frac{\delta r}{r} / G$.

The change in decade-box resistance ΔR is equivalent to a corresponding change in length of one of the strain gages. That is, $\left(\frac{\delta \ell}{\ell}\right)_{\text{equivalent}} = r_2 \Delta R / R^2 G$.

In order to obtain a calibration it is only necessary to divide the equivalent change in length by the deflection d milliamperes of the null-indicating output meter corresponding to the change ΔR. Hence the calibration formula is $S = r_2 \Delta R / dR^2 G$ per milliammeter deflection, where r_2 is the strain-gage resistance, R is the decade-box resistance, ΔR is the change in R, d is the output-meter deflection corresponding to the change ΔR, and G is the gage factor.

APPENDIX D

A QUALITATIVE ANALYSIS OF REVERSIBLE PERMEABILITY AS A FUNCTION OF REMANENT STATE

The reversible permeability observed at different remanent states is due to two distinct mechanisms which have additive effects but are essentially independent phenomena. The two mechanisms are Domain Rotation and Reversible Domain-Wall Motion. The effect of the remanent state on these mechanisms will be considered and experimental data examined in the light of this analysis.

Domain rotation is the result of the torque $\vec{M} \times \vec{H}$, which is proportional to the sin θ where θ is the angle between the moment $\vec{M}$ and the field $\vec{H}$. The magnetic moment M of a domain, in the absence of an applied field, is along a direction determined by the effective domain anisotropy K_d. The first order restoring torque supplied by the crystalline anisotropy for a small angular displacement $\Delta\theta$ of the magnetic moment would be proportional to $\Delta\theta$. Therefore the displacement $\Delta\theta$ due to the application of a small field ΔH would be proportional to the applied torque: $\Delta\theta \propto \Delta H \sin\theta$. The change in the magnetic moment ΔB of this domain, in the direction of field, is proportional to the change in the cos θ. Hence $\Delta B \propto \sin\theta\, \Delta\theta$. Therefore since $\Delta\theta \propto \Delta H \sin\theta$ we may express the permeability μ_{rot} entirely in terms of the angle θ: $\mu_{rot} = \frac{\Delta B}{\Delta H} = A \sin^2\theta$, where A is a constant involving the saturation moment, and the effective domain anisotropy constant K_d.

Since $\sin^2(\theta + 180) = \sin^2\theta$, only a change in the distribution of the angle θ throughout the material will affect the average over-all permeability of a sample. Therefore, between 90° and 180° domain walls, only the position of 90° walls will affect the permeability. The average permeability μ_{rot} can be expressed in terms of an integral relationship, viz. $\mu_{rot} = A \int_0^\pi f(\theta) \sin^2\theta \, d\theta$, where $f(\theta)$ is the angular distribution of the domain magnetization about the direction of the applied field and $\int_0^\pi f(\theta) \, d\theta = 1$. The μ_{rot} will therefore be small if the magnetization of the domains are closely aligned to the field since $f(\theta)$ would be very narrow.

Reversible domain-wall motion will also cause reversible permeability, μ_{wall}. This contribution to permeability will be proportional to the domain wall area. The relative 180° domain wall area present at any remanent state, B_r, as compared to that at the demagnetized state will be calculated on the basis of the following simple model. For a unit cross-section of the material a single domain of reverse magnetization will be considered with a cylindrical 180° domain wall.

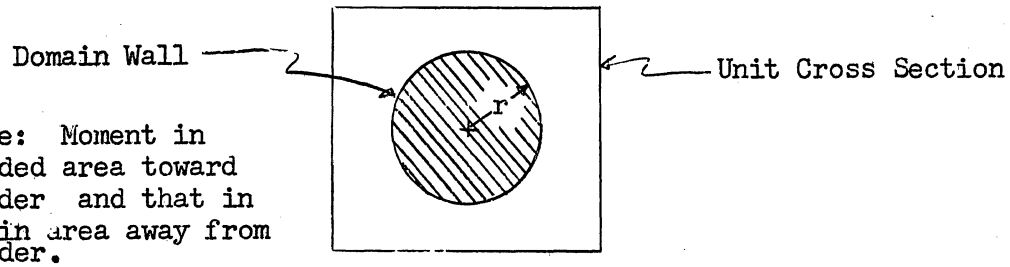

The remanent state can be calculated on the basis of this model: $B_r = B_s(1-\pi r^2)$, where B_s is the saturation flux density. Solving for r we obtain the following relationship: $r = \sqrt{1 - \frac{B_r}{B_s}} / \pi$. Since the wall area is proportional to r and the μ is proportional to the domain wall area we may obtain $\mu_{wall} = B \sqrt{1 - \frac{B_r}{B_s}}$ for the reversible permeability at remanence, where B is a constant involving the saturation

moment and the domain-wall energy surface density.

For the above discussion it had been tacitly assumed that the field was aligned parallel to the magnetic moments in the domains. A first-order correction for the effect of an angular displacement θ of the magnetic moment from the applied field can be made. The small reversible displacement of a domain wall is proportional to the applied force which in turn is a linear function of the cos θ. Since the change in magnetization due to the wall displacement is also proportional to the cos θ, the permeability will vary with the $\cos^2 \theta$. An average permeability can be obtained by integrating $\cos^2 \theta$ throughout the material:

$$\mu_{wall} = B \sqrt{1 - \frac{B_r}{B_s}} \int_0^{\pi} f_r(\theta) \cos^2 \theta \, d\theta$$

for any remanent state.

The ratio of the total permeability, $\mu_{tot} = \mu_{rot} + \mu_{wall}$, at remanence over that for the demagnetized state, $B_r = 0$, gives the ratio $\frac{\mu_{rem}}{\mu_i}$ reported in the literature for materials of various remanent states.[11] Therefore using the derived expressions for the average contribution of μ_{rot} and μ_{wall} one obtains:

$$\frac{\mu_{rem}}{\mu_i} = \frac{A\int_0^{\pi} f_r(\theta) \sin^2 d\theta + B \sqrt{1 - \frac{B_r}{B_s}} \int_0^{\pi} f_r(\theta) \cos^2 \theta \, d\theta}{A\int_0^{\pi} f_i(\theta) \sin^2 d\theta + B \int_0^{\pi} f_i(\theta) \cos^2 d\theta}$$

where $f_r(\theta)$ and $f_o(\theta)$ are the angular-distribution functions of domain magnetization about the direction of the applied field for the remanent and demagnetized states, respectively.

This equation readily shows that if there is not a significant change in $f(\theta)$ between the remanent and demagnetized state the only

dependence of $\frac{\mu_{rem}}{\mu_i}$ on the remanent state would come from the coefficient $\sqrt{1 - B_r/B_s}$ which is due to wall motion. Since in general for most ferrites A is large compared to B, the term containing $\sqrt{1 - B_r/B_s}$ can enter only when $f(\theta)$ is very narrow, because of an extreme grain-to-grain alignment of the crystallite moments, making $\sin^2\theta$ very small. In this case μ_{wall} predominates :

$$\frac{\mu_{rem}}{\mu_i} \leq \sqrt{1 - \frac{B_r}{B_s}} \quad \frac{\int_0^{\pi} f_r(\theta) \cos^2\theta \, d\theta}{\int_0^{\pi} f_i(\theta) \cos^2\theta \, d\theta} \leq \sqrt{1 - \frac{B_r}{B_s}} ,$$

$$\text{since } \int_0^{\pi} f(\theta) \cos^2\theta \, d\theta \leq 1.$$

Therefore, as $B_r/B_s \rightarrow 1$, μ_{rem}/μ_i should approach a very low value.

When a high grain-to-grain alignment does not exist, the $\overline{\cos^2\theta}$ would be very low; the μ_{rot} will predominate and

$$\frac{\mu_{rem}}{\mu_i} \leq \frac{\int_0^{\pi} f_r(\theta) \sin^2\theta \, d\theta}{\int_0^{\pi} f_i(\theta) \sin^2\theta \, d\theta} ,$$

which for $f_r(\theta) \leq f_i(\theta)$ would approach the limit of 1.

Therefore, the low value of μ_{rem}/μ_i obtained in square B-H loop ferrites would be indicative of a high alignment and 180° domain wall motion. On the other hand, the high $\mu_{rem}/\mu_i \leq 1$ obtained in nonsquare-looped ferrites would indicate just the opposite, being caused by domain rotation or 90° domain-wall motion.